APPLE BRUISE MEASUREMENT BY IMAGE ANALYSIS

A thesis

submitted in partial fulfilment of
the requirements for the degree
of
Master of Horticultural Science
in
Agricultural Engineering
at
Massey University
Palmerston North
New Zealand

LI OUYANG

1995

ACKNOWLEDGMENTS

I would like to thank Dr Cliff J. Studman, supervisor (Department of Agricultural Engineering, Massey University), for his generous advice, thoughtful guidance, and encouragement throughout this study.

I wish to express my appreciation to Professor Gavin Wall, head of the Department, for his encouragement and support of this study, Mr Ian A. Painter and Mr R.L. Bolter for their assistance with laboratory experiments and construction of apparatus, and other members and postgraduates of the Department of Agricultural Engineering for their friendship.

In particular, I wish to express my appreciation to Mr. George Brier (AgResearch, Hamilton) for his helpful suggestions and cares.

Finally, I wish to thank my husband Jiafa for his encouragement and understanding, without which this study would have been impossible.

TABLE OF CONTENTS

LIST OF FIGURES

LIST OF TABLES

ABSTRACT

Apple bruising is one of the main problems causing loss of apple quality during harvesting and post-harvesting process. The degree of bruising may be described by bruise surface or volume, but manual measurement of these variables is tedious and often inaccurate. Image analysis techniques could be more accurate and reliable. This study was therefore designed as part of a project to develop a semi-automatic system to determine apple bruise size, by establishing an effective method of image analysis for measuring apple bruises in the laboratory.

Systems for image analysis of apple bruises were set up using the VIPS (Vision Image Processing System) computer language, a program developed at Massey University. Bruises on fresh and stored "Granny-Smith" apples were made using a falling pendulum, and steel and hockey balls dropped vertically in a series of experiments. Parameters such as bruise width and depth in the bruise cross-section were measured by traditional manual methods and compared with semi-automatic image analysis values. The surface bruise area was also measured by both methods. Bruise volume assessments were made both by estimation from single cross-sections and by taking several cross-sections through the bruise and measuring their thickness. In order to test repeatability of the measurement technique, apple bruises were measured by independent assessors and their results were compared with image analysis data.

Bruise width and depth measurements from a radial cross section were the same for the manual method and image analysis. Bruise volumes calculated from these two methods by assuming a geometric shape also gave similar results, regardless of the way in which

the bruise was made. However, the standard deviation of bruise volume among the replicates technique from the image analysis was half that for the manual measurement method.

Direct measurement of the bruise surface area (after skin removal) by image analysis was five times less variable than by manual measurement. The manual method, however, consistently overestimated bruise area by 10% compared with the image analysis.

An improved method to estimate bruise volume using image analysis is proposed, which does not require a geometric shape of the apple bruise to be assumed. This involves taking a series of sections parallel to the skin. This method was more amenable to image analysis techniques and appears to be more accurate than the traditional manual radial cross-section method for bruise volume assessment.

CHAPTER 1

INTRODUCTION

1.1 General introduction

Apples are one of the major fruits grown in New Zealand for export and local consumption. Bruising is currently one of the most important reasons for rejection of apples from export grade. Apple bruising can cause significant loss of apple quality during harvesting, sorting and transporting, and reduce the income of apple growers. According to Banks and Studman (1991), Granny Smith apple growers lost between $6m and $10m due to bruising in 1991 in New Zealand. Sober *et al.*, (1989) found that 81% of 'McIntosh' apples were bruised during harvesting. After transport to the packaging house, 93% of the apples were bruised. Most bruising occurs as a result of impacts against a variety of surfaces, and during impacts with other apples (Pang *et al.*, 1992).

Mechanisation of fruit harvesting, sorting, and packing can lead to mechanical damage of fruit. In recent years this has drawn a lot of attention from researchers and fruit growers. Mechanical impact due to external forces can result in fruit cutting, peeling, and bruising. Modern handling systems have virtually eliminated fruit cutting and peeling during handling, but bruise damage is still a major cause of quality loss in fresh fruit.

1.2 Definition of a bruise

Bruising has been defined as damage to plant tissue by external forces causing a physical change in texture, and/or eventual chemical alterations that result in changes of colour, flavour, or texture (Mohsenin, 1970). Bruising does not break the skin of an apple, but influences its appearance. Hence it will reduce the acceptability of the apple to the consumer.

Since bruising can be caused by compression, impact or vibration forces in almost all processes from harvest to consumption, a study on fruit bruising can be complex. However, bruise area and bruise volume are two basic parameters for describing the size of the bruise. Other terms for defining fruit bruising are based on these parameters. For instance, bruise susceptibility (Klein, 1987; Vergano *et al.*, 1991), bruise resistance coefficient (Schoorl and Holt, 1980), bruising threshold (Brown *et al.*, 1990; Bollen and Cox, 1991; Pang *et al.*, 1992; Schulte *et al.*, 1992) and bruise factor (Pang, 1994) have been used in the study of fruit bruising. These are all based on measurements of bruise surface area or bruise volume. Furthermore, the values of bruise surface area or bruise volume indicate the amount of damage directly (Topping and Luton, 1986; Brusewitz and Bartsch, 1989). The sizes of bruise surface area and bruise volume are related to other parameters, such as drop height, impact energy, and surface conditions, etc (Schoorl and Holt, 1977; Topping and Luton, 1986; Chen and Yazdani, 1991). In practice, bruise surface area of fruits is the main standard used by the industry for assessment, while most researchers use bruise volume measurements. Thus the precise measurement of both bruise area and volume is essential in the study of fruit bruising.

1.3 Machine vision systems

Machine vision is useful as a tool for automated visual measurement, and has become an active area of research in the last decade. Owing to the advances in computing and electronic technology and the decline in the price of computing and imaging hardware, machine vision technology has been considered for many applications in agricultural and food production processes. Machine vision is a machine eye-brain (camera-computer) system which provides some of the capabilities of human visual perception (Hodgson, 1984).

Machine vision systems are becoming more useful as an alternative to manual methods for irregular shape, size measurement and automation in the agricultural and horticultural industries. To meet the increasing demand for high quality produce and reduce waste cost, automation of the evaluation of fruit quality would generate significant economic and labour saving benefits to the fruit industry. One of the major requirements in developing machine vision systems for sorting fruit and vegetables is the ability to analyse an image accurately and quickly (Chen and Sun, 1991). However, before an automated mechanism can be designed, the possible bruise damage needs to be considered. In some cases it may be necessary to determine the likely proportion of the product which will be unavoidably damaged. This has to involve the determination of bruise damage quantity in terms of bruise surface area and bruise volume. These are two key factors in the design and modification of machines for fruit handling. A machine vision system could not only be applied for automation in fruit industries, but also used as precise equipment for accurate and fast measurement of irregular shape and size of objects in agriculture and horticulture in general.

This thesis presents research work on an application of machine vision technology for apple bruise measurement. The emphasis is on the application of image analysis techniques to measure bruise size by developing machine vision methods for measuring bruise area and bruise volume, once fruit have been cut to reveal the damage clearly. Thus, the project is aimed at developing a device to aid researchers to measure bruises, and not as a production line system for detecting bruises.

1.4 Objectives

The objectives of this study were:

- To become familiar with hardware and software techniques in image analysis;
- To develop a semi-automatic system to measure bruise width and depth from cross-sectional area and hence calculate the bruise volume of apples;
- To develop a semi-automatic system to measure bruise area and volume of apples;
- To develop a reliable method for applying image analysis to the measurement of bruise volume;
- To compare the accuracy of image analysis with manual methods for estimating bruise area and volume.

CHAPTER 2

LITERATURE REVIEW

2.1 Introduction

As outlined in Chapter 1, in studies of apple bruising, damage parameters such as bruise surface area and bruise volume are determined (Bollen and Cox, 1991; Brown *et al.*, 1987; Brown *et al.*, 1990; Holt and Shoorl 1977; Pang *et al.*, 1992). Bruising is generally measured by producing a bruise in the apple using a falling sphere, or by dropping the fruit onto a flat surface (Collett *et al.*, 1991). The bruise is then allowed to discolour over a period of time, the apple is sectioned, and the volume of the bruise is obtained by measuring bruise depth and width (Pang *et al.*, 1992). There are several different approaches to determine bruise area and bruise volume. Almost always manual measurement methods (Mohsenin, 1970; Holt and Schoorl, 1977) have been used, although there have been some exploratory investigations into the prospects for using machine vision systems (e.g., Collett *et al.*, 1991). This review considers first some definitions for assessing bruise size. Then the occurrence of bruising, and factors which affect bruising levels are outlined. Following this, bruise volume formulae are discussed. The remainder of the Chapter is concerned with reviews of image analysis principles, and applications to fruit and vegetables.

2.2 Apple bruising

Bruising means damage to plant tissue by external forces causing physical change in texture and/or eventual chemical alteration of colour, flavour, and texture. Bruising does not break the skin (Mohsenin, 1970).

Most fruit crops are subjected to various types of loading during harvest, handling, and transportation that cause bruising to the fruit and loss of product quality (Srivastava *et al.*, 1992). Apples are highly susceptible to impact damage during post-harvest handling (Studman and Banks, 1990). The impact damage may occur to individual apples during harvesting, filling of bins and on the packaging line. Damage to apples in bulk may take place due to vibration impact during handling and transporting of bins, corrugated containers and unitized pallets. Bruising may also occur due to compression of apples during storage (Banks and Studman, 1991).

2.2.1 Degree of bruising

The mechanics of fruit damage due to impact has been studied by many researchers. Holt and Schoorl (1977) studied the degree of bruising by using the bruise volume and energy absorbed, and found a strong linear relationship between bruise volume and energy absorbed during the impact of fruit into a flat surface in the range of impact energies from 0.3 to 2.2 J. Bruise volume can be calculated from the diameter of the apple, and the maximum depth and width of each bruise. Schoorl and Holt (1980) also suggested a method of measuring bruising. The degree of bruising was described as the bruise resistance coefficient of the fruit, defined as the bruise volume divided by the energy absorbed. Unfortunately this definition means that the bruising resistance increases as the fruit bruise more easily. It is preferable to term this ratio the Bruise Susceptibility (Studman and Banks, 1990).

By dropping fruit onto a wooden table, Klein (1987) found the susceptibility of apples to impact damage increased from early to late harvest time and decreased during storage at 1 °C. Mowatt and Banks (1994) measured bruise susceptibility using a method involving dropping a hockey ball onto the fruit. They reported that bruise susceptibility could be characterised by the size of a bruise resulting from a standardised impact. They found that apples with high bruise susceptibility incurred greater areas of bruising during normal postharvest handling than those with low bruise susceptibility.

Pang (1994) measured a term called the bruise factor by impacting apples from different drop heights onto a flat steel surface using a pendulum. He concluded that bruise factor related reasonably well to the number of bruises produced by the mechanical fruit grader. A larger number indicated more sensitivity to bruise damage.

Thus, the degree of bruising can be described by bruise volume, bruise area, bruise susceptibility and bruise factor. However, the bruise area which is measured on the skin of the fruit is more important in commercial situations, because (1) bruise volume is not measured since fruit cannot be cut; (2) in practice, fruit is graded by bruise area; (3) consumers selecting fruit are choosing on visual appearance of fruit.

2.2.2 Effect of storage time and temperature on apple bruise

Temperature and storage time are important environmental factors that could govern susceptibility of fruit to bruising. Kader (1985) found that each increase of 10 °C above optimum, the rate of several deterioration increases by two- to three-fold. Quality apples need to be kept in coolstore regardless of whether they are for export or local consumption. Correct storage temperatures can increase the storage period while maintaining the quality of fruit. An understanding of how apples bruise related to temperature and storage time would help in designing the handling, packaging, and storage systems to minimize bruising and maintain product quality.

Zhang (1992) reported that bruise susceptibility of 'Golden Delicious' was significantly lower than that of 'Red Delicious'. The report concluded that in the temperature range from 0 °C to 21 °C, in general, the colder the apple was, the higher the bruise susceptibility would be. Within the experimental period (about 5 weeks), storage time did not have a significant effect on bruise susceptibility. However, in the same time period, the apple firmness continually decreased with time. Klein (1987) reported that bruise susceptibility increased with lateness of harvest and decreased over storage time. Storage appeared to be more significant than harvest date in governing susceptibility to damage. However, Schoorl and Holt (1977) found increased bruise susceptibility with increasing storage time.

From the mechanical point of view, Mohsenin (1970) reported that while apple at lower temperatures are "firmer", they are less resistant to internal cell rupture as manifested through their lower values of bioyield force. The higher yield force exhibit at the higher temperature could be due to the reduced turgidity which enabled the plant cell to undergo a greater deformation without rupturing.

Pang and Studman (1992) reported that fruit at low temperature had a high bruise susceptibility. They concluded that handling fruit at low temperature may result in more bruising, so that apples should be graded at room temperature to reduce bruise damage.

Experimental results of Ouyang (1993) showed that the bruise susceptibility of fresh 'Royal Gala' apples was not significantly different from that of apples stored for one week at room temperature (16 ^{o}C). The bruising method used was to drop the apples onto a flat wooden surface. All testing was at room temperature. However, failure force and stress measurements of 'Royal Gala' apples were higher than values measured after one week of storage at room temperature.

Due to the different treatments and methods used, it is not easy to compare results obtained by researchers. The question of the effect of storage temperature and storage time on the bruise susceptibility of apples remains open, and it needs to further study. Most importantly, the research methods for apple bruise measurement should be developed.

2.2.3 Colour changes in apple bruised tissue

Detection of bruise colour changes following impact is critical both to the science and industry. It has been generally believed that colour of bruises takes 1 or 2 days to develop by New Zealand apple industry (Samim and Banks, 1993a). The study of bruise colour change in 'Granny Smith' apples conducted by Samim and Banks (1993a) indicated bruises should be allowed to develop for a period of 4 - 14 h before sectioning to assess bruises at their most intense degree of discolouration. They concluded that the discolouration of apple bruises generally developed with time of impact but subsequently faded as both water and dry matter are lost from the bruise. The further study (Samim and Banks, 1993b) showed that storage of apples in different moisture conditions did not seriously affect bruise discolouration in 'Granny Smith' apples.

2.3 Methods for determination of apple bruise sizes

There is no standard method for estimating bruise damage, and consequently researchers have often designed their own procedures.

2.3.1 Estimation of apple bruise

- ***Bruise surface area***

In order to measure bruise surface area (A) manually, it is generally assumed that its shape is ellipsoidal (Pang and Studman, 1992). Thus the bruise area is calculated from measurement of the major and minor diameters (d_1 and d_2) of the ellipsoid, using the formula:

$$A = \frac{\pi d_1 d_2}{4} \qquad 2.1$$

- ***Bruise volume***

Bruise volume has been measured by excavating the bruised tissue and measuring the mass of tissue (Klein, 1987). However, this method is too time consuming for practical purposes, and subject to human error, so normally, bruise volume is measured in terms of width and depth of the bruise. Bruise volume is calculated by assuming a geometric shape. A number of methods for calculating bruise volume have been suggested.

Mohsenin (1970) defined the bruise volume (V_{bruise}, mm^3) on the assumption that the shape of the bruise was spherical. This gives:

$$V_{bruise} = \frac{\pi h}{24}(3d^2 + 4h^2) \qquad 2.2$$

where h is the depth of bruise at the centre in mm and d the surface diameter of the bruise in mm. A cross-section of an idealised bruise showing the symbols used by Mohsenin (1970) is shown in Figure 2.1a.

Holt and Schoorl (1977) assumed that the shape of the bruise was spherical above and below the contact plane. The volumes of the bruise above the contact plane, V_2, and below it V_1 are shown in Figure 2.1b. Total bruise volume, (V_{bruise}, mm^3) of the bruise is then given by:

$$V_{bruise} = V_1 + V_2 = \frac{\pi h}{24}(3d^2 + 4h^2) + \frac{\pi X}{24}(3d^2 + 4X^2) \qquad 2.3$$

where h is the height of the bruise below the contact plane in mm, and X is the height of the bruise above the contact plane in mm. This can be calculated from:

$$X = R - \sqrt{R^2 - \frac{d^2}{4}} \qquad 2.4$$

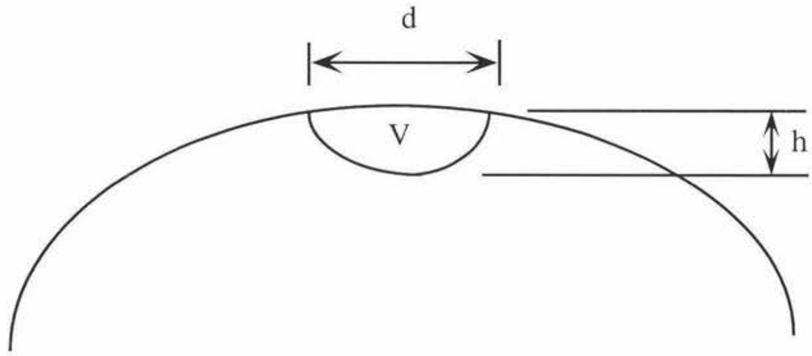

Figure 2.1a A cross-section of an idealised bruise showing the symbols used by Mohsenin (1970)

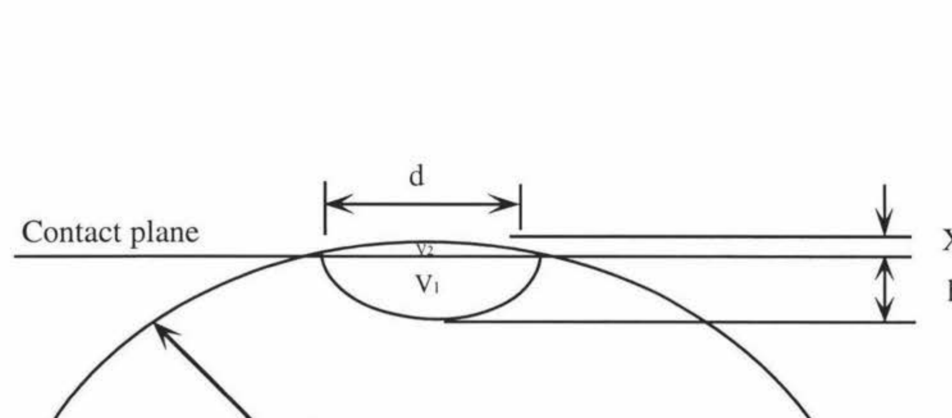

Figure 2.1b A cross-section of an idealised bruise showing the symbols used by Holt and Schoorl (1977)

where R is the radius of the apple in mm. A cross-section of an idealised bruise showing the symbols used by Holt and Schoorl (1977) is shown in Figure 2.1b.

A more simple formula was used by Chen and Sun (1981). The degree of bruise was evaluated by cutting through the centre of the bruise region and measuring the maximum width and depth of bruise with a scale. The shape of the bruise was assumed to be a semi-oblate spheroid, for which the bruise volume is given by:

$$V_{bruise} = \frac{1}{6}\pi\, hd^2 \qquad 2.5$$

2.3.2 Measurement methods

Current methods involve determining the size of the bruise by human eyes. This can be quite difficult, because the discolouration in some apples may be relatively hard to detect, and the shape of the bruised area may be irregular. Considerable subjectivity may be involved in bruise size determination. Therefore, there is a requirement for a device which enable the apple bruise to be measured rapidly, and to overcome the difficulty in measuring the irregular shape of bruise.

Machine vision systems have been considered as an alternative technique to detect and measure surface defects on apples (Davenel *et al.*, 1988). Numerous other auto-techniques for identifying and measuring apple bruise have also been reported, such as a X-ray transmission method (Diener *et al.*, 1970), an electrical resistivity method (Holcomb *et al.*, 1977), an optical reflectance method (Pen *et al.*, 1985), near-infrared reflectance method (Upchurch *et al.*, 1993), and a spectrophotometry method (Geoola *et al.*, 1994), but these will not be discussed in this report.

2.4 Machine vision systems

2.4.1 Equipment and techniques

For a general machine vision system, the basic equipment consists of a personal computer and video camera together with associated hardware and software. The software may be based on a computer language such as C^{++}. The video camera is used not only to get images of the object, but also to transfer the images to the computer (Collett *et al.*, 1991).

The most common kind of image analysis involves shape or line detection and image structure. Boundary chain coding techniques have been used to describe shape and size (Sarker and Wolfe, 1985). An image is digitised and divided into small regions, called picture elements or pixels. A grey level is given to each pixel based on the intensity of light received by the camera at each corresponding pixel location. An 8-bit A/D converter provides up to 2^8 or 256 grey levels of intensity for each pixel. Digitised images may be stored temporarily in computer memory or permanently on disk or tape (Paulsen and McClure, 1986; Roudot *et al.*, 1988).

Two terms commonly mentioned with computer vision systems are image processing and pattern recognition. Image processing involves steps taken to enhance an image and extract pertinent information. Pattern recognition involves procedures that allow the computer to identify and classify an object based on certain characteristics. There is no general theory in existence which allows a computer process or algorithm to be directly written to meet some specified need. Algorithms are developed by trial and error using interactive image processing computers (Hodgson, 1984). However, to make an algorithm for any particle application, normally the following three common main steps are followed: image capture, image segmentation with thresholding, and image size measurement.

Step 1: Image capture

Two image processing systems have been developed in the Production Technology Department of Massey University: an Opcon Industrial Line-Scan Camera hardware and associated software; and the VIPS digital image processing algorithm development environment, which is matrix image based. These two systems have been compared by Collett (1991).

The Opcon Line-Scan Camera system comprises a camera and dedicated CPU for image capture and analysis. A software package called Pixel Mechanic is used to program the system to look for "features" in the line-scan camera shot. These features could be simple edges, or collections of edges making up more complicated patterns. The Opcon system has the advantage that once the application has been specified, it runs on a dedicated hardware system and thus can be quite fast. However, its main disadvantage is its use of a line-scan camera. This requires taking multiple images to build up a two-dimensional picture. Also, the range of features which the system can be set up to recognise is limited, and success is heavily dependent on orientation. An advantage is that line-scan camera images take less memory and disk space, but this must be balanced against the fact that more images must be captured to provide enough information.

In contrast, VIPS is a software only system, running on a VAX mini-computer, although it has recently been ported to a Macintosh platform. This means it is slower in operation due to being on a shared computer system. However the fact that it is based on matrix-array camera images, and has such a wide range of image processing operations, makes it a powerful tool for machine vision. Matrix based images obviously take up a large amount of storage space, but they have the advantage that only one image needs to be captured to provide all the information needed.

Step 2: Image segmentation

There is a broad range of techniques available for image segmentation (Pen *et al.*, 1985). Generally, more than one segmentation technique is required because different methods present different features in images. With high contrast images collected under well controlled lighting conditions, simply thresholding the intensity level of every pixel may be sufficient to segment out most of the possible defective points or clusters of points. In many cases, more complex methods are required. If the contrast is poor, edge-based techniques are frequently appropriate. The thresholds can be set manually or calculated from histogram analysis, global or local statistics, or other methods (Yang, 1992).

The operator chooses a grey threshold level which transforms the image into a binary representation. Once the digitising process is completed, thus providing a means of checking the similarity of the enhanced binary, a different threshold grey level is chosen until a close agreement exists between the two images (Yanuka and Elrick 1985).

Step 3: Image size measurement

After image thresholding, the image will be a black and white pixel image. By counting black or white pixels, the size of an object can be measured in pixels or converted to a IS system and put in suitable data file.

2.4.2 Application of machine vision system in agricultural science and fruit industry

Image processing and analysis in horticulture has gained significant momentum in the last few years due to the development of computerised systems which provide fast and easy means of processing complicated data. The availability of low cost imagery hardware has in part been responsible for the recent interest and development of video imagery systems. Video imagery systems are able to supplement or even replace human vision as a data gathering and data analysis tools. Image analysis techniques have been well developed and are applied in many areas of horticultural research and industry.

Applications of machine vision system cover a broad range of industrial and farming operations, including automated harvesting (Slaughter and Harrell, 1987) and inspection and grading of commodities (Rehkugler and Throop, 1986; Sarker and Wolfe, 1985). Interest is increasing in the development of machine vision systems to replace human visual inspection. Computer analysis of visual images (McDonald and Chen, 1990) is potentially of great importance in horticulture. Machine vision systems can be used for automatic machine operation in fruit industries and offers the potential to automate many manual grading practices. As microprocessor speeds continue to increase and costs decline, machine vision is likely to become a more cost effective solution for many inspection situations (Shearer and Payne, 1990).

Monochromatic systems

While studying the identification of mushroom cultivars using image analysis (Vooren *et al.*, 1991; 1992), Vooren *et al* (1992) concluded that it exhibited a significant improvement over previous methods which used only manual assessments of length, width, and a range of more or less complex shape descriptions to determine bean size (Vooren *et al.*, 1993).

Applications of machine vision systems have been employed in the sorting of many products, including sorting products by length, size (or projected area), and shape. Kassler *et al* (1993) investigated the use of machine vision to sort prawns by size and shape. They identified three key parameters. The parameter exhibiting the greatest potential was the "number of boundary points" or the parameter length of individual prawns. They also suggested the development of a qualitative shape standard by which prawns could be graded.

Machine vision system was also tested by Hodgson (1984) for kiwifruit grading. He separated the automatic inspection and grading of kiwifruit into three distinct tasks: non-contact size grading, shape defect detection, and area defect detection. In principle, non-contact size grading could be carried out by counting the number of small rectangles or picture elements covered by a fruit image and multiplying the number by a calibration factor. While this required a minimum of image processing followed by a simple count of occupied picture elements (or pixels in contrast). Size and shape defect detection required considerable more processing to be done.

Colour systems

In most colour sorters the measurements are often global or average readings and are obtained by integrating over the whole surface of a product (Yang, 1992). The use of colour in digital image processing systems increased the information constant of the image, and enabled the basic ideas of image analysis to incorporate chrominance, in addition to luminance. The judgement of colour and its faithful reproduction is an important concern in the commercial and industrial world (Gunasekaran *et al.*, 1987).

Sarkar and Wolfe (1985) investigated the application of image analysis and pattern recognition techniques for sorting tomatoes for colour surface scars. Boundary chain coding techniques were used to describe shape and size. An interference filter was used to enhance images for colour sorting by thresholding, and orientation was determined by analysing gradient intensity profiles. Their studies included developing a vision based inspection system for tomatoes.

Shearer and Payne (1990) investigated machine vision for sorting bell peppers by colour and defect. They concluded that the peppers could be sorted according to colour by mapping the red-green-blue (RGB) values to one of eight possible hues, and statistically classifying the frequency distributions. When this approach was applied to sorting with respect to damage it was found to be only marginally effective. Colour sorting of peppers use criteria which range from the pepper being too light a shade of green in colour to rejecting peppers exhibiting even the slightest hint of red. Pale green or light coloured peppers are generally caused by poor cultivation practices, while colour variations from a slight reddish cast to bright red are a direct result of senescence. In either case, Shearer and Payne (1990) suggested that a simple characterisation of the visual spectrum of light reflected from the pepper surface would provide sufficient information to support an accept reject decision.

Miller and Delwiche (1989) investigated computer vision as an alternative to manual sorting and grading for peaches. A laboratory system for acquiring colour images of peaches was developed and image analysis algorithms were used to compare peach colour to standard peach maturity colours. Their results suggested that machine maturity classification agreed with manual maturity classification in 54% of the test samples, and was within one colour standard in 88% of the tests. The correlation coefficient between machine and manual estimates of blush surface area was 0.92. The effect of cultivar on ground colour classification and blush measurement was significant. Overall system performance was comparable to manual capabilities of sorting and grading fresh market peaches.

Other applications in agriculture and horticulture

Machine vision systems have been also applied in many applications in agriculture. In plant science, applications range from assessing leaf areas (Storlie *et al.*, 1989), and root lengths (Kokko *et al.*, 1993), to map area measurement and photoanalysis (McDonald and Chen, 1990). The system has been used to evaluate seed coat and cotyledon cracks in soybeans (Gunasekaran *et al.*, 1987; 1988). They found that white light in the front-lighting mode with a black background for the soybeans was the best condition for acquiring video images of soybeans suitable for subsequent processing. Crack detection was most successful when seeds were positioned carefully such that the cracked region of the soybean end was viewed directly by the camera. Using the algorithms developed, 96% of the soybeans with seed coat cracks and 100% of the soybeans with cotyledon cracks were correctly detected from the samples tested.

In soil science, machine vision systems have been successfully applied in the measurement of the physical properties of soil (McBratney *et al.*, 1992; Volkmar, 1993; Koppi *et al.*, 1994). The significance of image analysis for quantifying the porosity of soils and the ratio between pore space area to total area has been discussed by Yanuka and Elrick (1985). Morrison and Chichester (1991) also described a similar machine vision system for determining percentage residue cover on soil.

Image analysis has also been used to measure the dimensions of pigs, from which pig weight and growth rate can be estimated (Minagawa *et al.*, 1993; Schofield, 1993). In a study by Minagawa *et al* (1993), mean central projective image area of the pigs was calculated and related to their live weight. An exponential relationship between the mean central projective image area and the weight was obtained with a standard error of $\pm$ 2.4 kg (54 pigs, from 7 kg to 105 kg).

2.4.3 Application of machine vision systems in apple bruise detection and measurement

Since the physical and chemical properties of tissues in bruised area and unbruised areas of apples are different (Samim and Banks, 1993a), machine vision systems can be applied in apple bruise detection (Davenal *et al.*, 1988). Various techniques for distinguishing bruised from unbruised regions on apples have been reported. The level of x-ray energy transmitted through bruised apple tissue is less than through unbruised apple tissue (Diner *et al.*, 1970). On unpeeled fruit, for large bruises (> 200 mm^2), the bruised area has lower reflectance than the unbruised area, and thus can be characterised by dark pixels upon digitisation. The bruise area can then be determined by counting the number of dark pixels. However, this can be difficult if the bruise is small, or if the apple has a striped or variable colour.

The reflectance of apple flesh, both bruised and unbruised, using visible and infrared light sources has been examined by Upchurch *et al* (1993). The results showed that there was a significant difference between bruised and unbruised flesh. Using an image processing algorithm, the bruised part of the apple could be distinguished from unbruised flesh in principle. Collett *et al* (1991) used machine vision systems to measure both parameters rather than manual measurement to calculate bruise volume. This study showed the potential possibilities of machine vision systems to measure bruises on the cut surface of apples. Upchurch *et al* (1993) investigated influence of time and bruise-type on near-infrared reflectance for automatic bruise detection. Throop *et al* (1993) developed an algorithm to process both old and new bruises from near-infrared reflectance images of stored Red Delicious apples.

Rehkugler and Throop (1986) developed an apple handling and sorting device using machine vision for bruise detection and classification into USDA grades which was based on bruise surface area measurement. The machine vision system provided a means for obtaining a digital image of an apple with a video camera, and then analysed the images to obtain information for making classification decisions about the apple. Grey level response to bruised tissue was represented by reduced image intensity. They used a rotating cone and wheel mechanism to orientate the fruit with the stem-calyx axis in the vertical direction. The fruit was rotated 360 degrees on a vertical axis and viewed by a 64 pixel line scan camera. The digital image captured by the camera and computer represented most of the surface of the apple. In their study, bruise areas on apples were predicted and compared with measured bruise areas with a correlation ranging from 0.63 to 0.84. Grade classification errors were presented as a comparison of the accuracy of grade predictions for the total quantity of fruit graded and on a grade-by-grade analysis of the errors in misclassification. A strong correlation between bruise depth and measured bruise surface area was found. They concluded that the current algorithm and system for bruise detection appeared to be equal to the accuracy of current manual bruise detection techniques for the selected verities of apples.

Rehkugler and Throop (1989) used a line scan camera of near-infrared reflectance from an apple surface for bruised tissue detection. The image data was thresholded to separate possible bruise tissue from the rest of the apple tissue in the image. Bruise area could be discriminated in the line scan image by the lower grey level of these areas in the unprocessed image. From this information, the amount of bruise area in the fruit could be determined, and the fruit graded. They concluded that the application of computer vision enabled bruise area prediction with correlation coefficients of 0.64 to 0.73 in comparison to a human inspector.

Taylor *et al* (1984) reported on the use of line scan cameras for detecting apple bruises. They concluded that apple bruise detection using digital imaging techniques was as accurate as human graders, and that the line scan camera seemed more promising for implementation in real time. They developed an automated system for detection of apple bruises based on the previous line scan camera work. Despite the apparent successes of these system, no commercial bruise detection device using image analysis has been produced. This suggests that the determination of bruise area by image analysis in uncut fruit is still a challenging problem.

Throop *et al* (1989) used computer vision for watercore detection by apple weight density and by apple light transmission. While an apple weight density algorithm correctly separated 86.7% of a 60-apple test sample with 5.0% misclassified as being watercore free, use of computer vision approximation has been shown to be a good method to define apple volume: a light transmittance algorithm correctly classified watercore presence in 100% of the 60-apple test sample. This technique proved to be more accurate and was an easily applied detection method requiring little computation. However, it was not possible to distinguish the degree of watercore damage. The economic value of misclassified fruit may determine the viability of using these sorting methods.

Foster *et al* (1991) described and reported the development of an algorithm to detect the presence of apple stem end splits which may be suitable for use in automatic inspection systems. The location of the stem end split and the difficulties of providing adequate illumination, together with the need to detect fine splits effectively camouflaged by the apple stripes, at image integration times of 500 microseconds, presented a serious challenge. The problem was overcome in principle, but the financial viability of the system was debateable.

2.5 Discussion and conclusions

Manual methods for bruise measurement involve determining the size of the bruise by human eye and assuming a geometric shape. This can be quite difficult and inaccurate at times, because the discolouration in apples may be relatively difficult to detect, and the shape of the bruised area and volume are often irregular. There could be considerable subjectivity in the values used to determine the size of the bruise. Therefore, more accurate and useful methods for determining bruise size are required for further study of apple bruising.

A survey of image analysis techniques has been completed. The principles, techniques, and validity for each application have been discussed. Most papers show that machine vision systems can be a powerful and intuitive means of examining shape. Its power lies in its ability to transform the structure of objects into simpler forms and then to enhance their interpretation. From a practical standpoint, the tools of image processing are easily implemented. Using a small set of fundamental programming operations, many diverse applications can be addressed, including shape recognition and textural analysis. Because of this flexibility, image processing has great potential in the field of apple bruise study. This thesis will now focus on one aspect which has not been examined in detail previously: ie, the use of image analysis to measure bruise volume and area in experiments where fruit is cut and sectioned to reveal bruised regions clearly.

CHAPTER 3

BRUISE VOLUME ESTIMATION BY CROSS-SECTIONAL MEASUREMENTS: A COMPARISON OF IMAGE ANALYSIS AND MANUAL METHODS

3.1 Introduction

Bruise volume parameters play a major role in the study of mechanical damage to fruit. In most research studies, the bruise volumes for apples have been calculated by measuring apple diameter, bruise width and bruise depth at the central cross-section of the bruise (Schoorl and Holt, 1980). By assuming a geometrical shape, the volume can be estimated. These three parameters are normally measured directly with vernier callipers. Bruise width and depth are the two main parameters required for the determination of apple bruise volume, and they vary with impact energy, drop height, and other impact conditions (Schoorl and Holt, 1980; Chen and Sun, 1981; Brown *et al.*, 1990; Pang and Studman, 1992).

This chapter describes experimental studies using a machine vision system to measure bruise depth and width from the central cross-section of a bruise.

3.2 Objectives

The purposes of the study were:

- To develop algorithms for bruise detection and measurement;

- To investigate image analysis for measurement of bruise width and depth from the central cross-sectional area of the bruise produced by impact against various objects.

- To compare bruise volume calculated from bruise width and depth measured by image analysis and manual methods.

- To test for variation of bruise parameters measured by image analysis with comparison of manual methods.

3.3 Experimental sample preparation

3.3.1 Fruit preparation

'Granny Smith' apples were used for this study. Experiments were conducted on both stored and fresh apples.

For stored fruit preparation, freshly picked 88 count 'Granny Smith' apples were selected at their commercial harvest date on 31 March 1994. They were graded over a standard grading table in a Hawke's Bay packing shed, placed into 88 count apple cartons and shifted to Massey University. They were held in cold storage at 1 ^{o}C until required. The experiments were conducted in October 1994 after the apples had been stored for 7 months. A sample of 80 apples was selected at random from fruit with no visible bruises. Apples were allowed to reach ambient temperature before testing. Apple diameter ranged from 72 - 80 mm.

The fresh apple experiment was carried out on the following season's apples. Freshly picked Count 88 'Granny Smith' apples were selected at their commercial harvest date on 1 May 1995 in Palmerston North. The experiments were conducted within 24 hours of picking. A sample of 60 apples with no visible bruises was selected at random from fruit collected for the study. Apple diameter ranged from 74 - 82 mm.

3.3.2 Bruising method

Bruises were produced in three ways: (1) by impacting apples onto a flat steel surface using a pendulum device; (2) by dropping a hockey ball onto apples; (3) by dropping a steel ball (having a relatively smaller curvature than the hockey ball) onto apples. Equipment used for producing bruises is illustrated in Figures 3.1, 3.2 and 3.3. These three devices have often been used for fruit bruising studies in the Department of Agricultural Engineering at Massey University (Pang, 1994; Mowatt and Banks, 1994). Three experiments were designed and conducted as follows.

<u>Experiment 1: Different bruise sizes obtained by the pendulum impact device</u>

Experiment 1 was designed to focus on comparison of the measurement of different bruise sizes by image analysis and manual measurement. Seventeen stored apples were impacted by the pendulum device (Figure 3.1). The diameters of the apples were recorded before bruising. Each apple had a hole through the centre along the calyx to stalk axis, which was produced by a cork borer 10 mm in diameter. This allowed the apple to be slipped onto the pendulum arm, and aligned with the impact point. This was arranged at the centre of percussion of the pendulum arm, at 500 mm from the pivot point. The apple was released from the select

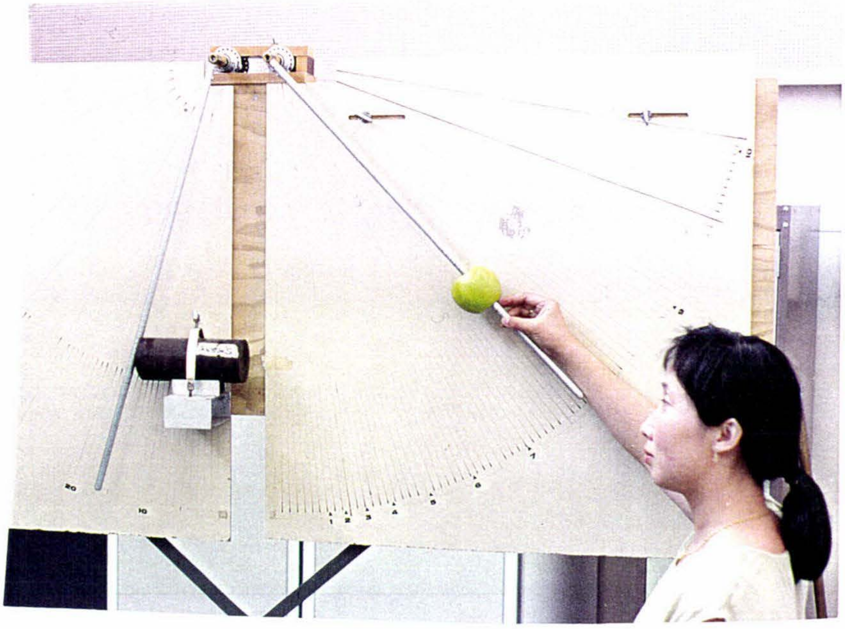

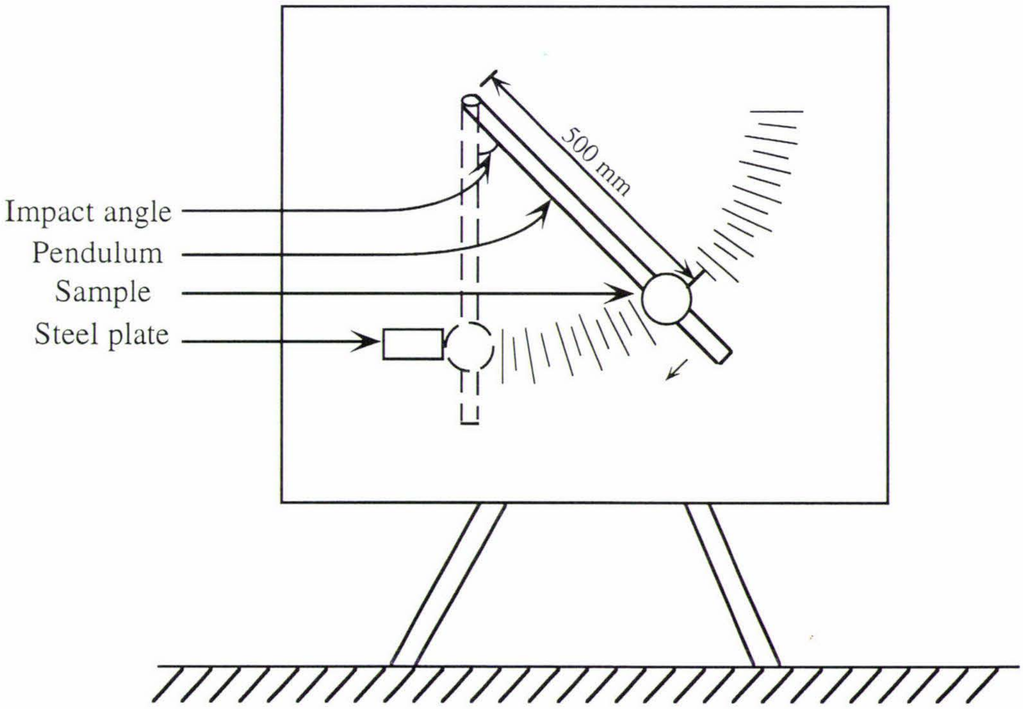

Figure 3.1 Pendulum impact device

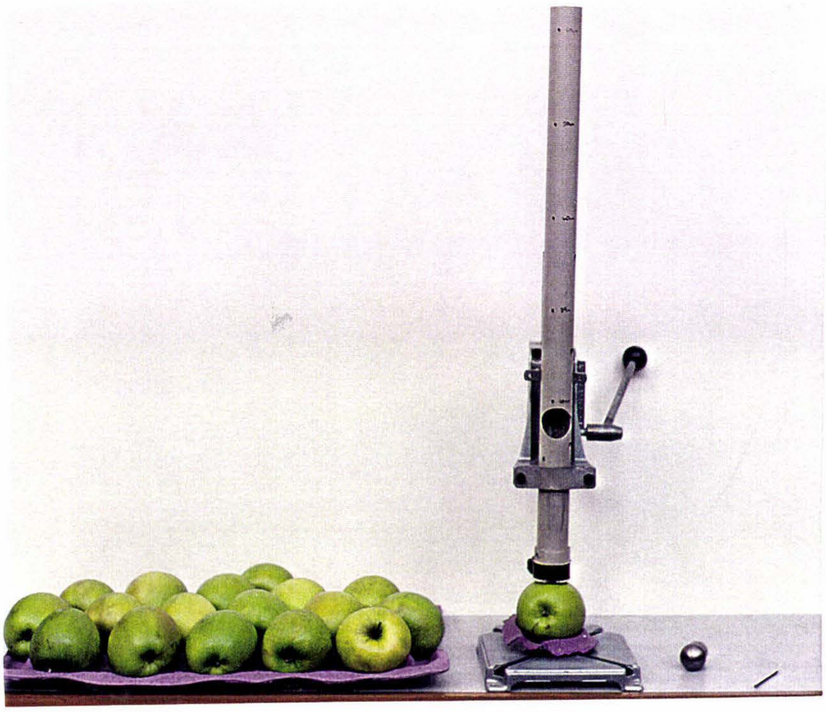

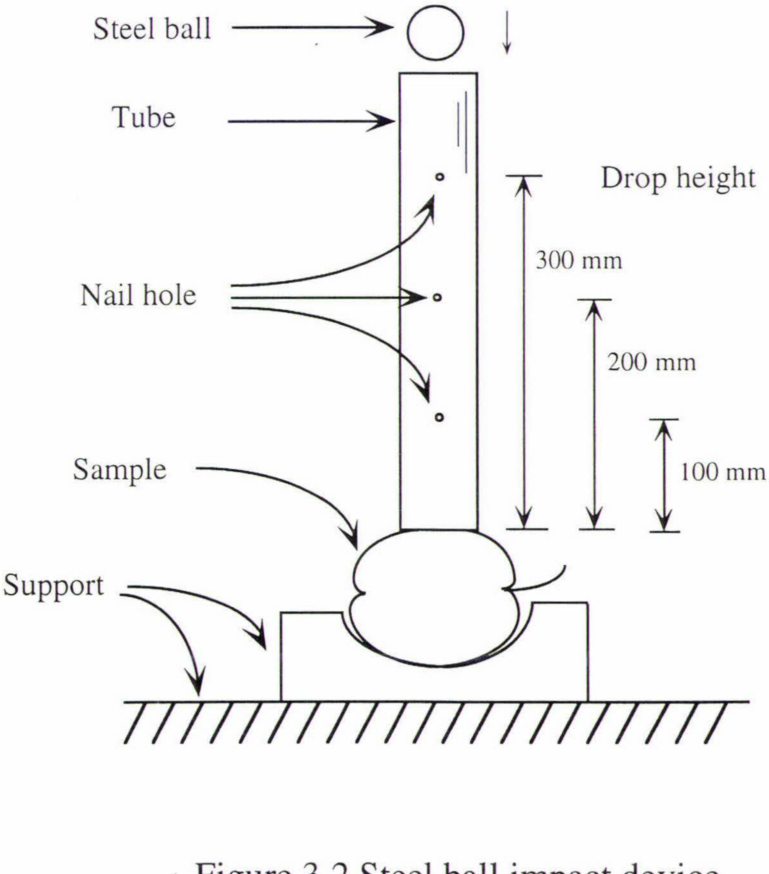

Figure 3.2 Steel ball impact device

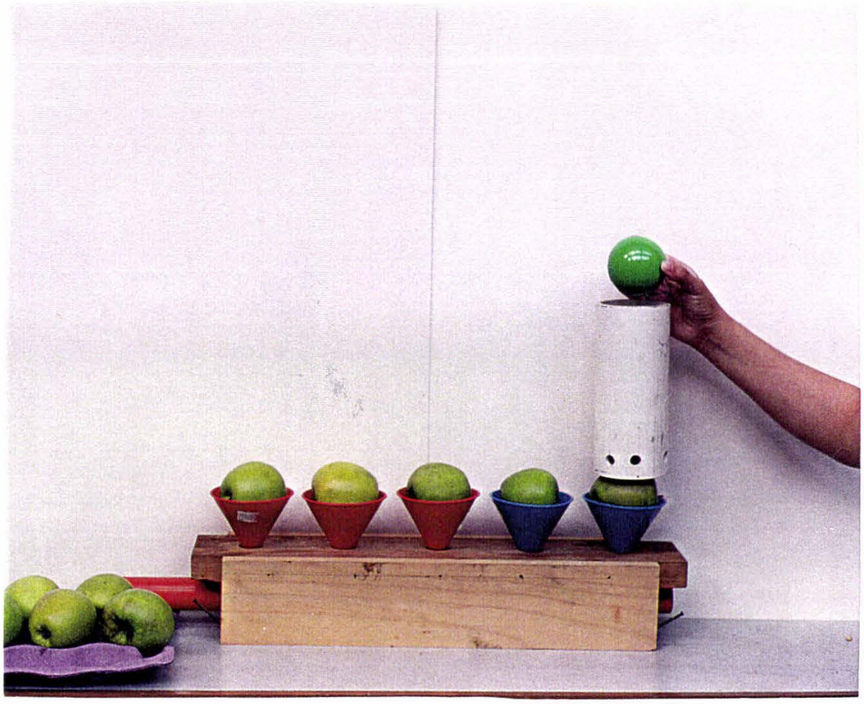

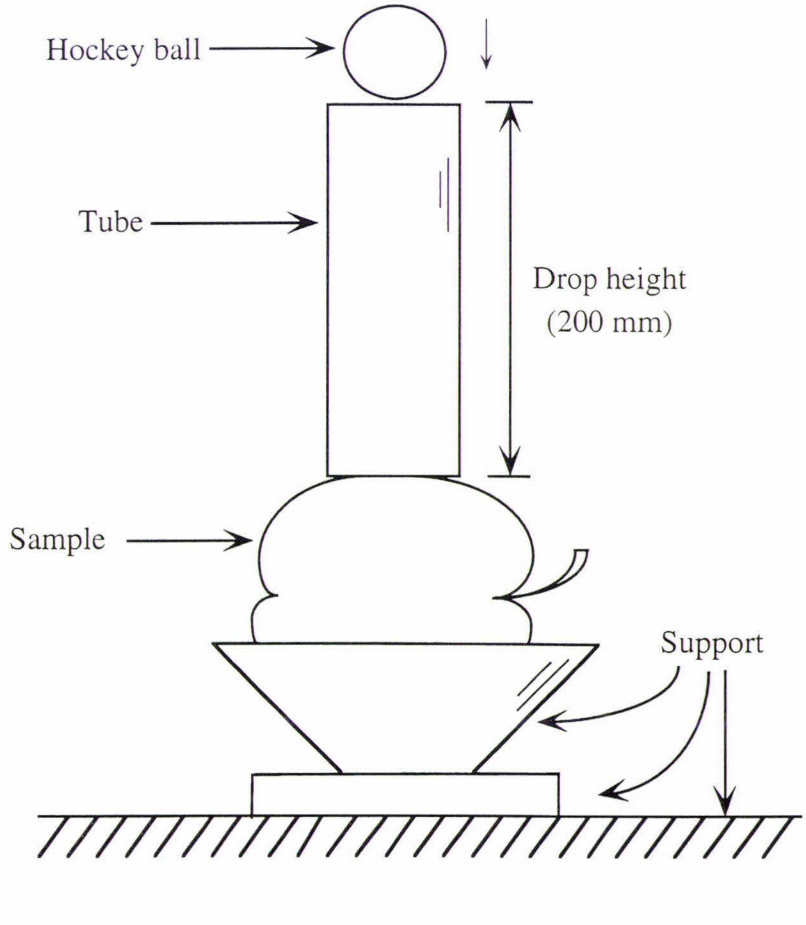

Figure 3.3 Hockey ball impact device

impact angle, and caught by hand after the first impact in order to avoid a second impact. The apple was then rotated 120° around the pendulum arm to another target position, and released from the next impact angle. Three impact angles were chosen to achieve 3 different sized bruises on each apple. The impact angles were 30, 45, and 60 degrees from vertical. The impact surface of the pendulum was marked by white powder. When apples were impacted onto it, the impact contact area on the apple would be marked by the powder. The area was then marked by a marker pen. It is important to do this, especially for small sized of bruises, since small bruises are not always visible with the skin on the apple later on.

Twenty fresh 'Granny Smith' apples were impacted by the pendulum technique at an angle of 60 degrees only. This allowed for comparison of image analysis with manual measurements.

Experiment 2: Fruit bruised by different sized balls

Experiment 2 was designed to investigate the possible effects of different impact curvatures on image analysis and manual measuring techniques. Two spheres of identical mass (158 g) were used for this experiment. Both were allowed to fall down a vertical tube from a stationary position 200 mm vertically above the apple surface (Figures 3.2 and 3.3). Each apple was subject to one impact from each sphere at two different points on its surface chosen so that they exhibited similar maturity in colour. The impact energies from the two types of sphere were identical (same mass and height), but impact curvatures were different as the steel ball had a radius of 14.54 mm and the hockey ball a radius of 35.65 mm. This experiment was carried out on 30 stored and 20 fresh apples. Each apple had two bruises, one from each ball.

Experiment 3: Measurement repeatability

Experiment 3 was carried out to test variation and accuracy of the image analysis system, and repeatability of bruise volume determined by both image analysis and the manual method. Three standard sized black circles which have been used as standard sizes for area measurement in the Image Analysis Unit at Massey University, were measured 20 times by the image analysis system. The diameters of the circles were 10 mm, 20 mm, and 30 mm.
Three apples were selected from the fresh apple sample and impacted by the steel ball from three different heights. The drop heights were 100, 200, and 300 mm. Each apple received one bruise. After allowing the bruises to develop for 24 hours, the apples were cut to reveal the bruise cross-sectional area. Width and depth of the bruise were measured by image analysis, and then the same bruises were measured by ten people. To prevent further browning after sectioning a thin layer of vaseline was used over the cut cross-section before the measurements were made. All the assessments were completed within 30 minutes of cutting the apples.

3.4 Bruise measurement

After impacting, bruises were allowed to discolour for 24 hours at room temperature before measurements were taken. Both the image analysis and the manual method for measuring the bruise size were conducted at the same time. After the diameter of the apple was measured by using an electronic vernier calliper, a cut was made through the centre of the bruised region in line with the flower to stalk axis. This exposed the central cross-section of the bruise. A typical image for measurement of bruise parameters from the centre cross-sectional area of the bruise is illustrated in Figure 3.4. Bruise volume was calculated using the formula given by

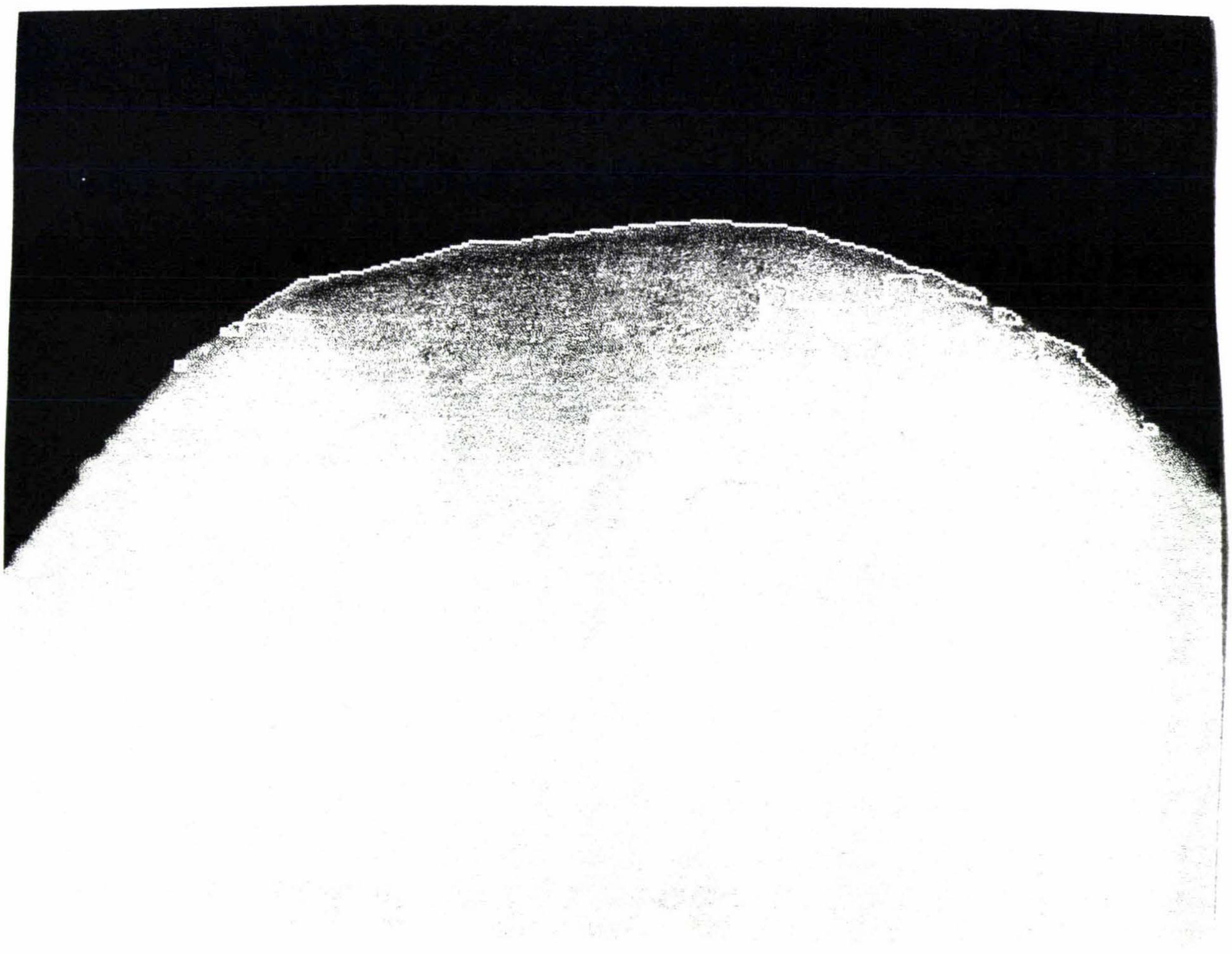

Figure 3.4 A typical bruise image for measurement of bruise parameters from the centre of cross-sectional area of the bruise

Schoorl and Holt (1980) (Equations 2.3 and 2.4). Bruise width and depth measured by both image analysis and manually were used for bruise volume estimation.

In the manual measurement method, bruise width and depth were measured directly by using an electronic vernier calliper, with judgement of the extent of bruise's central cross-sectional width and depth being made by human eye. In the image analysis, bruise width and depth were measured from the same cross-sectional area. The details of the image analysis will be further explained in the following sections.

3.4.1 Image analysis system

The machine vision system used for this study is illustrated in Figure 3.5. The system consisted of four main parts: Camera, Computer, lighting set, and system support. Associated equipment was required.

- **Part 1. Camera**: A CCD (charge-coupled device) colour camera (MODEL KP-C553E/K HITACHI) with cosmicar television lens (50 mm, 1:1.4 + 46 mm + 2) was used for getting the image information of apple bruises. The camera can provide matrix-array images.

- **Part 2. Computer**: A 486DX2/66 PC computer, with a 420 Megabyte hard disk, 16 MB of RAM, and equipped with VIPS software, was used. Both image display and processing can be done on this computer, one monitor being required. An image with 512 X 512 pixels from 0 to 256 grey level based on different intensity of colour of the bruise

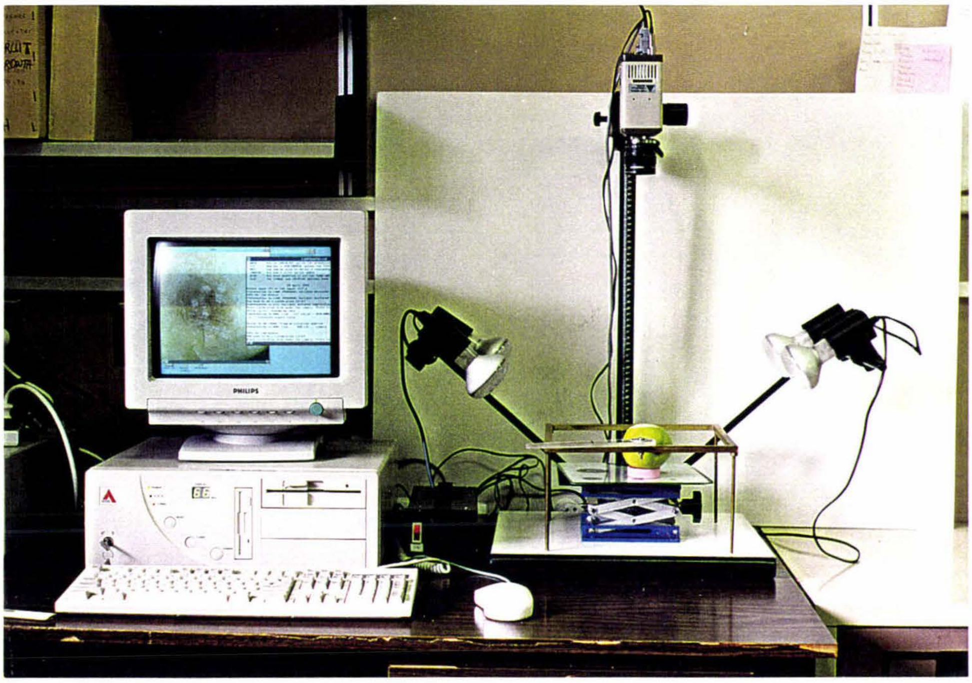

Figure 3.5 Machine vision system used in this study

- cells could be displayed on the screen. Algorithms were written with software package VIPS (Vision Image Processing System) version 4.1 (VIPS manual, 1992).

- **Part 3. Lighting set**: The equipment for lighting contained four 100 watt lamps, four 40 watt florescent lights, and a stand. The stand was used for supporting the four lamps and the camera. The four 40 W fluorescent tubes were fitted on the ceiling of the room. No other light sources were used in the experiment.

- **Part 4. System support**: The distance between apple bruise surface and camera lens should be the same for each individual bruise image captured. A device for adjusting the distance for each individual apple was used.

- **Associated equipment:** digital electronic vernier callipers, sharp knife, peeler, and board.

In order to make the system easy to operate and the results comparable for each bruise measurement, standard conditions were maintained for illumination of the system, position of the camera, position of the apple bruise surface, and the image processing algorithm.

3.4.2 Measurement procedure for image analysis

- **Lighting**: A standard lighting set up was used for image capture.

- **System calibration**: A system calibration was used to convert the data from image capture to real bruise size. It was necessary to calibrate the system with a particular measurement distance to the camera. Position of the apple bruise surface was adjusted to give a fixed distance between the surface and camera lens.

- **Sample placement**: By using a positioning device (Figure 3.5), the apple was kept at the same distance from the camera and the measuring area was kept parallel with the camera lens. The positioning device had a plexiglass flat plate at a fixed height, and was adjusted on the scissor stand to bring the surface to the correct height.

- **Image capture**: The image to be measured was displayed on the computer screen and recorded.

- **Image processing**: The image processing was automatically conducted by the software by running an algorithm. This process included image segmentation, image thresholding, area chain, and calculations.

- **Area selection**: The algorithm included a request to the operator to select the area to be measured. This was performed manually by pointing at the area with the mouse and pressing the Enter key. This was necessary to ensure the program began in the correct area.

- **Bruise measurement**: After selecting bruise area, the bruise width and bruise depth were measured. The VIPS command CHAIN RECTANGLE was used for the measurement of the bruise width and depth (Ref. VIPS manual pp. 54-55).

- **Data recording**: Data was saved automatically by the algorithm. The data file could then be transferred into a spreadsheet for further analysis later.

3.4.3 Algorithms

The key to image analysis work is to have a suitable algorithm. There is no standard algorithm for a particular measurement. However, there are many ways which can be used to make an algorithm solve one particular measurement. The suitable algorithm should:

- be able to carry out the measurement easily with minimal operator inputs;
- have accurate results;
- be readily repeatable.

The algorithm developed was based on the analysis of the grey levels on the profiles of the bruise image (Figures 3.6a and b). Two different types of bruise image came from the two different bruising methods. So, two algorithms were made for this study which are presented in Appendix 1. These algorithms were designed for different types of bruise measurement where cross-sectional areas differed with different impacts. Before the main experiments were carried out, experiments were conducted in order to develop the algorithm. About 100 bruises produced with the three bruise methods were tested by various versions of the algorithm before the main experiment was conducted.

3.4.4 Statistical analysis

The computer package Quattro Pro for windows version 5.0 was used for all data processing in this study. A Paired Two Sample Means test was used for a statistical comparison of bruise measurement using image analysis and manual measurement.

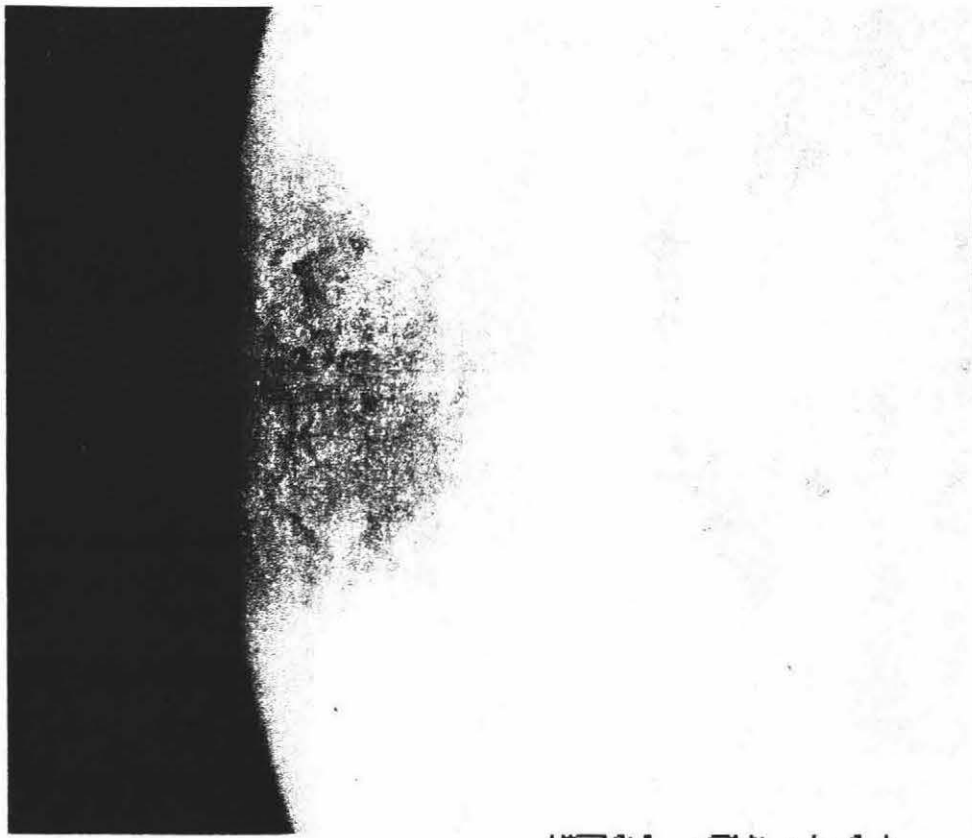

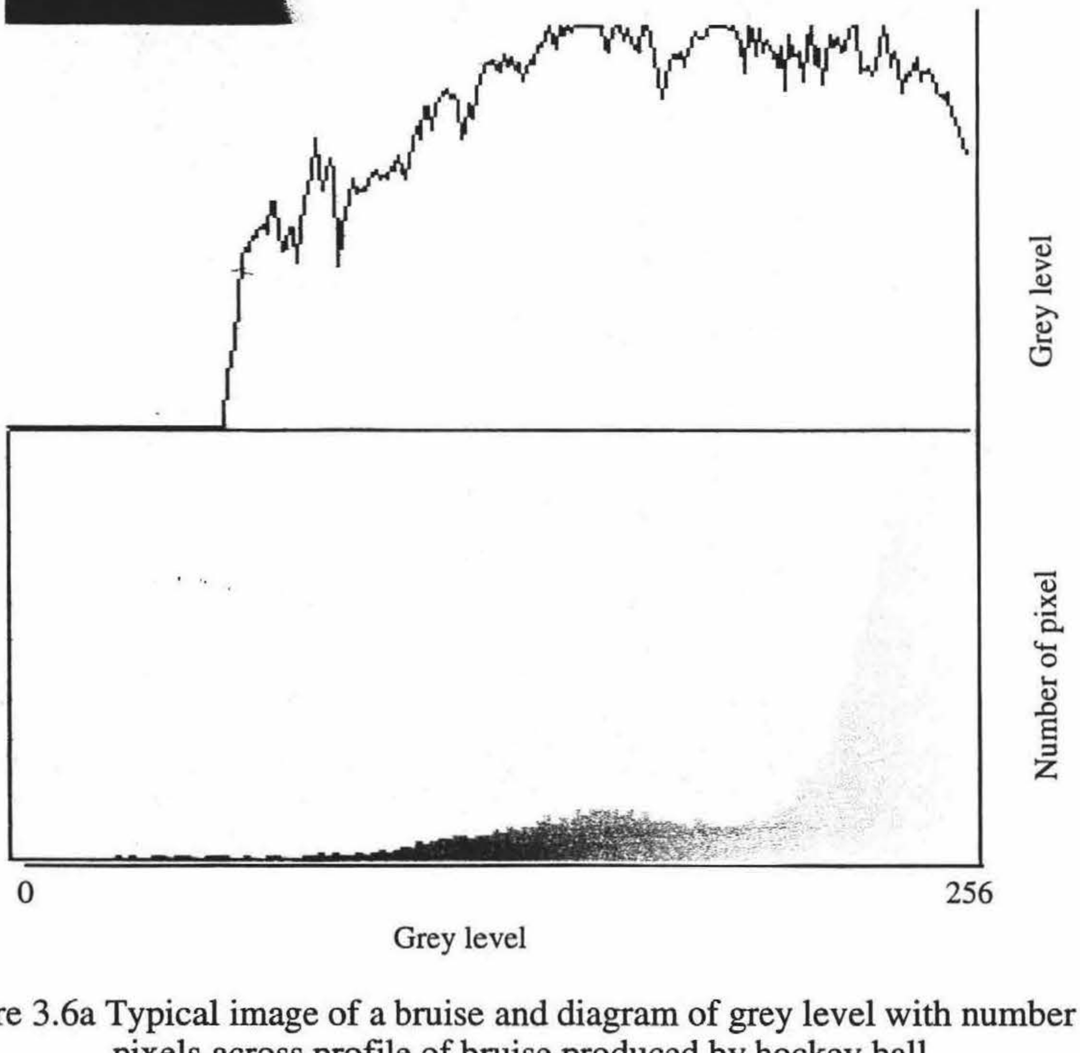

Figure 3.6a Typical image of a bruise and diagram of grey level with number pixels across profile of bruise produced by hockey ball

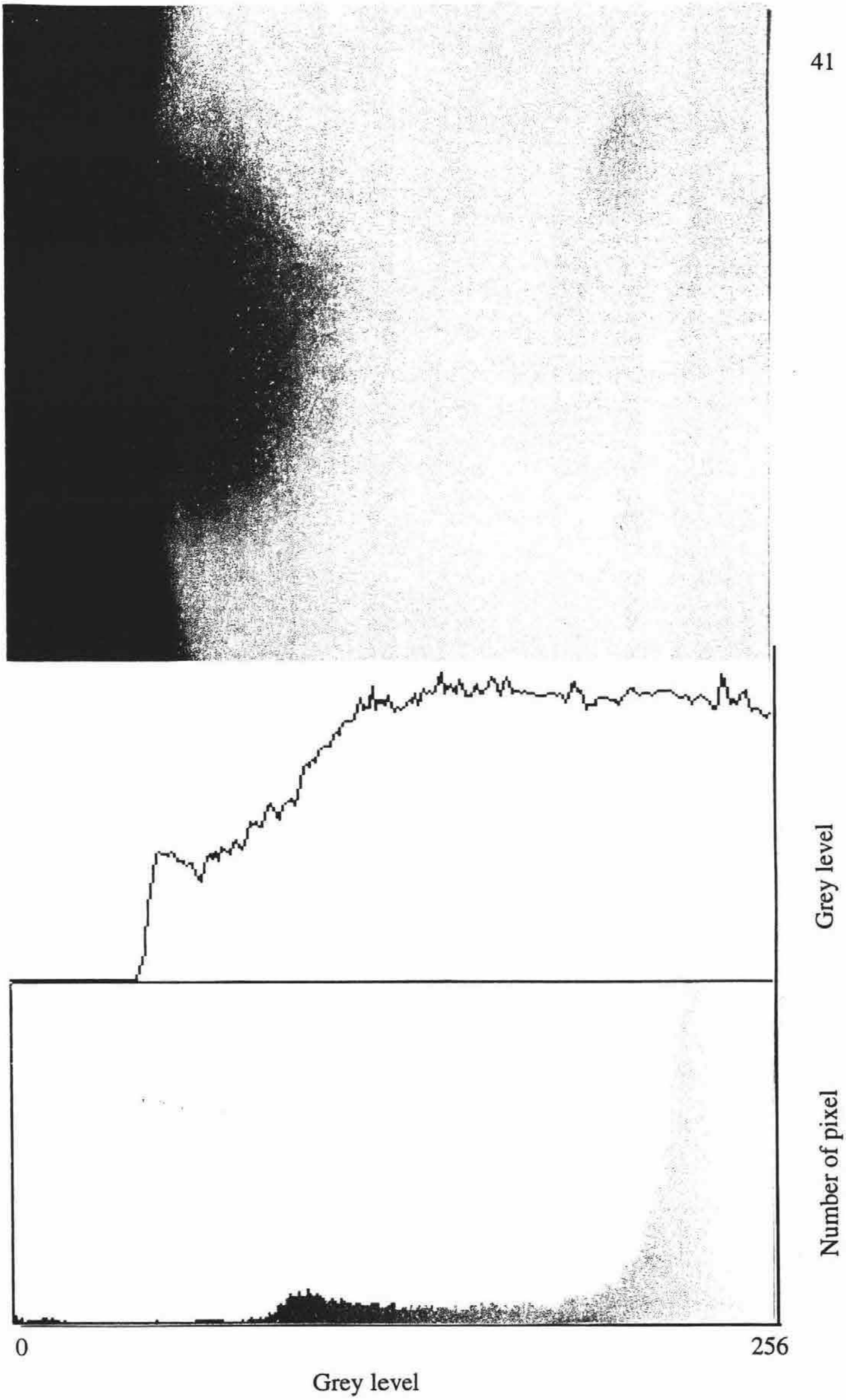

Figure 3.6b Typical image of a bruise and diagram of grey level with number pixels across profile of bruise produced by steel ball

3.5 Results

3.5.1 Experiment 1: Bruise produced by Pendulum impact

Different sizes of bruise were made due to different impact energies caused by the three impact angles. The results of bruise width, depth and volume determined by image analysis and the manual method for both the stored and fresh apples are summarised in Table 3.1. Details of individual bruise width, depth, and volume measurement by both image analysis and manually on the stored and fresh apples are shown in Figures 3.7a, b, and c, and 3.8a, b, and c. The regression coefficients (R^2) between bruise width, depth, and volumes, produced at different impact angles, measured by image analysis and manually were 0.93, 0.78 and 0.93, respectively (Figures 3.7a, b, and c). The means and standard deviations of the bruise width, depth and volume for the stored apples at different impact angles are shown in Figures 3.9a, b, and c.

The bruise width and depth measured by image analysis and manually were not significantly different ($p > 0.05$) either for the stored or fresh apples (Table 3.1). The differences in the mean bruise widths measured on the stored and fresh apples by both methods were less than 4%. The differences in the mean bruise depths measured by image analysis and the manual method were 13%, 7%, and 8% for the stored apples at 30, 45 and 60 degree impact angles, and 3% for the fresh apples at the 60 degree impact angle.

Bruise volumes were estimated from bruise width and depth by using Equations 2.3 and 2.4. Although there were variations in bruise volume for individual apples measured by image analysis and manually, there was no statistical difference in bruise volumes for all the three

Table 3.1 Pendulum impact, measured from cross-section of the bruise

Apple condition		Stored apples						Fresh apples	
Number of sample		17		17		17		20	
Impact angle (°)		30		45		60		60	
Measurement method		IA	MU	IA	MU	IA	MU	IA	MU
Bruise width (mm)	Min . value	6.79	9.14	16.57	16.49	19.61	18.93	24.18	24.27
	Max. value	18.74	17.78	29.05	27.31	34.69	31.98	32.77	30.41
	Mean value	13.50	13.82	19.89	19.92	23.65	23.28	29.19	27.96
	Comparison	p = 0.44		p = 0.94		p = 0.25		p = 0.08	
Bruise depth (mm)	Min . value	2.86	2.89	4.43	4.60	5.99	5.86	6.14	6.96
	Max. value	7.52	6.10	8.33	8.11	8.85	9.43	9.20	8.92
	Mean value	4.47	4.77	6.24	6.40	7.38	7.57	7.90	8.13
	Comparison	p = 0.10		p = 0.36		p = 0.10		p = 0.34	
Bruise volume (mm^3)	Min . value	86.78	133.7	718.85	931.11	1212.60	1099.45	2570.61	2246.05
	Max. value	1285.20	1003.9	2570.42	2335.49	5439.42	4473.80	5636.59	4446.79
	Mean value	486.45	516.95	1379.64	1443.42	2334.56	2345.87	3928.46	3615.27
	Comparison	p = 0.28		p = 0.32		p = 0.89		p = 0.30	

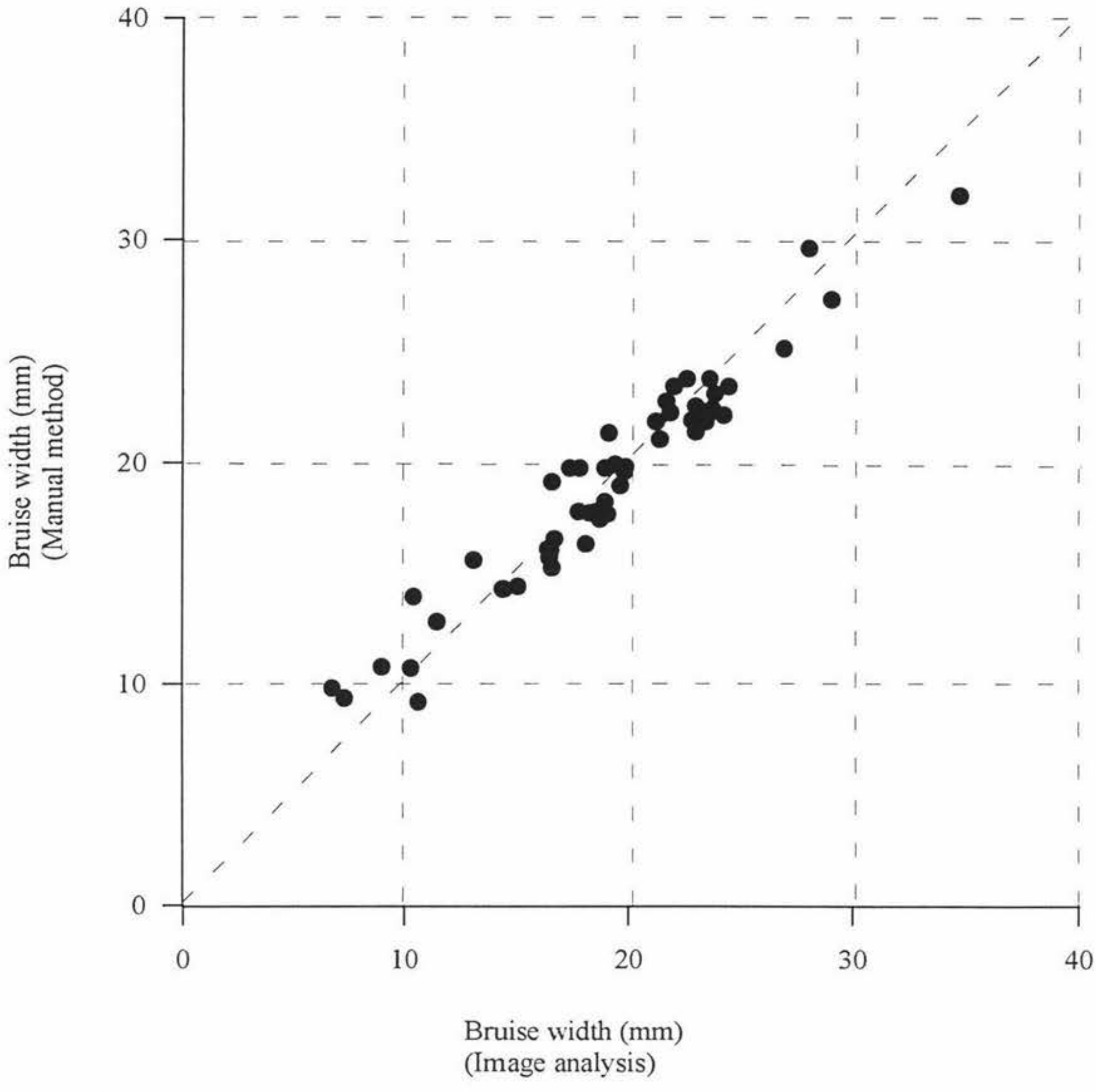

Figure 3.7a The relationship between bruise widths measured by image analysis and the manual method for bruises produced by the pendulum on stored apples.

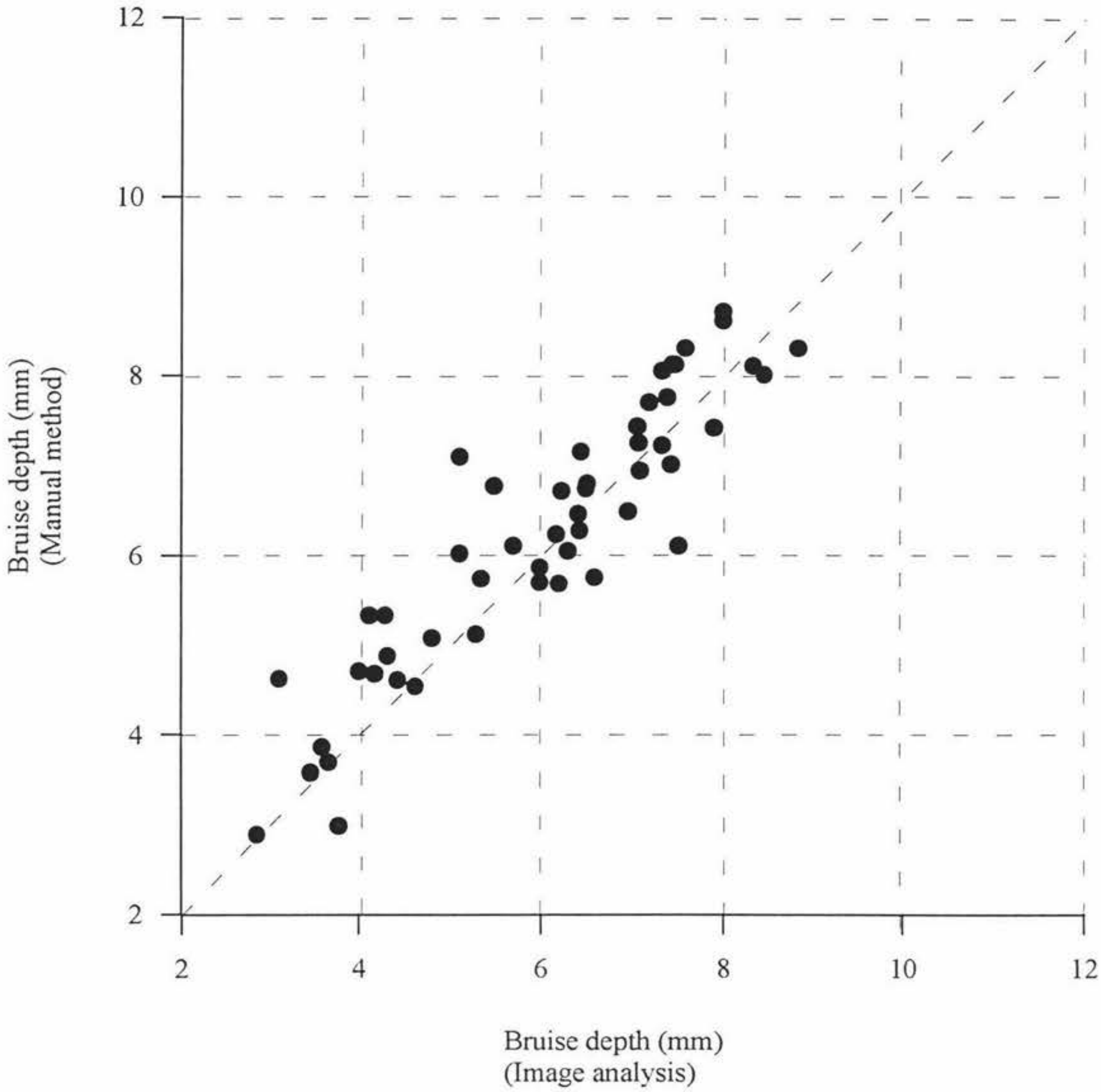

Figure 3.7b The relationship between bruise depths measured by image analysis and the manual method for bruises produced by the pendulum on stored apples.

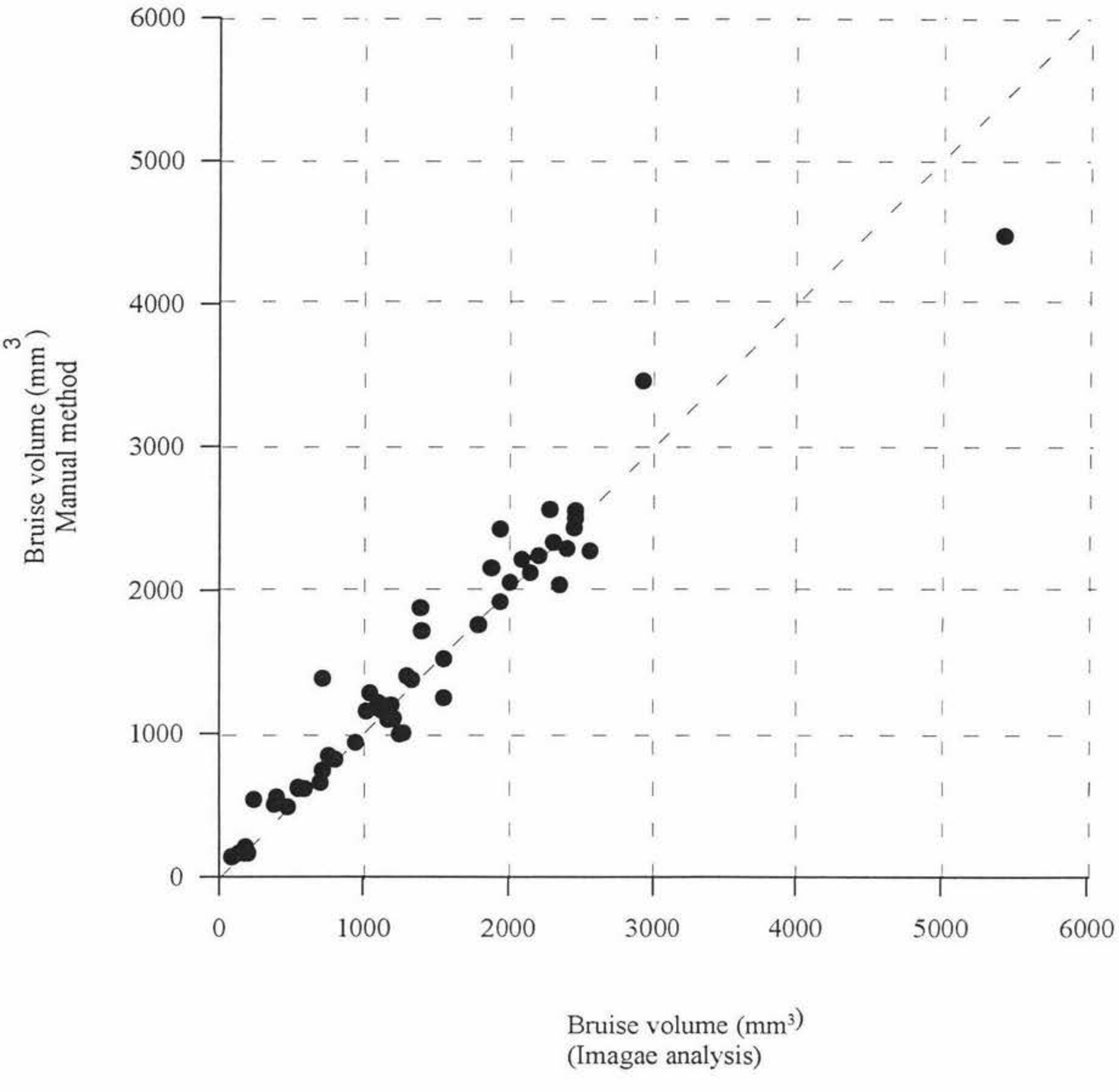

Figure 3.7c The relationship between bruise volumes measured by image analysis and the manual method for bruises produced by the pendulum on stored apples.

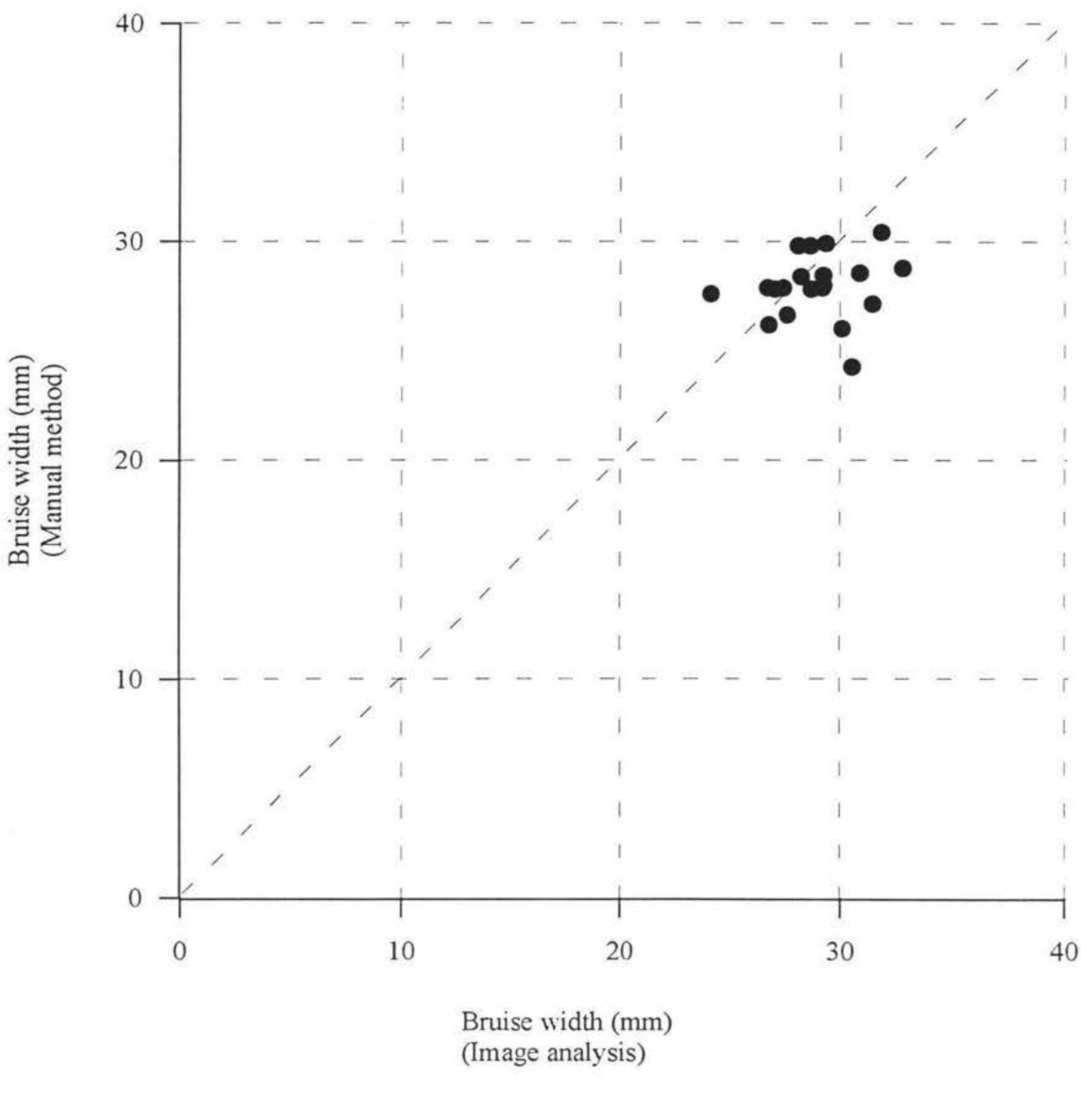

Figure 3.8a The relationship between bruise widths measured by image analysis and the manual method for bruises produced by the pendulum on the fresh apples.

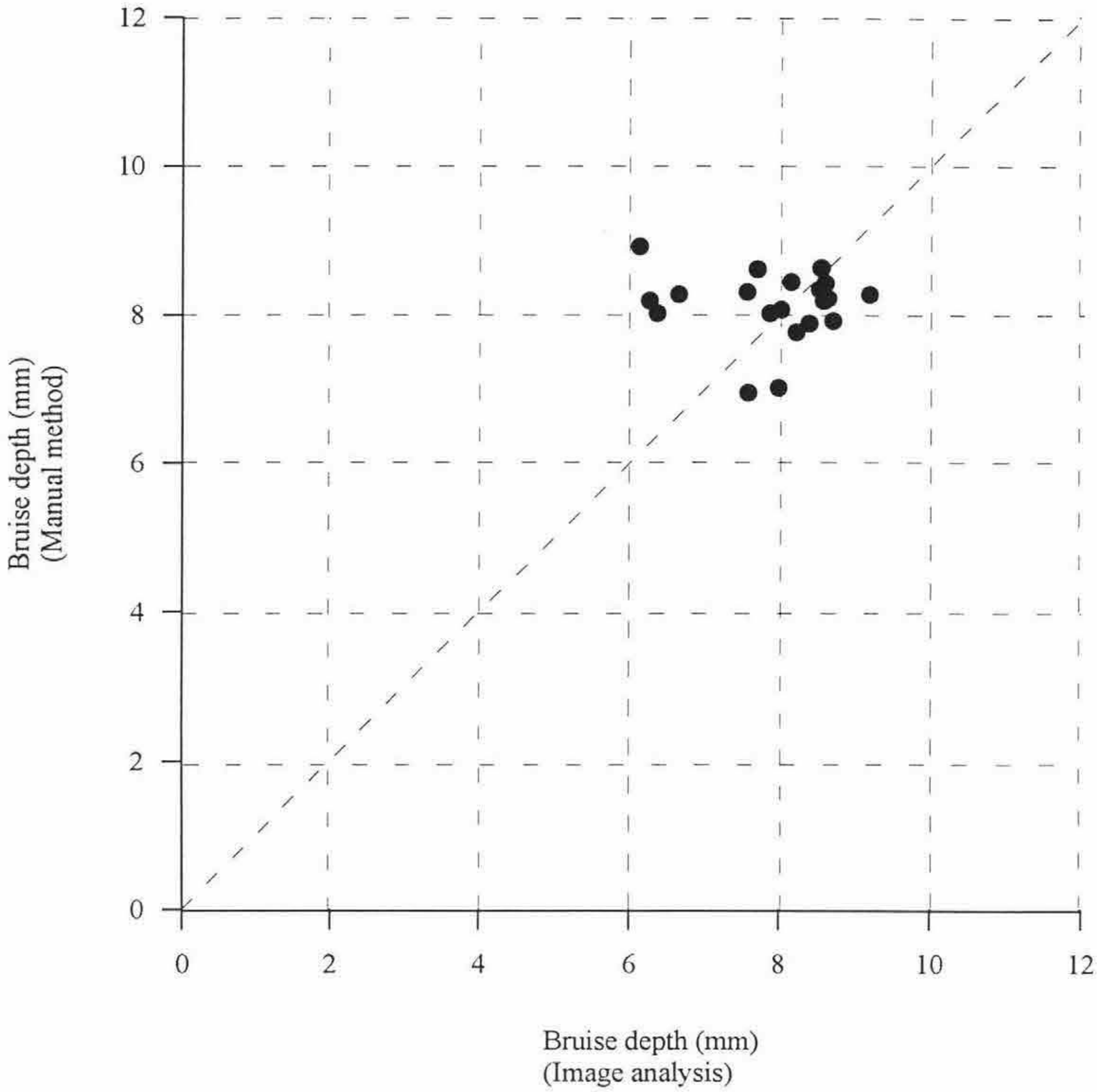

Figure 3.8b The relationship between bruise depths measured by image analysis and the manual method for bruises produced by the pendulum on fresh apples.

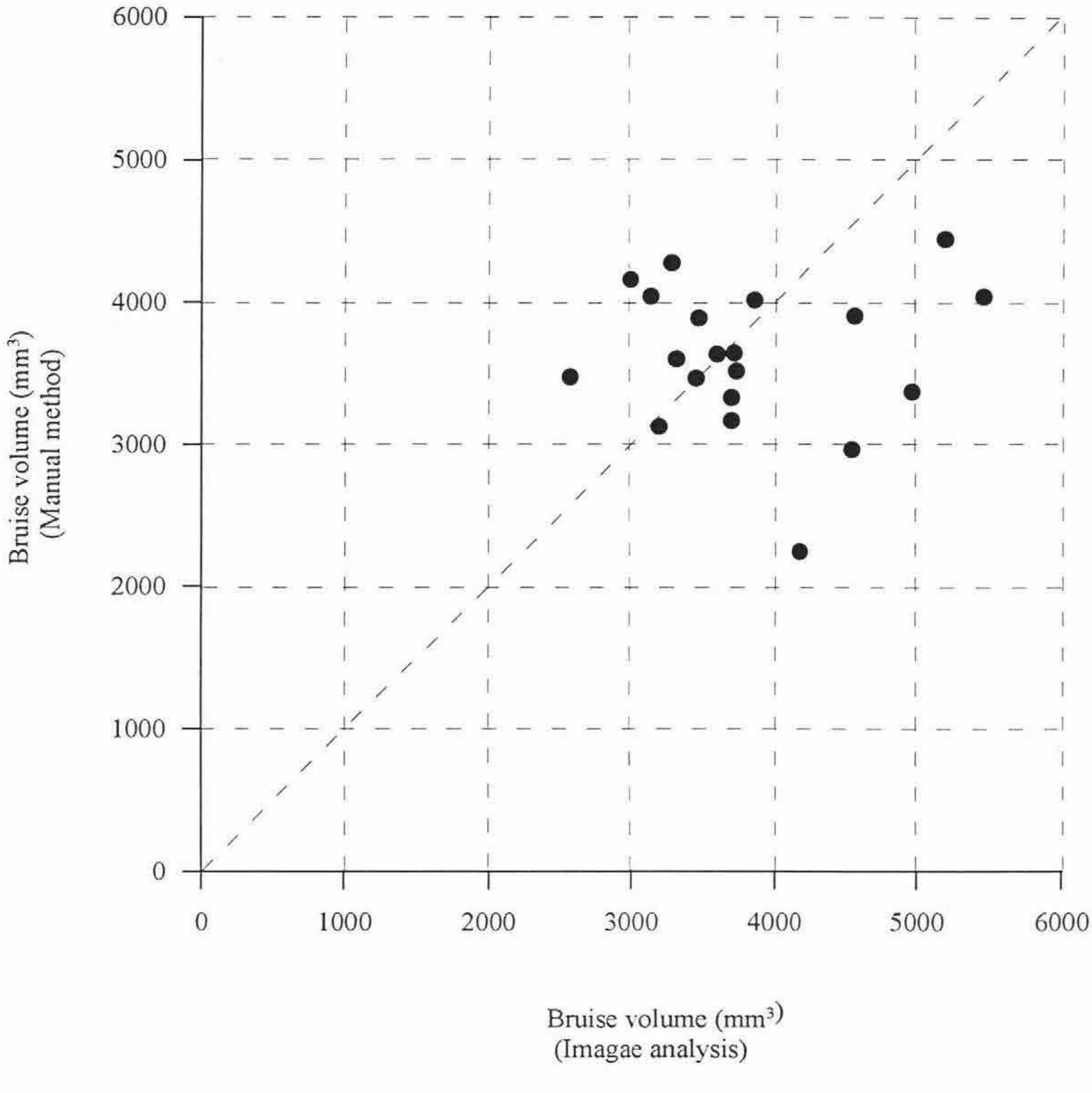

Figure 3.8c The relationship between bruise volumes measured by image analysis and the manual method for bruises produced by the pendulum on fresh apples.

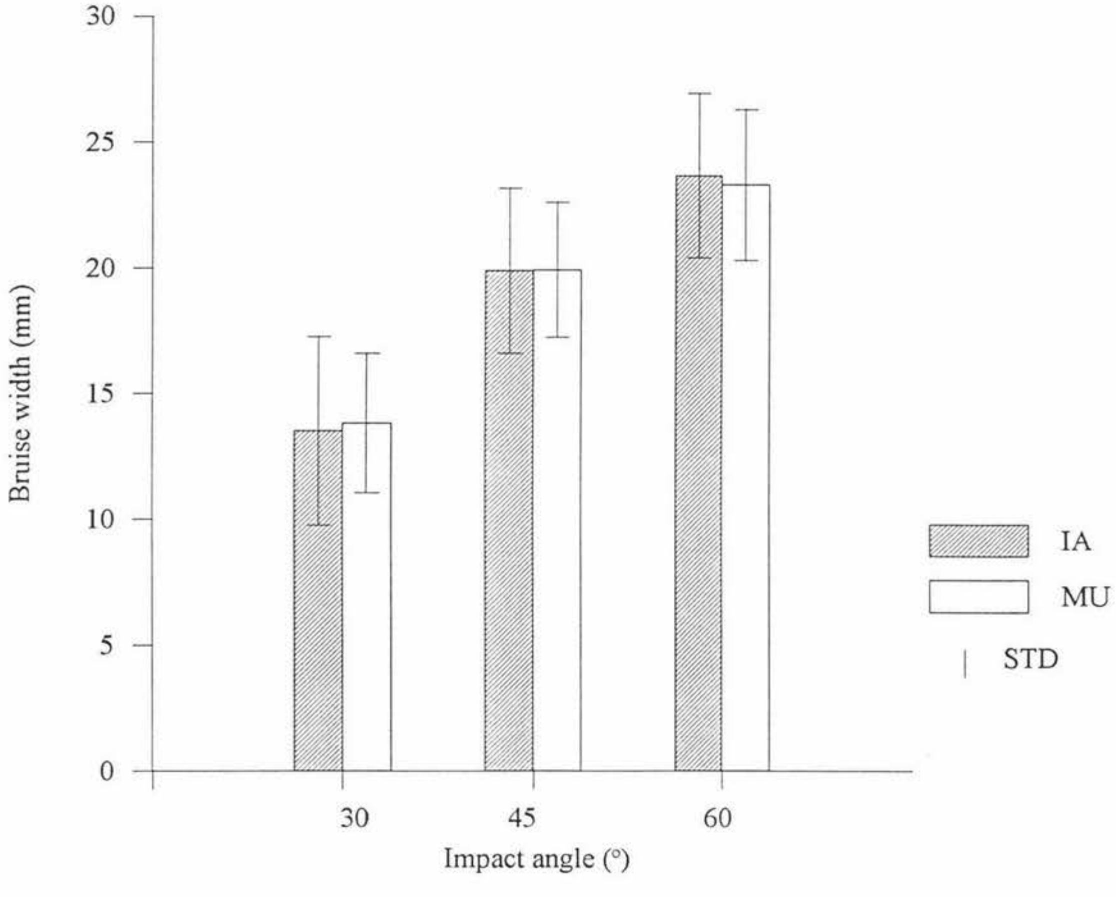

Figure 3.9a Measured bruise widths on stored apples produced by Pendulum

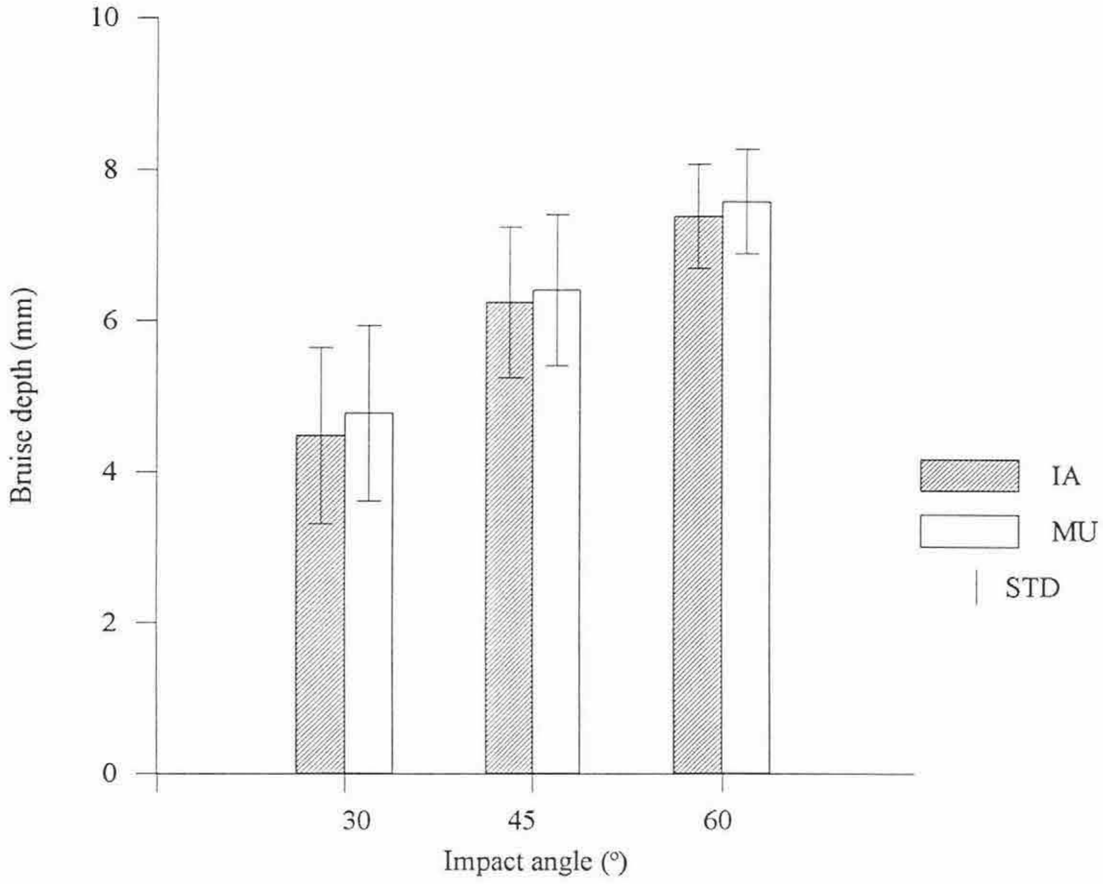

Figure 3.9b Measured bruise depths on stored apples produced by Pendulum

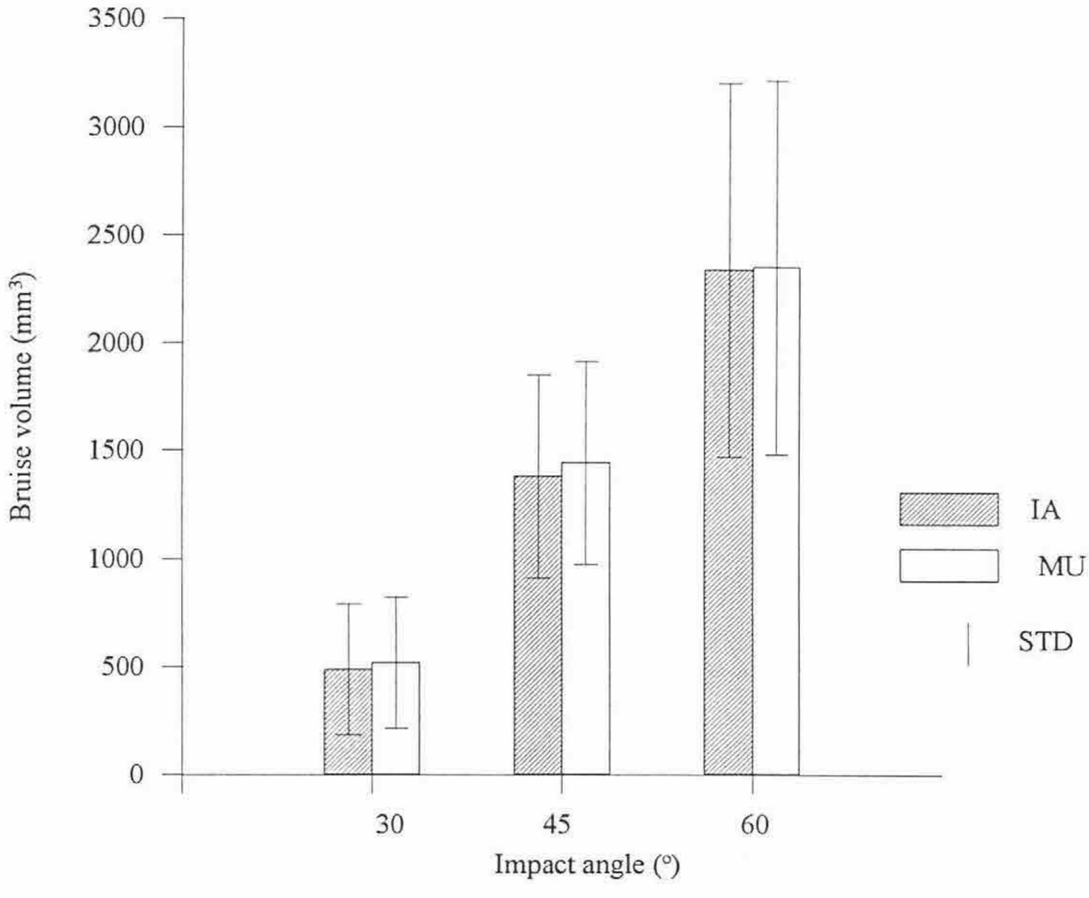

Figure 3.9c Measured bruise volumes on stored apples produced by Pendulum

impact angles for both stored and fresh apples ($p > 0.05$) (Table 3.1). The difference in the mean bruise volumes measured by image analysis and manually were 10%, 6%, and 3% for the stored apples at 30, 45, and 60 degree impact angles, and 6% at the 60 degree impact angle for fresh apples. The differences in bruise volume at the three impact angles were obviously due to the differing impact energies. With respect to bruising in individual apples, there was always a good linear relationship by both methods regardless of impact angle and apple storage time (Figures 3.7c and 3.8c). The data for each bruise volume estimated by image analysis and the manual method are attached in Appendix 2.

3.5.2 Experiment 2: Steel ball and hockey ball impact

Bruise images between the bruises produced by the two balls at the same impact energy were quite different. Because the image of the bruise produced by the steel ball impact was darker than that produced by hockey ball (Figures 3.6a and b), image segmentation, image thresholding, and area chain code should be different for the bruises produced by the two balls. Therefore different algorithms were used for each type of ball impact.

The results of bruise widths, depths, and volumes measured by image analysis and manually for stored and fresh apples are summarised in Tables 3.2 and 3.3. The means and standard deviations of the bruise width, depth and volume from the bruises produced by both balls measured by using the two measuring methods for stored and fresh apples are shown in Figures 3.10a, b, and c; and 3.11a, b, and c.

Table 3.2 Steel ball impact, measured from cross-section of the bruise

Apple condition		Stored apples		Fresh apples	
Number of bruise		30		20	
Measurement method		IA	MU	IA	MU
Bruise width (mm)	Min. value	13.18	14.43	15.95	15.61
	Max. value	19.63	17.58	22.34	19.88
	Mean value	16.89	16.59	19.02	17.84
	Comparison	p = 0.39		p = 0.18	
Bruise depth (mm)	Min. value	6.01	6.49	6.25	7..57
	Max. value	8.57	8.03	9.53	9.04
	Mean value	7.37	7.29	8.09	8.29
	Comparison	p = 0.29		p = 0.32	
Bruise volume (mm^3)	Min. value	572.96	757.96	881.56	1084.29
	Max. value	1773.56	1275.13	2342.59	1834.87
	Mean value	1166.26	1094.94	1633.89	1474.93
	Comparison	p = 0.24		p = 0.11	

Table 3.3 Hockey ball impact, measured from cross-section of the bruise

Apple condition		Stored apples		Fresh apples	
Number of bruise		30		20	
Measurement method		IA	MU	IA	MU
Bruise width (mm)	Min. value	14.35	15.92	18.48	17.98
	Max. value	22.54	20.45	24.83	23.97
	Mean value	18.26	18.00	20.89	19.81
	Comparison	p = 0.59		p = 0.86	
Bruise depth (mm)	Min. value	4.68	5.43	5.97	5.93
	Max. value	8.11	7.46	8.85	8.73
	Mean value	6.34	6.55	7.12	7.15
	Comparison	p = 0.25		p = 0.87	
Bruise volume (mm^3)	Min. value	487.32	780.12	1082.95	997.79
	Max. value	1942.42	1589.65	3024.96	2750.81
	Mean value	1156.19	1127.22	1707.88	1523.56
	Comparison	p = 0.74		p = 0.96	

The results showed that there were no significant differences between the two measuring systems studied when determining the bruise parameters and volume, irrespective of the freshness of the fruit or the method of fruit production (Tables 3.2 and 3.3).

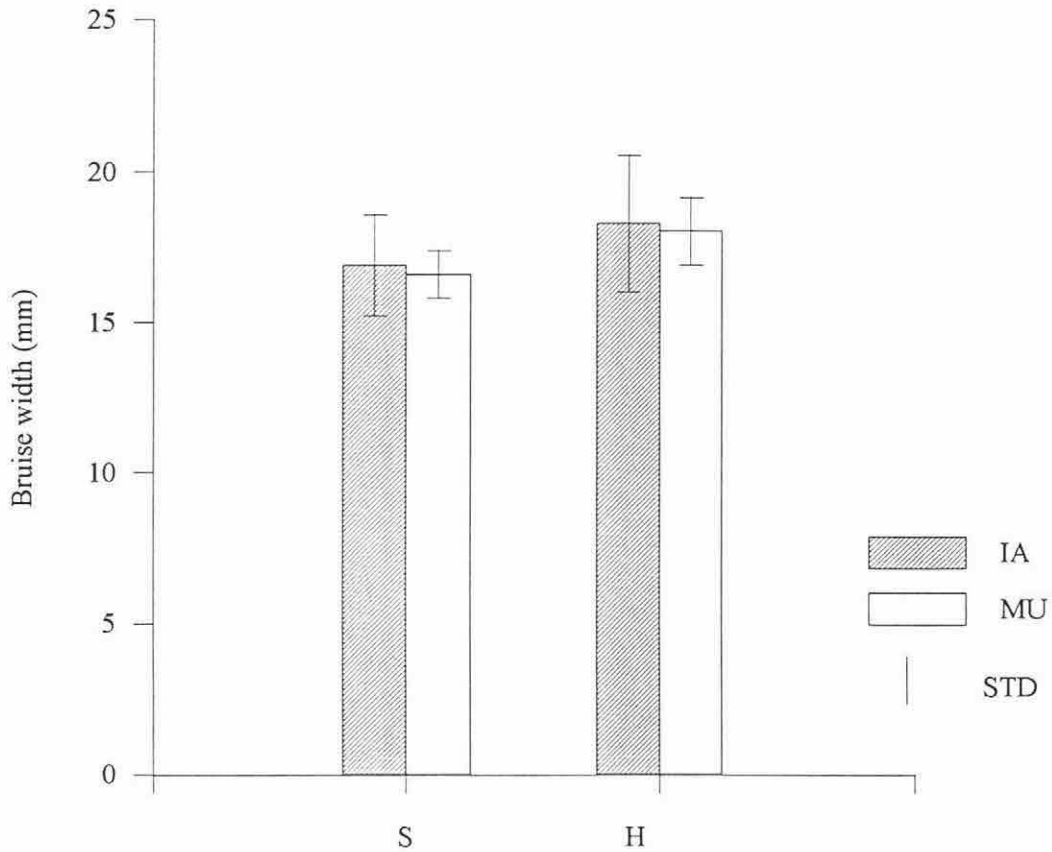

Figure 3.10a Measured bruise widths on stored apples produced by Steel ball (S) and Hockey ball (H) impacts

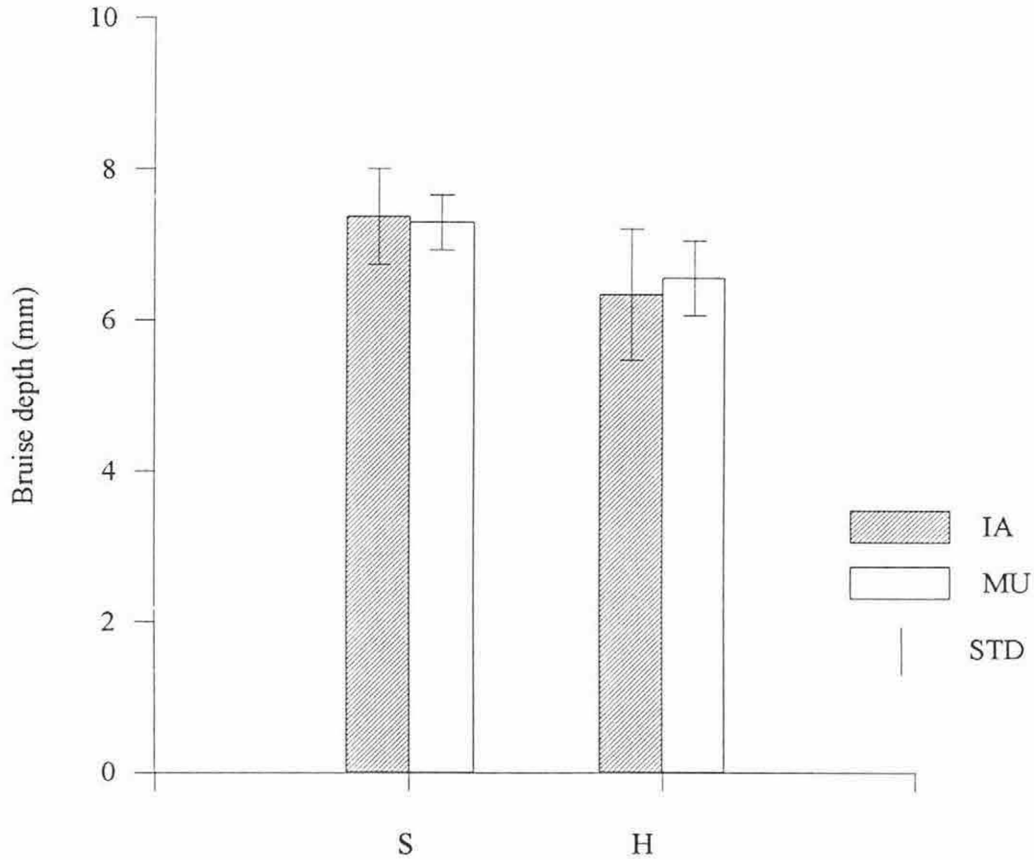

Figure 3.10b Measured bruise depths on stored apples produced by Steel ball (S) and Hockey ball (H)

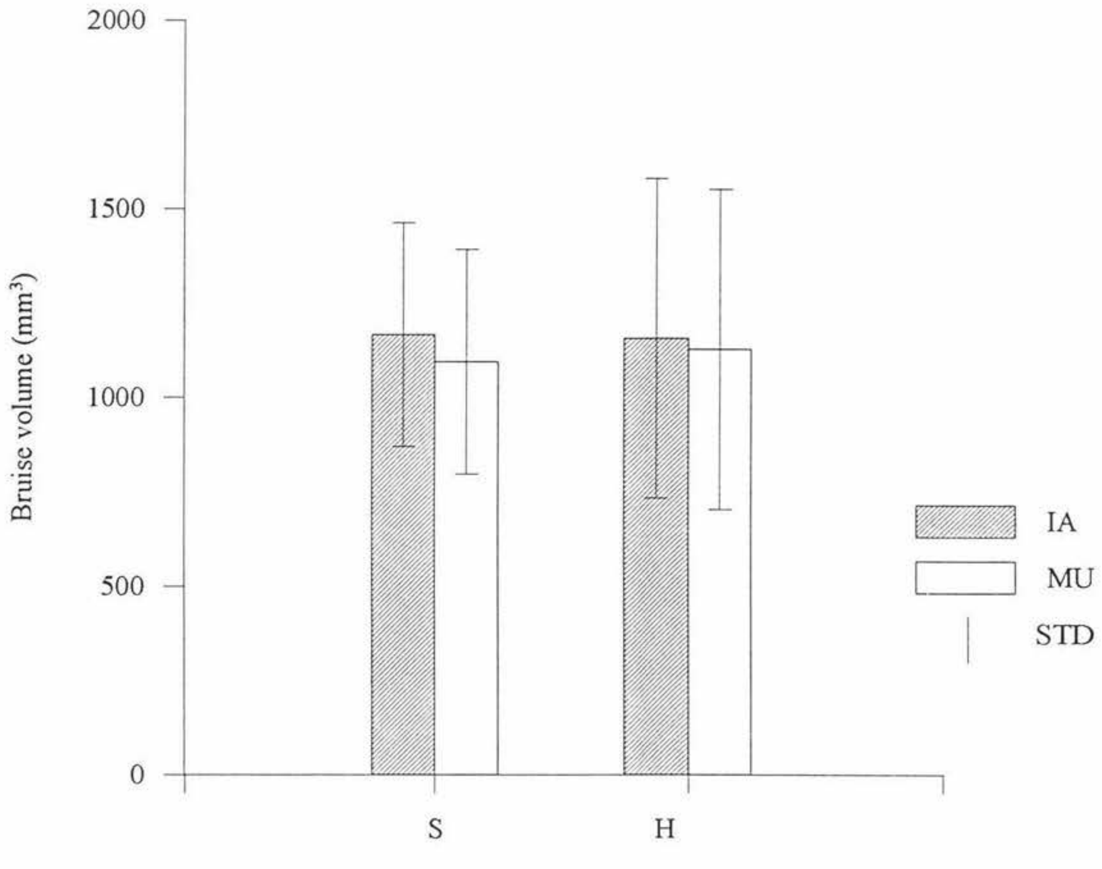

Figure 3.10c Measured bruise volumes on stored apples produced by Steel ball (S) and Hockey ball (H)

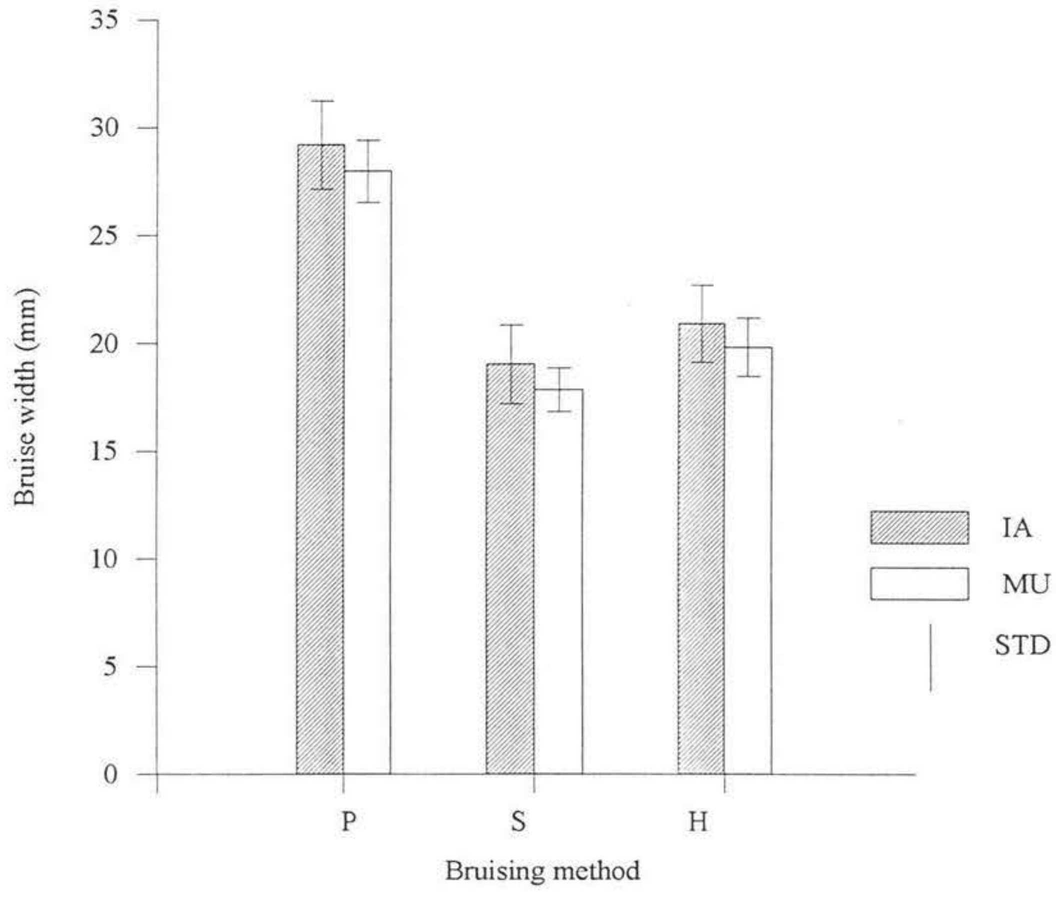

Figure 3.11a Measured bruise widths on fresh apples produced by Pendulum (P), Steel ball (S)and Hockeyball (H)

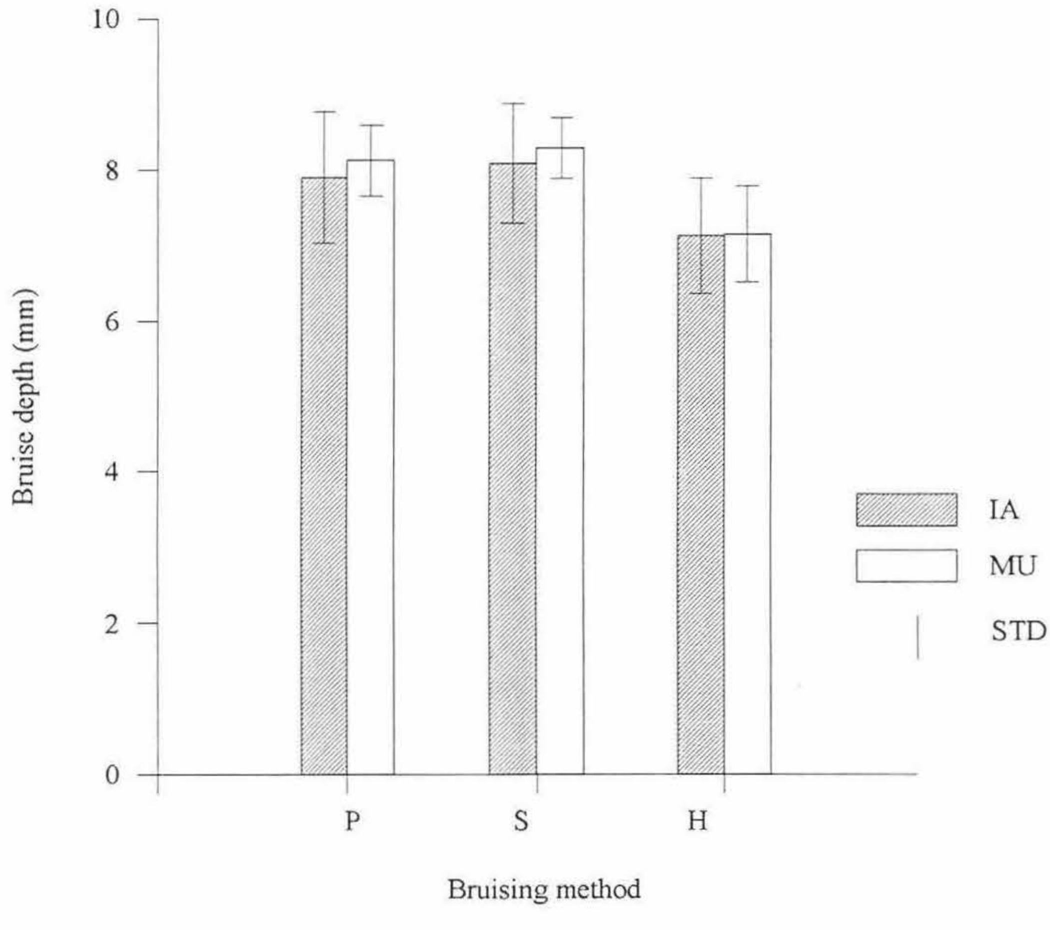

Figure 3.11b Measured bruise depths on fresh apples produced by Pendulum (P), Steel ball (S), and Hockey ball (H)

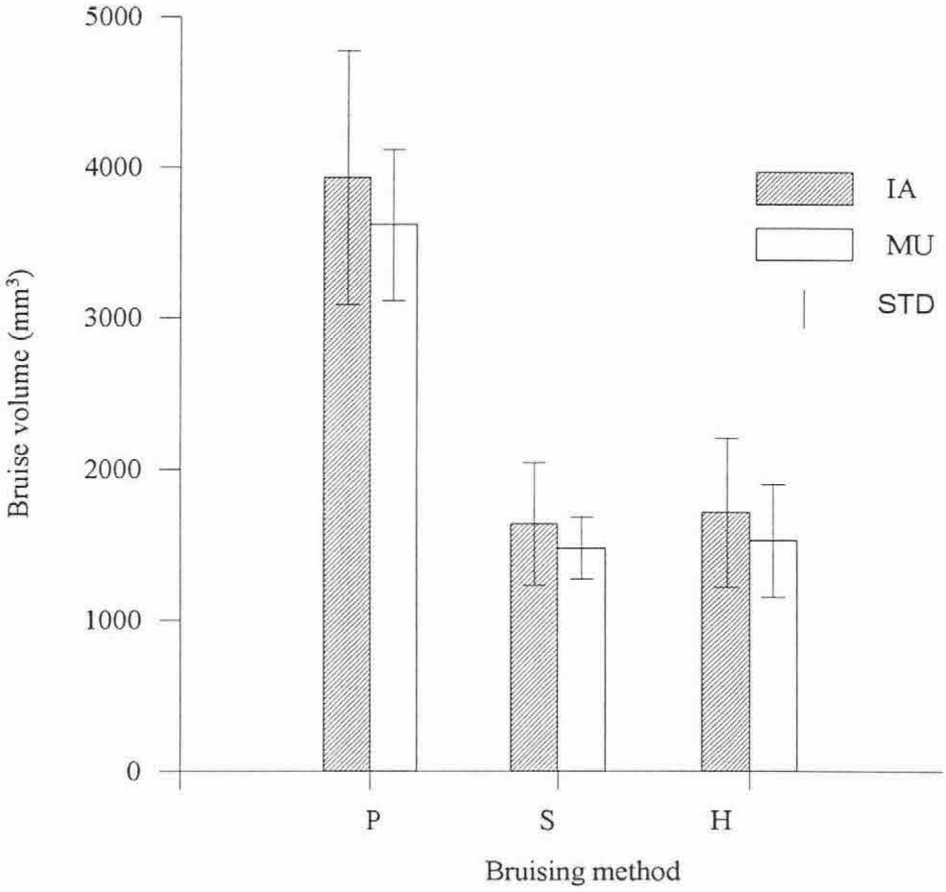

Figure 3.11c Measured bruise volumes on fresh apples produced by Pendulum (P), Steel ball (S), and Horkey ball (H)

The bruise width (both on stored and fresh apples) measured manually from the hockey ball was significantly larger than that from the steel ball ($p < 0.05$). However, the hockey ball made bruise with significantly less depth than the steel ball ($p < 0.05$). The bruise volumes, calculated from bruise width and depth, were not statistically different between the two types of ball at the same impact energy ($p > 0.05$). Again results obtained using image analysis and the manual method were the same (Tables 3.2 and 3.3).

3.5.3 Variability test

The results from the image analysis system variation test is shown in Table 3.4. The standard deviation of a known length measured by the system was small. The results of variations in bruise volume determination with image analysis and manually are shown in Tables 3.5 and 3.6. Variation of bruise volume among the replicates estimated by bruise width and depth obtained from the image analysis was half that of the manual measurement method.

Table 3.4 Variation of the area measurement in image analysis

Diameter (mm)			
	Circle 1	Circle 2	Circle 3
Standard value	10	20	30
Measurement 1	10.0019	20.0671	30.0545
Measurement 2	10.0004	20.0697	30.0052
Measurement 3	9.9992	20.0412	30.0545
Measurement 4	10.0035	20.0349	30.0051
Measurement 5	10.0008	20.0325	30.0340
Measurement 6	9.9967	20.0464	30.0038
Measurement 7	9.9824	20.0290	30.0097
Measurement 8	9.9992	19.9968	30.0006
Measurement 9	10.0000	20.0023	30.0123
Measurement 10	10.0000	20.0132	30.0575
Mean	**9.9984**	**20.0333**	**30.0237**
STD	**0.0056**	**0.0233**	**0.0226**
SE	**0.0018**	**0.0074**	**0.0071**

Table 3.5 Variation of bruise volume measured by image analysis from bruise cross-section area

Time Number	Bruise number 1 d (mm)	h (mm)	V (mm^3)	Bruise number 2 d (mm)	h (mm)	V (mm^3)	Bruise number 3 d (mm)	h (mm)	V (mm^3)
1	16.67	7.75	1188.13	17.02	6.77	1043.61	21.70	9.86	2613.54
2	16.41	7.68	1141.93	17.72	6.72	1118.20	20.53	9.87	2367.26
3	16.59	7.33	1095.26	17.16	8.05	1318.63	23.31	9.80	2969.73
4	17.15	6.74	1049.58	16.28	8.10	1213.93	22.32	9.38	2590.61
5	17.29	7.89	1297.79	17.21	7.91	1295.15	22.58	9.88	2822.09
6	17.24	7.59	1227.89	17.88	7.46	1289.38	20.86	9.43	2296.11
7	16.97	7.11	1098.38	16.57	7.43	1115.42	21.62	9.31	2415.56
8	17.25	7.69	1250.03	16.16	7.84	1146.23	21.32	9.28	2343.36
9	17.06	7.97	1284.32	16.74	8.01	1254.23	21.62	9.43	2454.12
10	17.30	8.02	1327.32	16.20	7.88	1159.12	21.91	9.23	2451.67
Mean	**16.99**	**7.58**	**1196.06**	**16.89**	**7.62**	**1195.39**	**21.78**	**9.55**	**2532.41**
STD	**0.31**	**0.38**	**91.34**	**0.58**	**0.49**	**87.70**	**0.77**	**0.26**	**207.43**
SE	**0.10**	**0.12**	**28.89**	**0.18**	**0.15**	**27.73**	**0.24**	**0.08**	**65.60**

Table 3.6 Variation of bruise volume measured by manual method from bruise cross-section area

People Number	Bruise number 1 d (mm)	h (mm)	V (mm^3)	Bruise number 2 d (mm)	h (mm)	V (mm^3)	Bruise number 3 d (mm)	h (mm)	V (mm^3)
1	15.56	8.45	1193.92	16.29	8.94	1398.49	19.52	10.51	2367.93
2	14.06	8.01	940.44	15.55	8.64	1234.99	19.03	10.46	2255.85
3	14.42	8.13	1000.09	16.42	8.46	1308.61	20.33	11.12	2745.81
4	14.30	7.47	871.21	15.77	7.97	1124.87	18.43	10.64	2198.36
5	14.61	7.56	917.83	16.23	8.64	1322.85	18.53	11.00	2331.79
6	14.37	7.76	928.06	15.28	8.27	1126.04	16.34	9.96	1652.81
7	14.90	7.30	902.83	16.40	8.40	1292.93	19.30	10.80	2418.34
8	14.09	7.50	855.61	15.06	8.20	1086.59	19.06	10.02	2126.44
9	15.28	7.18	921.55	16.48	9.09	1459.94	19.67	11.39	2697.49
10	14.48	8.37	1051.95	17.72	7.08	1189.48	25.03	10.18	3572.69
Mean	**14.61**	**7.77**	**958.35**	**16.12**	**8.37**	**1254.48**	**19.52**	**10.61**	**2436.75**
STD	**0.47**	**0.42**	**95.64**	**0.72**	**0.53**	**117.53**	**2.09**	**0.45**	**476.48**
SE	**0.15**	**0.13**	**30.24**	**0.23**	**0.17**	**37.16**	**0.66**	**0.14**	**150.68**

3.6 Discussion

3.6.1 Bruise image

The image analysis image captured from bruises produced by varying bruising methods showed some major differences. Among bruises produced by the three methods, the images from the pendulum impact were similar to those from the hockey ball impact (Figure 3.6a). The grey levels of the bruise image of the bruises produced by the pendulum and hockey ball impact were lower than those produced by the steel ball impact. The image of the bruise produced by the steel ball showed that bruised cells were more concentrated in the centre of the impact point, extended deeper from the surface toward the centre of the apple and were a darker colour than that of the bruises produced by the pendulum and hockey ball impact. Because the steel ball had a small surface curvature, apple tissues were badly damaged by it. These results are in good agreement with the elastics impact theory of two bodies (Mohsenin, 1970).

3.6.2 Accuracy and variation

The study showed that the variation of the image analysis system for a known diameter measurement was extremely small (< 0.067%). It also showed that the variation in bruise volume among the replicates as estimated from bruise width and depth obtained from the image analysis was up to 50% lower than that of the manual measurement method. These results indicated that the image analysis method was more consistent than the manual method.

Image analysis has other advantages over the manual measurement method. Firstly, it is easy to make a standard method for bruise measurement, and to make comparable results for individual studies. For instance, grey level could become a parameter for determining the bruise boundary; Secondly, image analysis for bruise measurement is relatively fast and could be automated.

3.6.3 Errors due to volume calculation formulae

In this study volume was estimated using both methods from bruise width and depth measurements. Bruise volume was calculated from a formula assuming a geometrical bruise shape. However, the shapes of bruises are usually irregular, so an error in apple bruise volume estimation may be incurred by assuming regular shapes. An accurate method for determining bruise volume may be attained by using the ability of image analysis systems to determine bruise area without using a formula, and this approach will be developed in the following Chapters.

3.7 Conclusions and further study

This present study demonstrated that similar estimates of apple bruise volume can be obtained using either image analysis or manual measurement. The study showed that image analysis provided a good alternative method for measurement and estimation of bruise width, depth, and volume. All the results obtained by image analysis were not significantly different to those obtained from manual measurement for the bruise produced on stored and fresh apples, irrespective of ways of making the bruise.

Variation of bruise volume among the replicates estimated from bruise width and depth obtained from the image analysis was up to 50% lower than that of the manual measurement method.

No other published studies have been found which use a video image analysis system to measure bruise width and depth in fruit. This trial indicated that this form of image analysis is very useful for studying bruising in apples.

CHAPTER 4

BRUISE SURFACE AREA DETERMINATION

4.1 Introduction

Many bruise parameters, such as bruise volume, bruise area, bruise susceptibility, and bruise factor, have been used to describe the degree of bruising in fruit. Among these parameters, bruise surface area seems to be the most important to the commercial fruit industry. This is because in practise fruit is graded by bruise area, and consumers select fruit on visual appearance. The size of bruise area measured with the skin on is a selection criteria used by the fruit industry. The New Zealand Apple and Pear Marketing Board allows any bruise area less than 100 mm^2 to be ignored for New Zealand export if the cumulative bruise area on the apple is not more than 100 mm^2 (Pang *et al.*, 1992). However, bruises sometimes can not be seen until the skin was removed (Pang, 1994). Pang found out that only 50% of bruises were visible on Gala apples without peeling the skin, 38% on Fuji, 48% on Granny Smith, and 82% on Splendour. No visible bruises were observed on Braeburn apples prior to peeling. But after peeling, bruises were clearly visible in all varieties in his study. Bruising may not always be visible, but it may affect the fruit quality as perceived by the eventual consumer. Therefore, bruise area measured after peeling has been generally used by researchers in the study of fruit bruising.

Currently, bruise surface area is determined by measuring a bruise area's maximum and minimum diameters, assuming its shape is ellipsoidal on apples (Equation 2.1, Chapter 2 (Pang and Studman, 1992)).

From the results of Chapter 3, it can be seen that the image analysis technique could be a useful tool to measure apple bruise parameters, and its application to bruise surface area was therefore investigated.

4.2 Objectives

This study focused on developing a machine vision system to measure bruise surface area directly with the apple skin peeled. The objectives of the study were:

- To set up a machine vision system for bruise surface area measurement of apples.
- To apply the image analysis system in the determination of bruise surface area automatically, and compare the method with manual methods.
- To compare variations of measurements of bruise surface area in image analysis and manual methods.

4.3 Materials and methods

4.3.1 Fruit preparation

Experiments were carried on both stored and fresh 'Granny Smith' apples. The apples used were from the sample described in Chapter 3.

Sixty 'Granny Smith' apples which had been stored for 7 months were randomly selected from the sample. Their diameters ranged from 71 to 82 mm. Sixty three fresh 'Granny Smith' apples were also selected randomly from the fresh apple sample. Their diameters ranged from 73 to 85 mm.

4.3.2 Experimental methods

The three bruising methods (falling steel ball, hockey ball, and pendulum device) have been fully described in Chapter 3. Three experiments were conducted.

Experiment 1: Measurement of different sized bruise areas

Experiment 1 was designed to test how well different sized bruise areas were measured by the image analysis system. A sample of 30 stored apples was used for this experiment. Small, medium and large sized bruises were produced by dropping the steel ball from 100, 200 and 300 mm on each 10 apples respectively (each apple had one bruise).

Experiment 2: Measurement of bruise areas of different types

To investigate how well the developed machine vision system measured bruise area on different types of bruises, this experiment was designed to conduct bruise area measurements on different conditioned apples (fresh and stored) and different bruise methods (dropping steel ball, dropping hockey ball, and pendulum impact). The experiments were conducted after the following preparations:

- 10 stored apples bruised by the steel ball dropped from 200 mm;

- 10 stored apples bruise by the hockey ball dropped from 200 mm;
- 10 stored apples bruised by the 500 mm radius pendulum falling through a 45 degree angle;
- 20 fresh apples bruised by the steel ball dropped from 200 mm dropping;
- 20 fresh apples bruise by the hockey ball dropped from 200 mm dropping;
- 20 fresh apples bruised by the pendulum falling through a 60 degrees;

Experiment 3: Variation test

System variation test

System variation testing was carried out on objects of known dimensions to check the accuracy and repeatability of the developed machine vision system for area measurement. The known sized objects used were three standard sized circles obtained from the Image Analysis Unit at Massey University. These were black circles on white paper, 78.54, 314.16, and 706.86 mm^2 in area. These three standard circles were measured by the image analysis system ten times each. The means and standard error were calculated.

Variation test comparing bruise surface areas measured by image analysis and manually

Three apples were selected from the fresh apple sample collection, and impacted by the steel ball from three different heights to give different sized bruises. The drop heights were 100, 200 and 300 mm. One bruise was made on each apple. Each bruise was measured ten times for maximum and minimum diameters by image analysis so the area could be calculated. The same bruise samples were then measured by ten people who had experience in fruit bruise measurement, for maximum and minimum diameters. After allowing the bruises to develop for 24 hours, the measurements were all completed within 30 minutes of removing the apple skin.

4.3.3 Bruise measurement

After the apples were impacted, the bruises were allowed to discolour for 24 hours at room temperature before measurements were taken. Bruise measurements were taken by both the image analysis and manually at the same time. The diameter and weight of the samples were recorded before the measurements were taken. The skin was peeled off in the region of the bruise. An area of 30 to 40 mm in diameter was peeled with a peel thickness of less than 1 mm where possible. Each apple was then placed onto the sample positioning device. The measurements using the image analysis were performed immediately following peeling. After the image analysis measurement, bruise parameters were measured using the manual method.

In the image analysis measurement, the basic procedures used were the same as those for measuring bruise cross-section in Chapter 3. However, due to the different types of images produced between bruise cross-sectional area and bruise surface area, the algorithm was modified slightly. In cross-section area measurement, the bruise image showed a background, bruise area and unbruised area in the image. However, in the bruise surface area measurement, the bruise image for the measurement shows only bruised and unbruised areas, and there was no need for background consideration. A typical graph of the bruise surface image analysis is shown in Figure 4.1. The algorithm

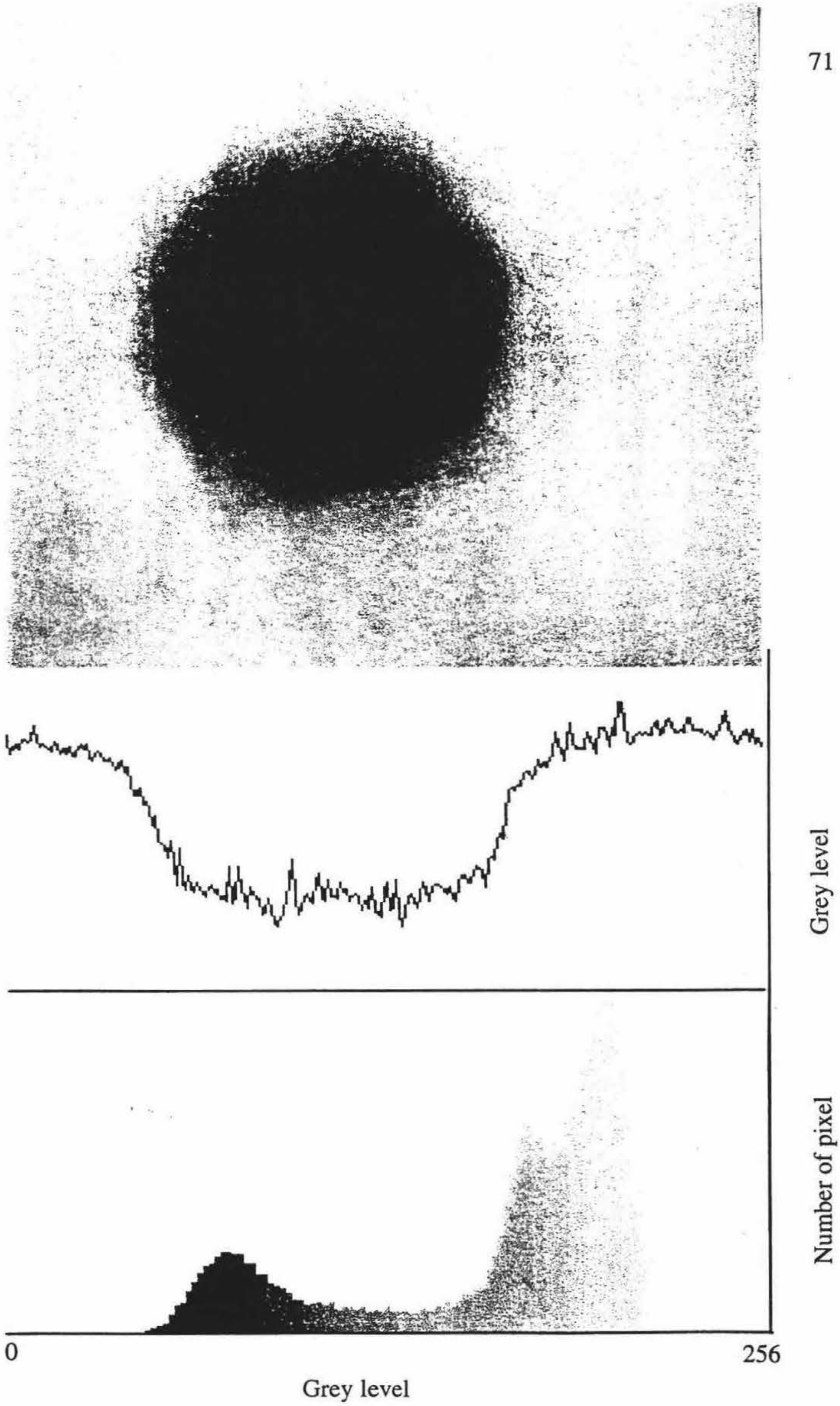

Figure 4.1 A typical bruise image and diagram of grey level with number of pixels across the bruise centre profile

used for this study is given in Appendix 1 as algorithm 2. In image analysis, bruise surface areas were determined directly by counting numbers of the pixels from the bruised area. At the same time, bruise maximum and minimum diameters were determined and recorded.

4.3.4 Bruise area determinations

Bruise surface area was determined in three ways using the image analysis and manual measurement:

- ***Method A***: Bruise areas were directly measured by image analysis and recorded in the computer without assuming a geometric shape;

- ***Method B***: Bruise areas were estimated by assuming their shape to be ellipsoidal, and the areas were calculated using Equation 2.1 (Chapter 2), where the bruise maximum and minimum diameters were measured by the image analysis.

- ***Method C***: Bruise areas were also calculated by Equation 2.1. However, the bruise maximum and minimum diameters were measured by manually.

4.4 Results

4.4.1 Bruise image

None of the bruises presented any difficulties for measurement by the developed machine vision system. There was no difference in the measurements even though there were slight differences in colours of the bruises. In general, the smaller the bruise area, the lighter the bruise colour. However, the bruise produced by the steel ball was slightly darker than that produced by hockey ball at the same impact energy. Since there were only bruised and unbruised tissues shown in an image bruise area measurement, no background was needed for the measurement. So, the bruise areas were relatively easy to measure using the developed machine vision system.

4.4.2 Different sized bruises

T-test analysis results for the bruise areas determined by the method A, method B and method C are shown in Table 4.1. Obviously, the bigger the drop height of the steel ball, the larger the bruise area produced, no matter how the bruise area was determined (Table 4.1). However, the bruise areas in Table 4.1 showed some differences between the three methods: there was no significant difference between bruise surface areas determined by image analysis (method B) and manually (method C) ($p > 0.05$); however significantly smaller bruise areas were measured directly by image analysis (method A) than were calculated from maximum and minimum diameters measured by image analysis (method B) ($p < 0.05$). The bruise surface areas from method B were on average 12% larger than those from method A. The results of individual bruise areas

Table 4.1 Comparison of bruise areas measured by the methods A, B, and C on the stored apples with the steel ball impact.

Number of bruises	Drop height (mm)	Bruise surface area (mm^2)		
		Method A	Method B	Method C
10	100	128.63 (5.36)[a]	144.25 (5.87)[b]	136.82 (7.44)[ab]
10	200	183.30 (3.26)[a]	195.00 (4.03)[b]	201.27 (4.32)[b]
10	300	308.85 (20.33)[a]	339.65 (24.46)[b]	315.13 (21.19)[ab]

Note: Values with the same letter in the same row are not significantly different;

Values in the brackets are standard errors of the mean.

from method A and method B are shown in Figure 4.2, which shows that the bruise areas from method A were always smaller. Figure 4.3 shows the individual bruise areas measured using method A and method C. The bruise areas from method C varied from method A, some being smaller and some larger than method A. There was no significant difference in the bruise areas measured by both method A and method C at 100 and 300 mm drop heights (Table 4.1). However, there were significant differences in the bruise areas measured by both method A and method C at the 200 mm drop height. This meant that bruise areas determined by measuring maximum and minimum diameters of the bruise (method B and method C) could show significantly different results for the true value of the bruise area.

4.4.3 Bruises produced by different methods

The comparison of results of bruise surface areas determined from methods A, B and C on fresh and stored apples for the bruises produced by the steel ball drop, the hockey ball drop, and the pendulum impact are shown in Table 4.2. In all cases, the bruise areas from method A were significantly smaller than those from method B.

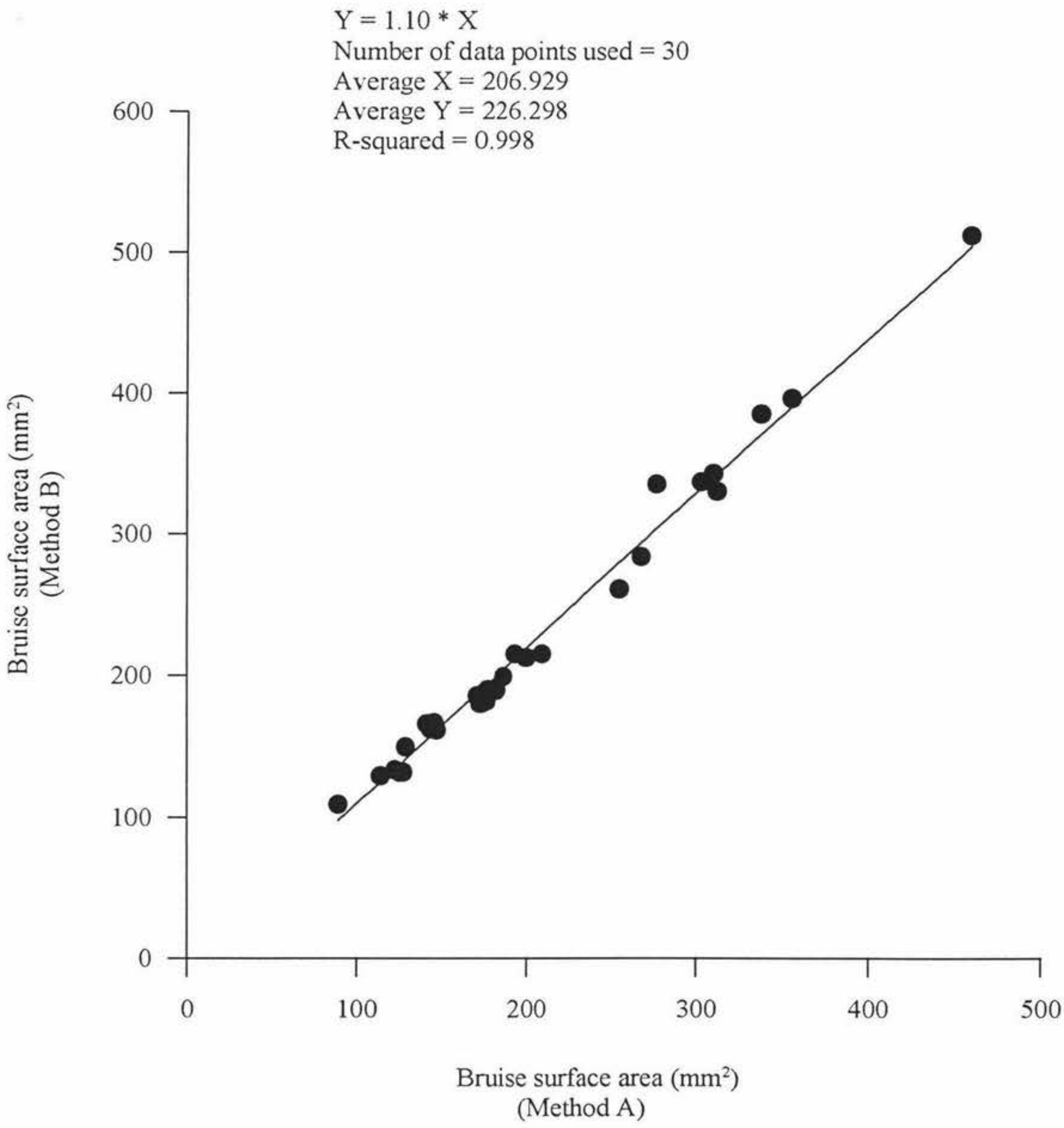

Figure 4.2 The relationship of bruise area determined directly using image analysis (method A) and calculated from maximum and minimum bruise diameters determined by image analysis (method B).

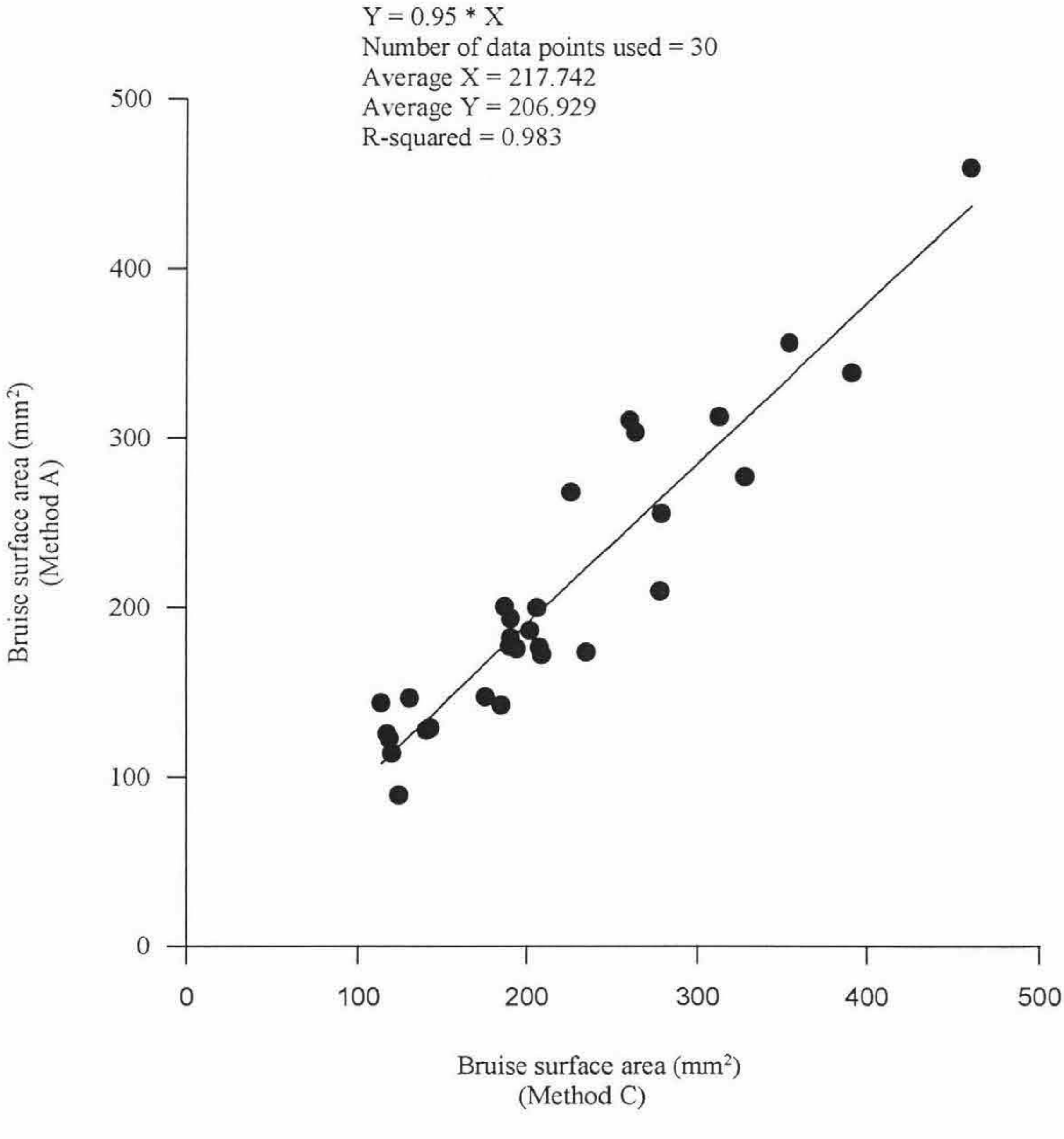

Figure 4.3 The relationship of bruise area determined directly using image analysis (method A) and manually (method C).

Table 4.2 Comparison of bruise areas measured by methods A, B, and C on stored and fresh apples with the three bruising methods

Apple Condition	Bruise production method*	Drop height or impact angle	Number of sample	Bruise area** (mm²)		
				Method A	Method B	Method C
Stored	S	200 mm	10	183.30 (3.26) [a]	195.00 (4.03) [b]	201.27 (4.32) [b]
Stored	H	200 mm	10	222.15 (5.15) [a]	242.59 (5.12) [b]	234.69 (5.00) [b]
Stored	P	45°	10	244.28 (12.1) [a]	286.88 (13.8) [b]	300.12 (12.3) [b]
Fresh	S	200 mm	20	208.55 (3.53) [a]	218.42 (3.66) [b]	212.28 (2.95) [ab]
Fresh	H	200 mm	20	218.30 (2.49) [a]	225.52 (2.91) [b]	230.49 (2.17) [b]
Fresh	P	60°	20	454.69 (9.42) [a]	466.34 (8.98) [b]	461.46 (7.34) [ab]

Note: * S, H, and P mean steel ball drop, hockey ball drop, and pendulum imapct respectively;

** Values with the same letter in the same row are not significantly different;

Values in the brackets are standard errors of the mean.

On the other hand, the areas measured by image analysis were the same as those measured by the manual method. When bruise surface areas were calculated from the diameters measured by image analysis, the areas were significantly larger than those obtained by direct image analysis. These results were expected, given that the largest dimensions of irregular bruises were measured by the image analysis method, and the areas were calculated from these larger values when regular bruise shapes were assumed.

4.4.4 Variations of bruise areas measured by image analysis and manually

The results from system variation test for standard area measurement are shown in Table 4.3. The results of variations in bruise area measured by image analysis and manually are shown in Table 4.4. The standard deviation in the diameter of the known object measured by the system was small. Variation of bruise area among the replicates obtained from the image analysis was one fifth that of the manual measurement method.

Table 4.3 Variation of the area measurement by image analysis for standard circles

Area measurement (mm^2)			
	Circle 1	Circle 2	Circle 3
Standard value	78.54	314.15	706.86
Measurement 1	78.19	314.31	706.61
Measurement 2	78.24	314.15	706.36
Measurement 3	78.23	314.17	706.26
Measurement 4	78.15	314.48	706.35
Measurement 5	78.14	314.34	706.37
Measurement 6	78.15	314.41	706.40
Measurement 7	78.16	314.35	706.28
Measurement 8	78.18	314.18	706.85
Measurement 9	78.16	314.12	706.13
Measurement 10	78.08	314.11	706.89
Mean	**78.17**	**314.26**	**706.45**
STD	**0.044**	**0.131**	**0.239**
SE	**0.014**	**0.041**	**0.076**

Table 4.4 Variation of bruise area measured by image analysis (methods A and B) and manually (method C)

Measure time or Person number	Bruise surface area								
	Bruise number 1			Bruise number 2			Bruise number 3		
	Method A (mm^2)	Method B (mm^2)	Method C (mm^2)	Method A (mm^2)	Method B (mm^2)	Method C (mm^2)	Method A (mm^2)	Method B (mm^2)	Method C (mm^2)
1	106.8	112.6	136.6	242.1	251.3	262.4	476.8	486.6	469.2
2	100.8	108.3	121.0	238.4	247.3	217.5	478.3	486.8	484.0
3	102.9	110.0	145.3	240.8	250.8	241.5	476.2	485.5	481.3
4	100.0	107.8	127.9	239.4	247.1	249.4	472.6	481.9	461.3
5	95.5	102.3	149.6	240.4	252.1	250.3	47.4	488.9	498.6
6	102.9	109.0	122.5	237.3	247.7	249.5	473.8	482.9	483.4
7	101.9	108.9	136.7	241.3	253.3	265.7	480.6	492.8	513.3
8	96.0	103.9	138.8	239.5	252.0	258.1	477.6	488.1	469.4
9	102.3	107.8	151.7	243.6	255.6	273.9	479.0	492.0	474.0
10	101.5	107.5	104.6	242.0	252.8	227.7	481.1	489.3	453.6
Mean	**101.1**	**107.8**	**136.2**	**240.5**	**251.0**	**249.6**	**477.3**	**487.5**	**478.8**
STD	**3.15**	**2.77**	**16.59**	**1.81**	**2.66**	**16.31**	**2.56**	**3.35**	**16.66**
SE	**1.00**	**0.88**	**5.25**	**0.57**	**0.84**	**5.16**	**0.81**	**1.06**	**5.27**

4.5 Discussion

From these experiments it was found that bruise surface area was clear and easy to measure by image analysis. The bruised area was easily separated from the unbruised area by the algorithm. High contrast in colour between bruised and unbruised areas is very important for accuracy and repeatability when using image analysis, and images of bruise areas were very suitable in this respect.

There was no significant difference between bruise surface areas determined by image analysis and manually, based on the measurement of bruise maximum and minimum diameters. Therefore, the image analysis method can be used for bruise surface area measurement. However, significant differences between bruise surface areas determined directly and calculated by the image analysis maximum and minimum diameter method (Tables 4.1 and 4.2) shows that bruise areas estimated by assuming a geometric shape would produce significant errors in bruise area measurements. From Figure 4.2 it is clear that measurements from diameters consistently over-estimated bruise area by 10%. It appears that this correction should be made to all such measurements, whether by image analysis or manually.

The estimates of bruise areas produced by the hockey ball impact demonstrate clearly the different results obtained between the three methods. Whether the maximum and minimum diameters of a bruise are measured manually or by image analysis, the same results are achieved, but assuming a regular bruise shape for calculations of bruise area leads to erroneous results. The study of bruise detection and measurement would be more accurate if a direct image analysis measurement as used in method A here was performed.

The variation test shows that the image analysis can be used for area measurement with a high degree of precision, as indicated by the low standard errors and coefficients of variation (Table 4.3). The estimates of area were quite close to the real area size, with less than 5% error, indicating that image analysis can provide accurate measurements of actual surface areas. The results of bruise area measurements in Table 4.4 indicated a large variation in manual measurements for bruise area determinations, suggesting that human error could be significant. In comparison, the variation in the image analysis results were small. The error of the manual measurement method was 5 times larger than the image analysis method (Table 4.4). Therefore, the method of image analysis for area measurement had an advantage over the manual measurement method in repeatability, as well as allowing accurate measurement of complex bruise areas without the need to assume a regular shape.

Image analysis can eliminate human error to a great degree. Measurements of bruises by humans can be a difficult and subjective task, since the boundary of the bruise region may not be clearly defined. Personal judgement is often not consistent. In addition, detailed measurements of apple bruising is hard work for the eyes and is a time consuming process. Introduction of image analysis into bruise area measurement could add accuracy and consistency to the whole procedure.

4.6 Conclusions

Bruise areas can be measured directly by image analysis without assuming a bruise shape. The variation of bruise area among the replicates measured by the image analysis was five times less than from manual measurement.

There were no significant differences in the estimation of bruise surface area from bruise maximum and minimum diameters measured by image analysis and manually. However, there was a significant difference in bruise area measured directly from image analysis and bruise area calculated assuming a geometric shape, with the latter consistently overestimating bruise surface area by 10%.

Using the developed image analysis system, accurate measurement of bruise surface area can be easily carried out for both fresh and stored 'Granny Smith' apples on bruises either produced by dropping balls or impacted by a pendulum device.

CHAPTER 5

A NEW APPROACH FOR BRUISE VOLUME DETERMINATION BY MULTIPLE SECTIONING USING IMAGE ANALYSIS

5.1 Introduction

Despite the commercial preferences discussed earlier, bruise volume is still an important indicator of apple bruising damage (e.g., Schoorl and Holt, 1977, 1981; Klein, 1987; Brusewitz and Bartsch, 1989; Schulte *et al.*, 1990; Bollen and Cox, 1991; Pang and Studman, 1992). Precise measurement of bruise volume is therefore still important.

Bruise volume is currently determined from the bruise cross-sectional area measurement derived from bruise width and depth (Chapter 3). Manual measurement is subject to the error of human subjectivity. By assuming a geometric shape, there are several possible formulas for the bruise volume calculation. These formulas were reviewed in Chapter 2 of this thesis. Assuming a geometric shape can produce an error in bruise volume calculations due to the naturally irregular shapes of bruises. This study was set out to find a new method to determine bruise volume by using image analysis techniques without assuming a geometric shape. Based on bruise surface area measurements using image analysis (Chapter 4), bruise volume may be determined accurately by integrating a series of bruise area measurements.

5.2 Objectives

The objectives of the study presented in this chapter were:

- To establish a new method for bruise volume determination using the developed machine vision system.
- To compare the results of bruise volume determined by the new method with those by manual measurement.
- To determine relationships between bruise volume, bruise surface area and bruise depth.

5.3 Materials and methods

5.3.1 Fruit preparation

Stored 'Granny Smith' apples were used in this study. Freshly picked 88 count `Granny Smith' apples were selected at their commercial harvest date on 31 March 1994. They were graded over a standard grading table in a Hawke's Bay packing shed, and were shifted to Massey University. They were held in cold storage at $1^{o}C$ until required. The experiments were conducted in October 1994 after the apples had been stored for 7 months. A sample of 34 apples was selected randomly from fruit collected with no visible bruises. Apples were allowed to reach ambient temperature before being tested. The apple diameter ranged from 72 - 84 mm.

5.3.2 Bruising methods

To produce bruises apples were impacted by the three impact methods which have been described in Chapter 3.

A sample of twenty four apples was selected randomly from the fruit collection. Opposite points in each apple showing similar maturity in colour were chosen for impacting. Different sized bruises were produced by dropping the steel ball or hockey ball from 100, 200, and 300 mm heights onto three groups of apples. The first group consisted of 7 apples, the second 8, and the third 9. The first and third groups were impacted by the steel ball. The second group of apples were impacted by the steel ball on one side and by the hockey ball on the other.

A further sample of ten apples was selected from apple collection for bruise production using the pendulum device. Each apple had a hole through the centre along the calyx to stalk axis, which was produced by a cork borer 10 mm in diameter. This allowed the apple to be slipped onto the pendulum arm, and aligned with the impact point. Each apple was placed onto the pendulum arm, aligned with the centre of impact point, released from the selected drop angle of 45 degrees (or drop height of 120 mm), and caught by hand after the first impact of the pendulum in order to avoid a second impact. Each apple was impacted once using this device.

5.3.3 Bruise sample preparation

After impacting, the bruises were allowed to discolour for 24 hours at room temperature before bruise samples were cut and measurements were taken. The bruise site on the apple could be easily distinguished by peeling the apple skin. Parts of apple containing the whole bruise were cut from the apple (Figure 5.1a), by slicing the apple on a plane parallel to the surface at the centre of the bruise. Experience showed that the thickness of the cut portion had to be equal to or larger than the maximum diameter of bruise surface area to make sure all the bruised tissue was included in the sample. Further cuts were made to remove the four edges of the sample piece (Figure 5.1b). However, a minimum of 10 mm of unbruised tissue was left around the bruise. This piece of apple (Figure 5.1c) was easy to hold for further slicing for bruise volume measurements.

5.3.4 Measurement of bruise volume

<u>New approach</u>

The machine vision system with the algorithm developed for bruise area measurement (Chapter 4) was used. The principle of the bruise volume measurement used in this technique was then to integrate a series of bruise areas measured by image analysis.

Bruise samples were placed on the sample positioning device of the machine vision system for measuring its bruise surface area (s_1), followed by recording its thickness using an electronic vernier calliper. At the same time as the bruise surface area was measured, the maximum and minimum diameters of the bruise were also recorded by image analysis. A thin slice parallel to the bruise surface was cut off from the sample after bruise surface area measurement. The thickness of the rest sample was recorded. Thus the thickness (t_1) of the first slice would be equal to the difference between the thickness of the sample recorded before and after cutting. The rest of the sample was placed on the machine again for a second bruise area measurement (s_2), followed by cutting another slice from the sample. The thickness of the rest of the sample

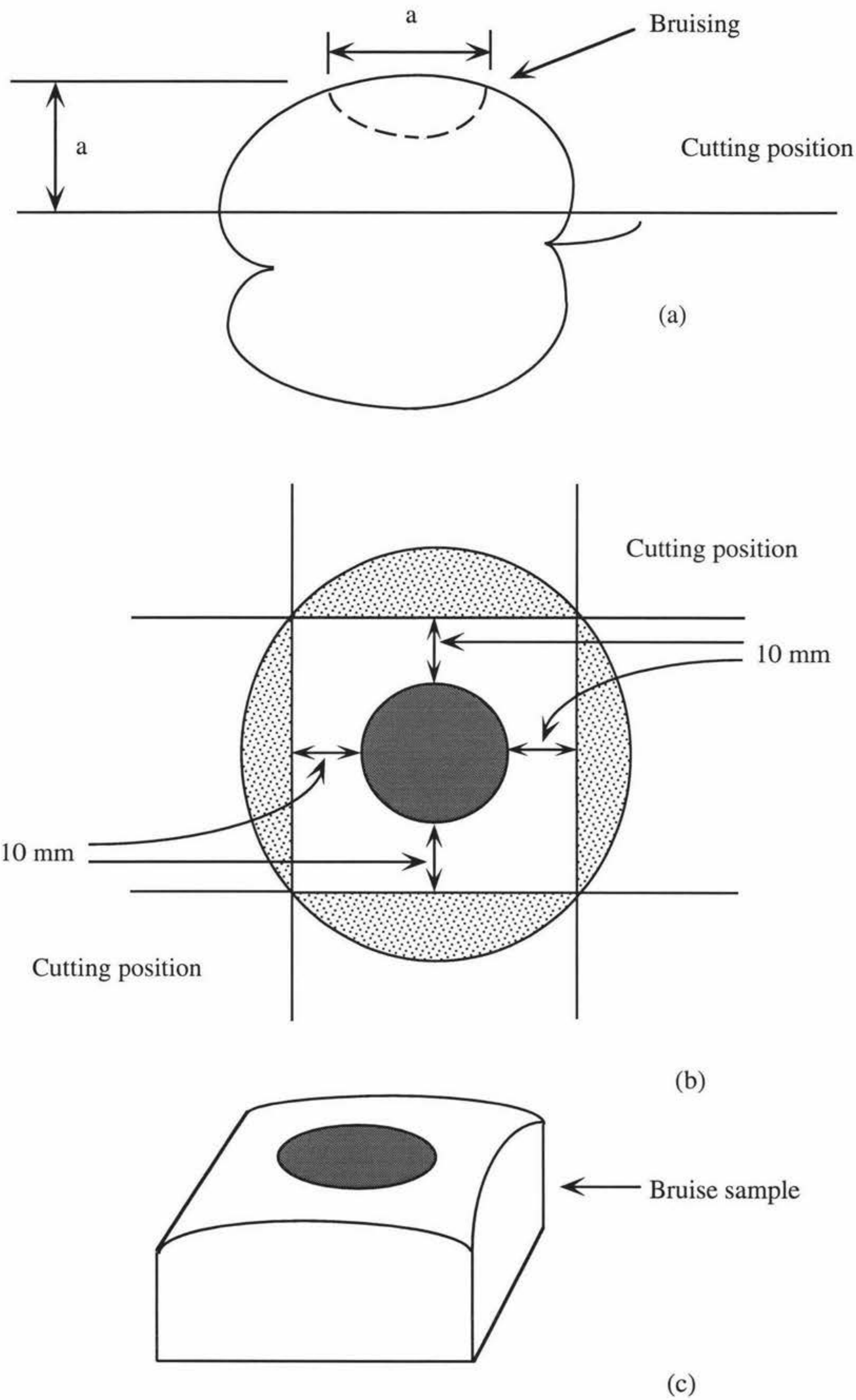

Figure 5.1 Bruise sample preparation

was measured again by electronic callipers. This process was continued until the last visible bruise area (s_n) was recorded.

In this method, the bruise area of each slice (s_i) was measured directly by image analysis. The thickness (t_i) of each slice was the difference between the thickness of the remaining piece of apple and its thickness before the last slice was remained so that the bruise volume (v_i) of each slice was equal to the bruise area (s_i) multiplied by the slice thickness (t_i). Thus the volume (V_{IA}) for the whole bruise is given by:

$$V_{IA} = s_1t_1 + s_2t_2 + \ldots\ldots + s_nt_n = \sum_{i=1}^{n} s_i t_i \qquad 5.1$$

A total of 34 bruises were measured in this way.

Manual method

For comparing the results from the image analysis, the bruise volume was also determined using the formulae normally used for manual calculations. Thus the bruise volume (V_{MU}) was determined using the Equation 2.2 (Mohsenin, 1970), Equations 2.3 and 2.4 (Holt and Schoorl, 1977), and Equation 2.5 (Chen and Sun, 1981) in Chapter 2.

The bruise width used in these formulae was the maximum diameter of the bruise measured by image analysis from the bruise surface area. The bruise depth used was the total thickness determined from the bruise slices.

5.4 Results

The comparison of results of the bruise volumes determined by both image analysis and the manual method are shown in Tables 5.1 and 5.2. The tables give means and standard errors of the bruise volume from individual experiments.

Table 5.1 Summarised results for bruise volume calculated from multiple image analysis slices and using the simple manual formula (given by Holt and Schoorl, 1977) on stored 'Granny Smith' apples

Number of bruises	Bruising method	Drop height or impact angle	Bruise volume (mm^3) Image analysis	Manual formula**
14	Steel ball	100 mm	449.56 (28.78)[a]	509.39 (30.57)[b]
8	Steel ball	200 mm	1017.78 (57.48)[a]	1204.08 (169.75)[a]
8	Hockey ball	200 mm	949.26 (43.50)[a]	1301.60 (183.80)[a]
18	Steel ball	300 mm	1851.71 (54.37)[a]	2731.95 (213.93)[b]
10	Pendulum*	45°	792.99 (57.52)[a]	1050.34 (94.47)[b]

Note: Values with the same letter in the same row are not significantly different at the 5% level; Values in brackets are standard errors of the mean.

* Pendulum drop height equivalent to 120 mm;

** Based on surface bruise diameters and bruise depth only.

Table 5.2 The results of the bruise volumes determined by image analysis and manual methods with three different formulae.

Bruise volume (mm^3)			
Image analysis	Manual formulae: Holt & Schoorl'	Mohsenin'	Chen & Sun'
449.66 (28.78)	509.39 (30.57)	453.81 (27.62)	518.47 (30.52)
1017.78 (57.48)	1204.08 (169.75)	1056.48 (122.37)	1163.55 (159.09)
949.26 (43.50)	1301.60 (183.80)	1003.26 (113.50)	1228.89 (149.18)
1851.71 (54.37)	2731.95 (213.93)	2229.94 (151.15)	2557.54 (186.54)
792.99 (57.52)	1043.70 (88.78)	809.36 (65.41)	1001.36 (79.77)

From Table 5.1, there was a significant difference in the bruise volume measured by image analysis and manually (calculated using the equations given by Holt and schoorl) on bruises produced by the steel ball dropped from 100 mm and 300 mm. However, there was no significant difference in the bruise volume measured by both methods on bruises produced by the steel and hockey balls dropped from 200. At the 100 mm drop height, the difference between the bruise volume measured by both image analysis and manually was an average of 13%. At 300 mm, there was a 47% difference on average between the methods. There was also a 32% difference in the bruise volumes determined by both methods for bruises produced by the pendulum.

There was about 12 - 30 % of difference among bruise volumes calculated from the three equations (Table 5.2), of which the same parameters were used. It is clear that the bruise volumes measured by the image analysis were closed to those calculted from Mohsenin's Equation.

The relationship between bruise volume and drop height for each bruise measured by both image analysis and the manual method are shown in Figure 5.2. There was a better linear relationship between bruise volume and drop height using image analysis (R^2 = 0.90) than using the manual method (R^2 = 0.66); A higher distribution of bruise volume value was estimated using the manual method than using the image analysis at the same dropping height.

The bruise volume is plotted against the product of bruise surface area and depth (as measured by image analysis) in Figure 5.3. R^2 of 0.97 indicates there was a good relationship between these parameters.

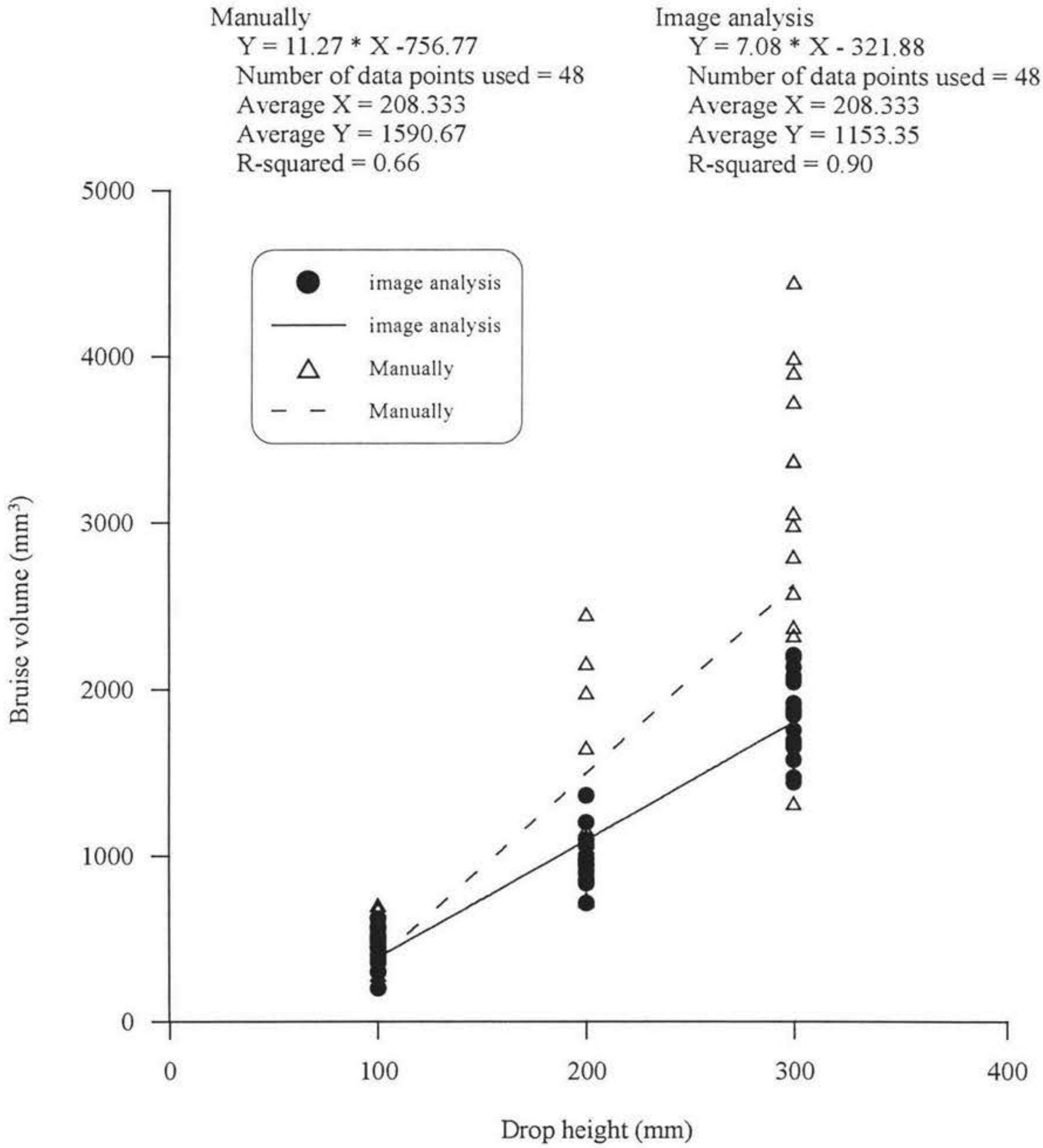

Figure 5.2 The relationship between bruise volume and drop height

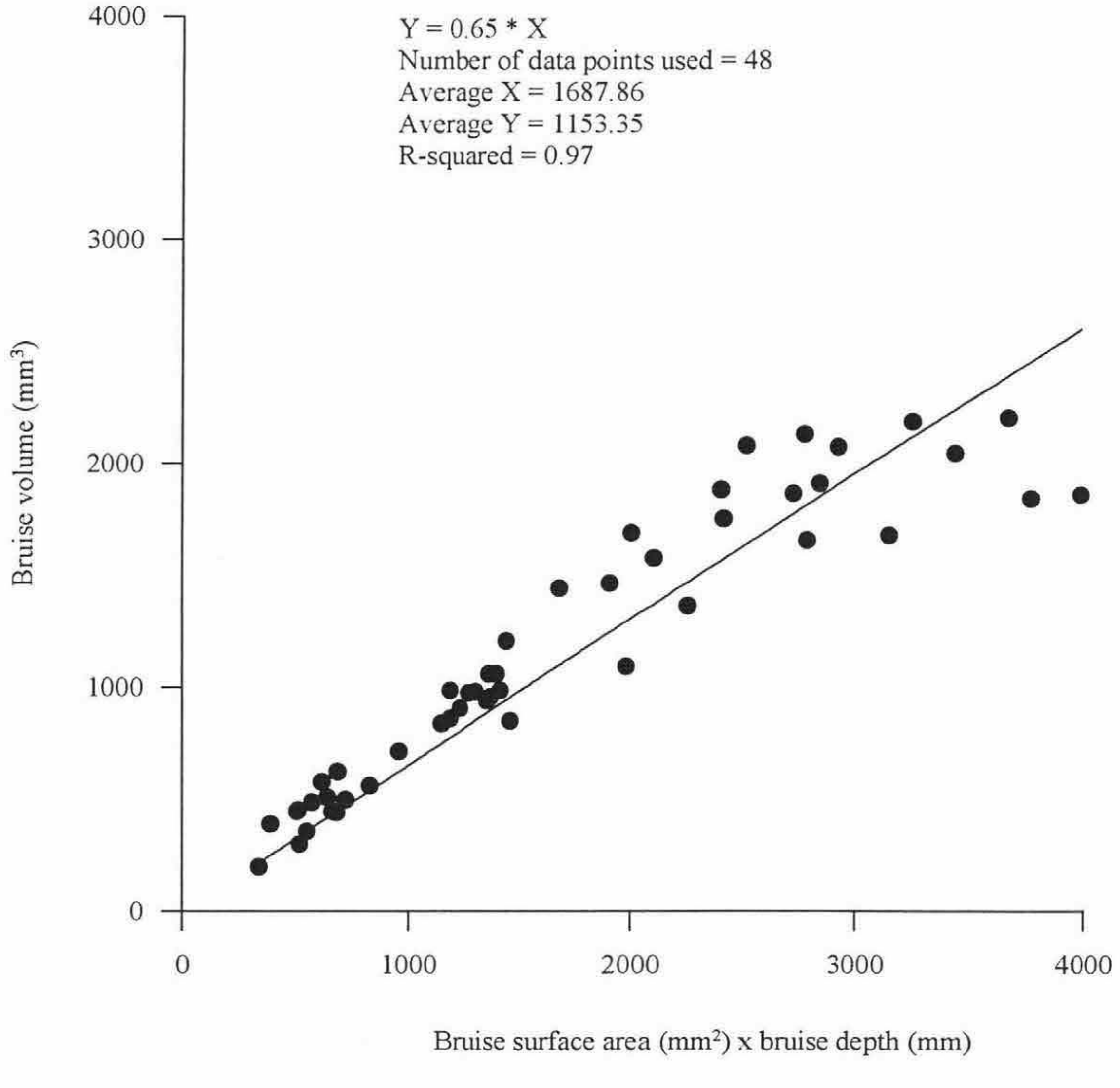

Figure 5.3 The relationship between bruise volume and multiplication of bruise surface area and depth

5.5 Discussion

5.5.1 Bruise volume measurement

This study demonstrated that the image analysis technique can be used for measuring apple bruise volume. Although the comparison results were not always consistent, the bruise volume measured by the two methods were statistically equivalent in cases (Table 5.1). The obvious difference was generally due to the equations used in the bruise volume calculation (Table 5.2). It is difficult to state whether the results obtained manually represented the "true" bruise volume due to the assumed geometric shape and formula used for the bruise calculations. However, image analysis offers a consistent way to obtain the bruise volume through a proper machine set up. The results in Figure 5.2 may imply that the higher the bruise volumes, the more variable the measurement will be using the manual formula. The variability of bruise volumes measured by the image analysis was much lower. This could have been due to real variability in bruise volume, but this is unlikely since such a variability would presumably have affected all the sets of data in the same way.

5.5.2 Bruise volume prediction

The apparently good relationship (Figure 5.3) between bruise volume and the multiplication of bruise surface area and bruise depth offers a good prospect for bruise volume estimation. This study has indicated that the bruise surface area and bruise depth can be readily measured using image analysis (Chapters 3 and 4). By taking regular sections, a direct estimate of bruise volume can be obtained without assuming a regular shape of a bruise. Relationships between the bruise volume and the bruise surface area and bruise depth could then be established for different types of apples and bruises (since there may not be a universal relationship between them).

5.6 Conclusions

Through this study, an image analysis technique for estimating apple bruise volume has been established. Based on the bruise area measurement by image analysis, the technique provided with a consistent way to measure bruise volume with less variability and without the subjectivity of manual measurements by experimenters. Estimation of bruise volume can be made by taking repeated cross-sections of bruise surface area and bruise depth, and both of these parameters can be readily measured by the image analysis technique.

CHAPTER 6

SUMMARY AND CONCLUSIONS

A series of experiments have been conducted on the use of machine vision technology for measurement of bruising in apples. Particular emphasis has been given to comparing both the image analysis and the traditional manual methods for apple bruise area and volume measurement.

The measurement of apple bruise size by manual methods requires both measurement and the assumption of a geometric shape of the bruise. Owing to the variation in bruise colour and shapes, significant subjectivity is required. The application of image techniques appears to provide a more accurate method for the measurement of bruising in apple.

A basic system using the image technology has been used for the detection and measurement of apple bruise. The system consisted of camera, computer, lighting set, system support, and associated equipment. The optimum illumination conditions of the system, appropriate positions of the camera and the apple bruise surface, and the suitable image processing algorithms were established and maintained for measurement throughout the whole study in order to make the results comparable.

Experiments were conducted on both stored and fresh 'Granny Smith' apples. Various sizes of apple bruises were produced by impacting apples using a pendulum device, or by dropping steel and hockey balls onto apples. Apple bruise width, depth, surface area, and volume were and compared with manual measurements.

The bruise width and depth from the central cross-section of a bruise measured by the image analysis and the manual method were not significantly different either for the stored and fresh apples, irrespective of the way in which the bruise was produced (Chapter 3). The bruise volumes calculated from measured bruise width and depth by the two methods were therefore not different. However, variations in the measured and estimated bruise parameters, including bruise width, depth, and volume, from the image analysis were less than those in the manual measurement (Chapter 3). The study also gave more consistent results using the image analysis. It was concluded that the image analysis could be used to measure and estimate apple bruise width, depth and volume reliably.

Measurement of apple bruise surface area without assuming a bruise shape using the image analysis was evaluated in the study (Chapter 4). Various types of apple bruise with varying colour, shape and size were all measured satisfactorily. The experiments confirmed that image analysis was a reliable method for measurement of apple bruise surface area due to far less variation in the bruise area among the replicates when compared with manual measurement. However, a significant difference existed in bruise areas measured directly from image analysis and bruise area calculated from maximum and minimum diameter measurements assuming a geometric shape. Bruise areas obtained by manual methods consistently overestimated bruise areas by about 10%.

A new approach for apple bruise volume determination by multiple sectioning using image analysis was developed (Chapter 5). In this approach bruise volume was determined by measuring a series of bruise slice areas. The method overcome errors in bruise volume calculations introduced by assuming geometric shapes, and offered a consistent way to determine bruise volume through a proper machine set up.

From the study it was concluded that the application of image analysis technology can offer an alternative way to detect and measure apple bruise. Compared with the traditional manual method, the technique can determine apple bruise width, depth, area, and volume accurately and quickly. The results of this study provide a basic image analysis technique for scientists and the fruit industry to give more precise measurement of fruit bruises during mechanical handling operations.

Due to the ease of bruise area measurement using the developed image analysis technology, the relationship between the bruise volume and bruise surface area may be worth further examination in order to estimate bruise volume from bruise area for different conditions of apple.

REFERENCES

Banks, N.H. and Studman, C.J. 1991. How to Reduce Bruises and Increase Returns. Technical Bulletin, New Zealand.

Bollen, A.F. and Cox, N.R. 1991. A Technique for predicting the probability of bruising for use with an instrumented sphere. The American Society of Agricultural Engineers Paper No. 91-6595.

Brown, G.K., Burton, C.L., Sargent, S.A., Schulte-Pason, N.L., Timm, E.J. and Marshall, D.E. 1987 Apple packing line damage assessment. The American society of Agricultural Engineers, Paper No. 87-6515.

Brown, G.K., Schulte-pason, N.L. and Timm, E.J. 1990 Impact classification using the instrumented sphere. American Society of Agricultural Engineers, Paper No. 90-6001.

Brusewitz, G.H. and Bartsch, J.A. 1989. Impact Parameters Related to Post Harvest Bruising of Apples. American Society of Agricultural Engineers, Vol. 32 (3), pp. 953-957.

Chen, P. and Sun, Z. 1981. Impact parameters related to bruise injury in apples. The American Society of Agricultural Engineers, Paper No. 81-3041.

Chen, P. and Yazdani, R. 1991. Prediction of apple bruising due to impact on different surfaces. Transactions of the American Society of Agricultural Engineers, Vol. 34(3), pp. 956-961.

Collett, A. Kerr, J., Ireland, M., Brownd, J. and Hall, D. 1991. The Design of a System for Measuring the Area of Bruise on Apples. Advanced Industrial Engineering. Massey University, New Zealand.

Davenal, A. Guizard, CH., Labarre, T. and Sevila, F. 1988. Automatic Detection of surface Defects on Fruit by Using a Vision System.

Diener, R.G., Mitchell, J.P. and Rhoten, M.L. 1970. Using an X-ray image scan to sort bruised apples. Agricultural Engineering, Vol. 51, pp. 356-357.

Foster, B.R., Hodgson, R.M., Browne, R.F. and Studman, C.J. 1991. Stem End Split Detection in Apples. 6th New Zealand Image Processing Workshop, pp. 157.

Geoola, Farh., Geoola, Fara. and Peiper, U.M. 1994. A spectrophotometric method for detecting surface bruises on 'Golden Delicious' apples. Journal of Agricultural Engineering Research, Vol. 58, pp 47-51.

Gunasekaran, S., Cooper, T.M., Berage, A.G. and Krichnan, P. 1987. Image Processing for Stress Cracks in Corn Kernels. Transactions of the American Society of Agricultural Engineers, Vol. 30(1), pp. 266 - 271.

Gunasekaran, S., Cooper, T.M. and Berlage, A.G. 1988. Soybean Seed Coat and Cotyledon Crack Detection by Image Processing. Journal of Agricultural Engineering Research, Vol. 41, pp. 139-148.

Hodgson, B. 1984. Automated inspection and grading. New Zealand Kiwifruit Special Publication. Vol. 4, pp. 32-34.

Holcomb, D.P., Cooke, J.R. and Hartman, P.L. 1977. A study of electrical thermal and mechanical properties of apples in relation to bruise detection. The American Society of Agricultural Engineers, Paper No. 77-3512.

Holt, J. E. and Schoorl, D. 1977. Bruising and energy dissipation in apples. Journal of Textural Studies Vol. 7, pp. 421-432.

Kader, A.A. 1985. Postharvest biology and technology: An overview in 'postharvest technology of horticultural crops, University of California, California. pp. 15-30.

Kassler, M., Corke, P.I. and Wong, P.C. 1993. Automatic grading and packing of prawns. Computer and Electronics in Agriculture. Elsevier Science Publishers B.V., Amsterdam. Vol. 9, pp. 319-333.

Klein, J.D. 1987. Relationship of Harvest Date, Storage Conditions, and Fruit Characteristics to Bruise Susceptibility of Apple. Journal of American Society of Horticulture Science. Vol. 112 (1), pp. 113-118.

Kokko, E.G., Volkmar, K.M. Gowen B.E. and Entz, T. 1993. Determination of total root surface area in soil core samples by image analysis. Soil & Tillage Research, Vol. 26, pp. 33 - 43.

Koppi, A.J., McKenzie, D.C. Douglas, K.T. 1994. Image of soil structure for illustration of machinery effects. Journal of Agricultural Engineering Research, Vol. 57, pp. 67 - 72.

McBratney, A.b., Moran, C.J., Stewart, J.B., Cattle S.R. and Koppi, A.J. 1992. Modification to a method of rapid assessment of soil macrospore structure by image analysis. Geoderma, Elsevier Science Publishers B.V., Amsterdam. Vol. 53, pp. 255-274.

McDonald, T. and Chen, Y.R. 1990. Application of Morphological Image Processing in Agriculture. Transactions of the American Society of Agricultural Engineers, Vol. 33 (4), pp. 1345-1352.

Miller, B.K. and Delwiche, M. J. 1989. A Colour Vision system for Peach Grading. Transactions of the ASAE, Vol. 32 (4), pp. 1485-1490.

Minagawa, H., Saito, S. and Ichikawa, T. 1993. Determining the weight of pigs with an image analysis system. In Livestock Environment IV, Fourth International Symposium University of Warwick, Coventry, England. 6 - 9 July 1993. Published by American Society of Agricultural Engineers. pp. 528-535.

Mohsenin, N. N. 1970. Physical Properties of Plant and Animal Materials. Gordon and Breach: New York.

Morrison, J.E. and Chichester, F.W. 1991. Still Video Image Analysis of Crop Residue Soil Covers. Transactions of the ASAE, Vol. 34(6), pp. 2469 -2474.

Mowatt, C.M. and Banks, N.H. 1994. Reduction of bruising in apples. Project report to ENZA international, New Zealand.

Ouyang, L. 1993. Mechanical Properties of biomaterials. (unpublished report which for assignment). Department of Agricultural Engineering, Massey University, New Zealand.

Pang, W., Studman, C.J. and Banks, N.H. 1992. Analysis of damage thresholds in apple-to-apple impacts using an instrumented sphere. New Zealand Journal of Crop and Horticultural Science, Vol. 20, pp. 159-166.

Pang, W. 1994. Prediction and quantification of apple bruising. PhD thesis, Department of Agricultural Engineering, Massey University, New Zealand.

Paulsen, M.R. and McClure, W.F. 1986. Illumination for Computer vision Systems. Transactions of the ASAE, Vol. 29 (5), pp. 1398-1404.

Pen, C.L., Bilanski, W.K. and Fuzzen, D.R. 1985. Classification Analysis of Good and Bruised Peeled Apple Tissue Using Optical Reflectance. Transactions of the ASAE, pp. 326-330.

Rehkugler, G.E. and Throop, J.A. 1986. Apple Sorting with Machine Vision. Transactions of the ASAE, Vol. 29(5), pp. 1388-1397.

Rehkugler, G.E. and Throop, J. 1989. Image Processing Algorithm for Apple Defect Detection. Transactions of the ASAE, Vol. 32 (1), pp. 267-272.

Roudot, A.-C., Duprat, F. and Nicolas, J. 1988. Slice Imaging to Quantify Kiwifruit Storage Defects. Sciences Des Aliments, Vol. 8, pp. 369-381.

Samim, W. and Banks, N.H. 1993a. Colour changes in bruised apple fruit tissue. New Zealand Journal of Crop and Horticultural Science. The Royal Society of New Zealand, New Zealand. Vol. 21, pp. 367-372.

Samim, W. and Banks, N.H. 1993b. Effect of fruit water status on bruise susceptibility and bruise colour of apples. New Zealand Journal of Crop and Horticultural Science. The Royal Society of New Zealand, New Zealand. Vol. 21, pp. 373-376.

Sarkar, N. and Wolfe, R.R. 1985. Computer vision based system for quality separation of fresh market tomatoes. Transactions of the ASAE, Vol. 28(5), pp. 1714 - 1718.

Schofield, C.P. 1993. Image analysis for non-intrusive weight and activity monitoring of live pigs. In Livestock Environment IV, Fourth International Symposium University of Warwick, Coventry, England. 6-9 July 1993. Published by American Society of Agricultural Engineers. pp. 503 - 510.

Schoorl, D. and Holt, J.E. 1977. The Effects of Storage Time and Temperature on the Bruising of Jonathan, Delicious and Granny Smith Apples. Journal of Texture Studies, Vol. 8, pp. 409-416.

Schoorl, D. and Holt, J.E. 1980. Research Note: Bruise Resistance measurements in apples. Journal of Texture Studies, Vol. 11, pp. 389-394.

Schulte, N.L., Brown, G.K. and Timm, E.J. 1992. Apple Impact Damage Thresholds. Applied Engineering in Agriculture, Vol. 8 (1), pp. 55-60.

Shearer, S.A. and Payne, F.A. 1990. Colour and Defect Sorting of Bell Peppers Using Machine Vision. Transactions of the American Society of Agricultural Engineers, Vol. 33(6), pp. 2045-2050.

Slaughter, D.C. and Harrell, R.C. 1987. Colour vision in robotic fruit harvesting. Transactions of the ASAE, Vol. 30(4), pp. 1144 - 1148.

Sober, S.S., Zepp, H.R. and Brown, G.K., (1989) Simulated packing line impacts for apple bruise prediction. American Society of Agricultural Engineers, paper No. 89-6047.

Srivastava, A.K., Mandhar, S.C. and Singh, M.D. 1992. Apple bruise prediction models using dimensional analysis. Agricultural Engineering Journal Vol. 1 (1), pp. 35-52.

Storlie, C.A., Stepanek, A. and Meyer, G.E. 1989. Growth Analysis of Whole Plants Using Video Imagery. Transactions of the ASAE. Vol. 32(6), pp. 2185-2194.

Studman, C.J. and Banks, N.H. 1990. The measurement of bruise susceptibility in apples and nashi. Proceedings of International Conference of Agricultural Engineering, Beijing, China, Vol. 3, pp. 31-36.

Taylor, R.W., Rehkugler, G.E. and Throop, J.A. 1984. Apple bruise detection using a digital line scan camera system. Agricultural electronics - 1983 and Beyond, The American Society of Agricultural Engineers, pp. 652-662.

Throop, J.A., Rehkugler, G.E. and Upchurch, B.L. 1989. Application of Computer Vision for Detecting Watercore in Apples. Transactions of the American Society of Agricultural Engineers Vol. 32 (6), pp. 2087-2092.

Throop, J.A. and Aneshansley, D.J. 1993. Improvements in an image processing algorithm to find new and old bruises. The American Society of Agricultural Engineers, paper No. 936534.

Topping, A.J. and Luton, M.T. 1986. Cultivar differences in the bruising of English apples. Journal of Horticultural Science, Vol. 61 (1), pp. 9-13.

Upchurch, B.L., Throop, J.A. and Aneshansley, D.J. 1993. Influence of time and bruise-type on near-infrared reflectance for automatic bruise detection. The American Society of Agricultural Engineers, paper No. 933596.

Vergano, P.J., Testin, R. J. and Newall, W. 1991. Peach Bruising: Susceptibility to impact, Vibration, and Compression Abuse. Transactions of the American Society of Agricultural Engineers, Vol. 34 (5), pp. 2110-2116.

Volkmar, K.M. 1993. A Comparison of minirhizotron techniques for estimating root length density in soils of different bulk densities. Plant and Soil, Vol. 157, pp. 239 - 245.

Vooren, J.G., Polder, G. and Heijden, G.W. 1991. Application of image analysis for variety testing of mushroom. Euphytica, Vol. 57, pp. 245 - 250.

Vooren, J.G., Polder, G. and Heijden, G.W. 1992. Identification of Mushroom Cultivars Using Image Analysis. Transactions of the American Society of Agricultural Engineers, Vol. 35(1), pp. 347-350.

Vooren, J.G. and Heijden, G.W. 1993. Measurement of the size of fresh beans with image analysis, Plant Varieties and Seeds, Vol. 6, pp. 47 -53.

Yang, Q. 1992. The Potential for Applying Machine Vision to Defect Detection in Fruit and Vegetable Grading. Agricultural Engineer Incorporating Soil and Water, pp. 75-79.

Yanuka, M. and Elrick, D.E. 1985. Application of Microcomputer-Based Image Digitisation in Soil and Crop Sciences. computers and Electronics in Agriculture. Elsevier Science Publishers B.V., Amsterdam. Vol. 1, pp. 59 - 73.

Zhang, W. 1992. Apple bruise susceptibility vs temperature and storage humidity. Paper of the American Society of Agricultural Engineers, No. 92-6009.

APPENDIX 1

Algorithm 1 (used in Chapter 3)

```
PROGRAM 0
IF %EXIST( calib_a ) = 0
LOAD cal.vip cal
BEEP 3
WRITE "You need to do a calibration first!" /LINE
LET camera = #1
RUN cal ,, camera
END
  set output /off
  WRITE "Place sample in right position."
  cap #1                              ! Capture from off the video
  get a (0 0) (512 512)
  set cursor
  disp a
  box ave a g (3 2)        ! Remove colour subcarrier interference
  INQUIRE "Enter your sample number " /LINE s_no
  FILE /WRITE/APPEND Data
  WRITE /FILE """" s_no """" /LINE
  BEEP 2
  WRITE "Image type:" /L "S - Slices" /L "H - Hockey ball" /L  "B - Ball
 bearing" /L "Q - Quit" /L
 INQUIRE "Enter your selection: " /ENT reply
 IF reply = "Q"
  EXIT
END
IF reply = "s"
  IF %EXIST( p1 ) = 0
    DECLARE LIST p1 p2
  END
  hist get g h
  HIST smooth h hs 9
  STAT hs ,,,, mn1
  STAT hs 0 mn1 ,, mbg
  LET a = g
  THRESHOLD a mbg
  CHAIN CODE a ck
  CHAIN SORT ck ckk 50 200          ! Discard noise bits
  CHAIN SIZE ckk p1 p2
  LET p2 = p2 - p1 + (31 31)
  LET p1 = (15 15) - p1
  CHAIN BRANCH ckk n
ELSE
  LET p1 = {(0 0)}
```

```
  LET p2 = {(512 512)}
  LET n = 1
 END
 LET total = 0.0
 LET total2 = 0.0
 FOR n = n 1 -1          ! Process each slice (or 1 for whole image)
  IF %EXIST(a) = 1
   DELETE a
  END
  DECLARE IMAGE %INDEX( p2 n ) a
  IF reply = "S"
   SELECT ckk cs n
   COPY g a %INDEX( p1 n )
   LET b = a
   TEST b
CHAIN DRAW cs b 255 /FILL %INDEX( p1 n )  !Get a mask for this
slice
   BOX MAX b c 5            Allow a boundary around the sides
   LET b = c
   AND c a
   LET a = c
   THRESH a 0 0
   CLIP a 0 mbg
   OR a c
   DISPLAY a         ! This slice
  ELSE
   LET a = g         ! Whole image
  END
  box enh a b 9 ! Enhance any boundaries
  box ave b c 5
  box enh c b 7
  box max b c 11        ! Remove cracks in the fruit
  box min c d 11
  disp d
  hist get d h
  hist sm h hs 9
  STATISTICS hs ,,,, mn1
  STATISTICS hs 0 mn1 ,, mn2
  IF reply = "B"
   LET hmin = (mn2 * 4 + mn1) / 5
  ELSE
   HULL hs mn2 mn1 hmin
   LET hmin = (hmin + mn1) / 2
  END
  STATISTICS hs mn1 ,,, mn1
  LET mn2 = (mn1 + mn2) / 2
  LET mn3 = (mn1 + mn2) / 2
  hull hs mn2 mn1 hmax          ! Find suitable threshold levels
  let e3 = d
  thresh e3 hmin hmax           ! Bruised regions
```

```
  BOX MIN e3 e
  BOX MAX e e3              ! Just tidy up a little
  chain code e3 cc
  DISPLAY a
  CHAIN DRAW cc d /disp    ! Overlay detected regions on original
  INQUIRE "Click on area you want to measure: " p
  IF p = (0 0)
  ELSE
   select cc cs  p
   test e3
   chain draw cs e3 /fill
   area cs csa
   LET csa = csa * calib_a
   write "Area is" csa " square mm"
   LET total = total + csa
   chain rectangle cs len wid
   WRITE ", or" (len * calib_w) " mm x" (wid * calib_w) " mm." /LINE
   WRITE /FILE csa (len * calib_w) (wid * calib_w)
   LET ci = cs
   CHAIN CUT ci 0.1 0.2
   SELECT ci cii p              ! Select middle bruise part
   area cii csa
   LET csa = csa * calib_a
   write "Area is" csa " square mm"
   LET total2 = total2 + csa
   chain rectangle cii len wid
   WRITE ", or" (len * calib_w) " mm x" (wid * calib_w) " mm." /LINE
   WRITE /FILE csa (len * calib_w) (wid * calib_w) /LINE
   CHAIN DRAW cii a /disp 0
   INQUIRE "Enter any comments: " /LINE comment
   WRITE /FILE """" comment """" /LINE
  END
 END

 IF reply = "Y"
  WRITE /LINE "Total areas are" total " sq mm, and" total2 " sq
mm"/LINE
  WRITE /FILE "Totals:" total total2 /LINE
 END
 FILE /WRITE/CLOSE
END
```

Algorithm 2 (used in Chapters 4 and 5)

```
PROGRAM 0
 IF %EXIST( calib_a ) = 0
  LOAD cal.vip cal
  BEEP 3
  WRITE "You need to do a calibration first!" /LINE
  LET camera = #1
  RUN cal ,, camera
  DECLARE colour colour
 END
  set output /off
 WRITE "Place sample in right position."
  cap #1                  ! Capture from off the video
  get colour (0 0) (512 512)
  colour colour a /green
  set cursor
  disp a
  box ave a g (3 2)
 INQUIRE "Enter your sample number " /LINE s_no
 FILE /WRITE/APPEND Data
 WRITE /FILE """" s_no """" /LINE
 BEEP 2
 BOX AVERAGE a b 5
 AVERAGE b c /ROW/FILL/MAX
 DIVIDE b c
 AVERAGE b c /COL/FILL/MAX
 DIVIDE b c
 BOX AVERAGE b c 5
 HISTOGRAM GET c h
 HISTOGRAM SMOOTH h hs
 HULL hs ,,, hv
 THRESHOLD c 0 hv
 CHAIN CODE c cc
 LET d = a
 CHAIN DRAW cc a 0         ! Overlay detected regions on original
 DISPLAY a
 INQUIRE "Click on area you want to measure: " p
 IF p = (0 0)
 ELSE
    select cc cs  p
    area cs csa
    LET csa = csa * calib_a
    write "Area is" csa " square mm"
    chain rectangle cs len wid
    WRITE ", or" (len * calib_w) " mm x" (wid * calib_w) " mm." /LINE
    WRITE /FILE csa (len * calib_w) (wid * calib_w) /LINE
    LET ci = cs
```

```
    SELECT ci cii p              ! Select middle bruise part
    DISPLAY COLOUR
    CHAIN DRAW cii a /disp 0
    INQUIRE "Enter any comments: " /LINE comment
    WRITE /FILE """" comment """" /LINE
   END

  FILE /WRITE/CLOSE
END
```

APPENDIX 2

(Data from Chapter 3)

Table 3.1 The date of bruise widths, depths, and volumes measured by image analysis and manual method for the stored apple with the bruise produced by the pendulum impact

Sample	Impact Angle	Bruise Width (mm)		Bruise Depth (mm)		Bruise Volume (mm^3)	
Number	(°)	IA	MU	IA	MU	IA	MU
1	30	10.66	9.14	3.59	3.86	200.33	165.30
2	30	9.04	10.74	3.77	2.99	167.88	165.73
3	30	10.33	10.71	3.47	3.58	181.61	201.84
4	30	18.13	16.27	3.11	4.62	555.21	620.96
5	30	6.79	9.80	2.86	2.89	86.78	133.70
6	30	7.32	9.31	3.67	3.69	767.61	837.74
7	30	15.06	14.35	4.17	4.68	141.35	161.77
8	30	16.48	15.66	4.32	4.88	473.73	485.07
9	30	17.79	17.78	7.52	6.10	599.31	609.19
10	30	16.43	16.06	4.00	4.70	1285.20	1003.90
11	30	16.57	15.22	5.11	6.02	550.73	615.37
12	30	10.46	13.92	4.28	5.32	724.81	735.55
13	30	13.17	15.53	4.62	4.54	240.03	531.30
14	30	14.44	14.26	6.30	6.05	403.83	551.92
15	30	11.50	12.78	5.35	5.73	702.52	652.07
16	30	18.74	17.43	4.11	5.33	380.71	500.72
17	30	16.56	15.98	5.69	6.10	808.01	816.06
18	45	29.05	27.31	4.81	5.08	2570.42	2269.42
19	45	26.93	25.10	5.48	6.76	2315.09	2335.49
20	45	18.56	17.73	6.18	6.23	1111.24	1216.33
21	45	22.78	21.86	6.97	6.49	1945.22	1919.42
22	45	19.88	19.81	6.23	6.71	1302.17	1397.91
23	45	19.42	19.88	5.29	5.11	1052.12	1277.80
24	45	18.29	17.70	4.43	4.60	1177.49	1093.71
25	45	19.78	19.55	6.52	6.80	1340.19	1369.59
26	45	18.77	17.70	6.44	7.15	1192.00	1198.06
27	45	17.38	19.72	8.33	8.11	1409.82	1716.50
28	45	19.15	21.31	7.19	7.70	1402.49	1878.08
29	45	19.10	17.64	7.90	7.42	1560.76	1244.45
30	45	16.57	19.13	5.11	7.09	718.85	1380.55
31	45	16.71	16.49	6.42	6.45	949.98	931.11
32	45	18.99	19.73	5.99	5.69	1127.83	1160.53
33	45	17.81	19.74	6.21	5.68	1025.57	1157.22

(Table 3.1 continues)

34	45	18.96	18.20	6.60	5.75	1252.72	992.01
35	60	34.69	31.98	7.08	7.25	5439.42	4473.80
36	60	28.03	29.59	6.50	6.74	2936.18	3460.21
37	60	21.39	21.04	6.43	6.28	1564.01	1519.53
38	60	24.19	22.08	7.39	7.76	2353.19	2036.37
39	60	21.68	22.71	7.43	7.01	1882.69	2149.44
40	60	24.45	23.41	7.47	8.12	2459.16	2435.82
41	60	21.20	21.84	7.10	6.93	2013.13	2054.03
42	60	22.98	21.39	7.33	7.22	1800.74	1759.69
43	60	22.97	22.50	7.34	8.05	2093.45	2209.49
44	60	22.01	23.41	7.44	8.12	1941.56	2426.86
45	60	23.68	22.38	7.07	7.43	2150.21	2118.02
46	60	23.82	23.05	8.00	8.62	2469.52	2500.22
47	60	21.87	22.19	8.47	8.01	2210.16	2237.43
48	60	23.40	21.81	8.00	8.72	2409.88	2292.38
49	60	23.58	23.75	7.59	8.30	2288.03	2557.10
50	60	22.57	23.76	8.85	8.31	2463.61	2549.93
51	60	19.61	18.93	5.99	5.86	1212.60	1099.45

Table 3.2 The data of bruise widths, depths, and volumes measured by image analysis and manual method for the fresh apple with the bruise produced by the pendulum

Sample	Impact	Bruise Width		Bruise Depth		Bruise Volume	
	Angle	(mm)		(mm)		(mm^3)	
Number	(°)	IA	MU	IA	MU	IA	MU
1	60	28.26	28.40	7.71	8.61	3471.31	3891.06
2	60	29.25	27.99	7.58	8.31	3711.40	3638.94
3	60	29.26	28.42	6.14	8.92	3135.64	4043.44
4	60	27.49	27.89	8.54	8.35	3595.76	3635.57
5	60	32.77	28.79	8.57	8.64	5460.57	4039.99
6	60	29.16	27.87	6.66	8.28	3316.87	3601.97
7	60	28.16	29.78	6.38	8.02	2992.98	4158.43
8	60	29.34	29.88	6.28	8.20	3283.05	4274.14
9	60	26.76	27.89	8.01	7.03	3195.74	3128.10
10	60	27.67	26.66	8.62	8.43	3700.04	3330.42
11	60	30.53	24.27	7.59	6.96	4183.99	2246.05
12	60	24.18	27.60	8.04	8.08	2570.61	3470.44
13	60	28.68	29.82	8.24	7.77	3857.13	4018.50
14	60	30.87	28.56	8.17	8.44	4564.86	3905.37
15	60	27.07	27.83	8.41	7.88	3454.23	3462.59
16	60	28.72	27.82	7.88	8.02	3730.09	3516.10
17	60	31.85	30.41	8.64	8.22	5197.02	4446.79
18	60	26.80	26.20	9.20	8.28	3698.85	3163.99
19	60	31.42	27.12	8.59	8.19	4969.74	3367.27
20	60	30.09	26.01	8.72	7.92	4541.64	2966.17

Table 3.3 The data of bruise widths, depths and volumes measured by image analysis and manual method for the stored apples with the bruise produced by the steel ball from 200 mm of drop height

Sample	Bruise width (mm)		Bruise depth (mm)		Bruise volume (mm^3)	
number	IA	MU	IA	MU	IA	MU
1	14.43	16.20	7.42	7.19	875.25	1022.84
2	17.78	16.33	6.83	7.15	1145.33	1032.69
3	19.34	16.66	8.57	6.96	1773.56	1036.49
4	17.55	17.01	6.38	6.85	1035.56	1059.29
5	17.10	17.47	6.44	6.92	989.59	1123.05
6	18.53	16.37	8.14	7.47	1537.82	1099.95
7	18.72	16.96	7.86	6.49	1496.17	983.79
8	15.52	16.25	6.61	7.42	849.99	1071.80
9	17.96	16.94	8.14	7.03	1446.66	1079.34
10	16.80	16.77	7.58	7.70	1171.38	1191.88
11	18.09	17.01	7.32	7.34	1291.81	1154.64
12	17.54	17.58	7.11	7.05	1170.83	1163.89
13	16.63	16.77	7.15	7.63	1068.17	1178.91
14	15.37	15.62	7.17	7.32	926.75	979.92
15	15.55	16.03	7.55	7.07	1014.89	980.64
16	19.57	17.49	8.42	7.40	1769.88	1222.34
17	16.29	17.34	7.35	7.62	1061.66	1244.44
18	15.09	16.49	7.79	7.15	1010.17	1049.53
19	16.73	16.92	7.40	8.00	1124.90	1271.42
20	17.01	17.42	7.5	7.63	1182.71	1262.55
21	17.26	16.82	8.23	7.79	1366.06	1213.35
22	18.59	15.7	7.65	7.53	1428.45	1031.09
23	17.47	17.39	6.91	7.61	1126.35	1257.53
24	17.74	17.27	6.56	7.49	1079.77	1205.94
25	19.63	17.32	8.31	7.20	1753.03	1161.18
26	16.77	16.06	7.15	7.07	1082.09	985.98
27	13.33	14.70	6.01	6.85	572.958	808.772
28	13.18	15.47	6.93	7.17	686.23	941.79
29	14.36	14.43	6.85	6.68	777.56	757.96
30	16.66	16.88	7.67	8.03	1172.35	1275.13

Note: Bruise volumes were calculated using Equations 2.3 and 2.4.

Table 3.4 Data of bruise widths, depths, and volumes measured by image analysis and manual method for the stored apples with the bruise produced by the hockey ball from 200 mm of drop height

Sample	Bruise width (mm)		Bruise depth (mm)		Bruise volume (mm^3)	
number	IA	MU	IA	MU	IA	MU
1	22.54	19.08	6.51	7.25	1773.60	1403.96
2	17.85	18.80	5.99	6.74	989.84	1253.37
3	18.75	18.14	5.91	7.04	1071.66	1221.48
4	21.51	18.81	7.77	6.85	1942.42	1285.54
5	20.77	17.79	5.71	5.65	1306.91	925.95
6	22.51	20.45	6.90	6.81	1862.22	1498.73
7	21.28	19.19	7.05	7.07	1699.88	1380.22
8	16.23	16.83	6.28	6.62	868.44	991.46
9	17.66	17.82	6.94	6.69	1148.73	1119.41
10	20.28	19.97	7.8	7.46	1725.32	1589.65
11	21.49	19.24	7.47	7.09	1853.48	1396.39
12	15.47	16.07	5.44	6.12	671.54	829.23
13	16.60	16.71	6.51	6.72	946.47	995.92
14	17.73	17.34	5.80	6.11	945.85	957.56
15	17.36	18.70	6.01	6.22	940.30	1135.97
16	17.24	17.99	6.67	6.65	1049.41	1136.41
17	17.28	17.03	7.55	6.43	1218.22	973.044
18	15.82	16.65	6.04	6.92	784.51	1019.61
19	20.59	19.37	7.33	7.17	1653.26	1426.45
20	18.22	18.77	5.69	7.12	974.55	1327.66
21	14.45	17.92	5.40	5.43	580.44	900.24
22	14.35	15.92	4.68	5.91	487.32	780.12
23	17.50	18.37	5.81	6.63	924.27	1180.60
24	17.42	17.82	5.57	5.93	875.17	981.19
25	16.73	16.6	6.57	6.68	966.10	971.44
26	17.17	18.14	5.42	6.75	814.80	1162.94
27	16.79	17.29	5.24	6.38	758.99	1001.46
28	19.72	16.67	8.11	6.19	1712.81	898.61
29	16.10	18.01	5.16	5.97	681.53	1004.43
30	20.25	18.46	6.74	6.03	1457.80	1067.64

Note: Bruise volumes were calculated using Equations 2.3 and 2.4.

Table 3.5 The data of bruise widths, depths, and volumes measured by image analysis and manual method for the fresh apples with the bruise produce by the steel ball from 200 mm of drop height

Sample	Bruise width (mm)		Bruise depth (mm)		Bruise volume (mm^3)	
number	IA	MU	IA	MU	IA	MU
1	19.88	17.58	8.95	8.16	1957.337	1392.168
2	19.47	17.41	8.58	8.9	1785.321	1541.208
3	19.26	18.65	8.87	8.73	1832.586	1694.488
4	18.82	18.27	7.26	8.53	1369.786	1584.502
5	18.49	18.33	8.22	8.39	1548.603	1565.078
6	18.34	19.88	8.16	8.19	1511.523	1765.638
7	17.13	16.03	8.21	7.75	1342.145	1107.107
8	19.86	17.19	8.58	7.99	1853.123	1302.12
9	19.34	18.57	7.76	8.14	1569.216	1541.36
10	19.94	17.73	7.78	8.51	1670.424	1503.021
11	15.95	15.61	7.55	7.87	1062.557	1084.295
12	19.15	18.99	9.05	9.04	1865.071	1834.874
13	16.41	18.24	6.25	8.42	881.5559	1554.687
14	19.81	17.35	8.97	8.11	1958.702	1354.023
15	16.18	19.39	6.76	8.62	947.6962	1797.14
16	17.65	17.7	9.53	8.59	1748.062	1519.33
17	16.69	16.83	7.96	7.89	1236.958	1240.456
18	17.15	17.9	7.51	7.73	1203.271	1350.108
19	19.56	17.36	7.64	8.57	1579.297	1465.733
20	17.47	17.78	8.18	7.57	1392.115	1301.35

Table 3.6 Data of bruise widths, depths, and volumes measured by image analysis and manual method for the fresh apples with the bruise produced by the hockey ball from 200 mm of drop height

Sample	Bruise width (mm)		Bruise depth (mm)		Bruise volume (mm^3)	
number	IA	MU	IA	MU	IA	MU
1	21.45	19.79	7.9	8.17	1964.85	1743.439
2	20.22	20.65	6.01	6.54	1298.579	1481.149
3	18.8	17.98	6.38	5.93	1184.09	997.7949
4	18.56	19.82	6.53	7.05	1183.477	1472.371
5	18.96	19.06	7.14	6.73	1378.497	1303.611
6	18.55	19.22	5.97	7.14	1082.947	1416.557
7	21.32	19.25	7.96	7.53	1965.854	1504.91
8	18.1	18.7	7.11	6.75	1247.537	1253.058
9	18.9	18.75	7.05	6.9	1342.847	1289.64
10	18.48	19.87	6.9	6.98	1252.983	1469.055
11	20.12	19.72	7.12	6.29	1533.618	1287.079
12	20.17	18.66	8.08	7.16	1781.867	1328.005
13	20.09	19.42	6.44	7.37	1380.847	1492.971
14	20.89	19.38	7.48	7.05	1758.978	1413.587
15	21.83	21.8	8.85	8.18	2326.327	2118.78
16	18.69	19.54	6.31	6.94	1160.895	1411.622
17	22.46	23.97	7.65	8.73	2082.006	2750.806
18	18.7	18.93	6.81	7.19	1258.547	1372.4
19	21.72	22.10	8.18	7.56	2096.726	1992.578
20	18.98	19.54	6.61	6.78	1256.968	1371.744

APPENDIX 3

(Date from Chapter 4)

Table 4.1 Data of bruise surface area measured on stored apples impacted by the steel ball from three drop heights

Sample number	Drop height (mm)	IA * D_1 (mm)	IA * D_2 (mm)	MU ** D_1 (mm)	MU ** D_2 (mm)	Bruise surface area (mm^2) IA	Bruise surface area (mm^2) IAC***	Bruise surface area (mm^2) MU
1	100	14.43	11.63	13.24	11.30	125.56	131.73	117.50
2	100	15.32	12.47	14.75	12.32	128.55	150.00	142.72
3	100	15.02	13.77	12.09	11.99	143.68	162.46	113.85
4	100	14.09	12.11	12.61	11.99	122.43	133.93	118.75
5	100	16.51	12.83	13.44	12.37	146.18	166.24	130.57
6	100	14.15	11.65	12.67	12.05	114.21	129.47	119.91
7	100	13.43	12.54	13.89	12.89	127.25	132.20	140.62
8	100	14.99	14.09	17.95	13.10	141.90	165.81	184.68
9	100	16.42	12.52	15.74	14.19	147.34	161.28	175.42
10	100	12.67	10.99	12.77	12.38	89.20	109.34	124.17
Mean		**14.70**	**12.46**	**13.92**	**12.46**	**128.63**	**144.25**	**136.82**
11	200	15.72	14.99	16.93	15.70	171.55	184.92	208.76
12	200	15.26	15.15	16.85	15.67	175.79	181.48	207.38
13	200	15.98	14.90	15.98	15.46	175.11	186.91	194.03
14	200	17.06	16.02	15.87	15.32	192.88	214.54	190.95
15	200	17.36	15.60	15.69	15.18	200.32	212.56	187.06
16	200	15.97	15.10	15.85	15.26	176.93	189.23	189.97
17	200	16.38	15.45	16.16	15.92	186.20	198.74	202.06
18	200	15.91	15.14	16.03	15.17	181.69	189.10	190.99
19	200	15.20	15.12	17.82	16.81	173.01	180.41	235.27
20	200	16.75	16.13	16.55	15.87	199.55	212.09	206.28
Mean		**16.16**	**15.36**	**16.37**	**15.64**	**183.30**	**195.00**	**201.27**
21	300	25.14	19.49	26.17	19.03	338.40	384.74	391.14
22	300	21.64	20.16	20.01	16.51	309.92	342.46	259.47
23	300	17.20	15.94	18.57	19.07	209.51	215.27	278.13
24	300	19.28	18.73	17.73	16.22	268.05	283.47	225.87
25	300	21.59	19.87	17.66	19.00	302.87	336.68	263.53
26	300	21.64	19.44	22.04	18.06	312.39	330.23	312.62
27	300	29.06	22.44	29.36	19.96	459.54	511.99	460.26
28	300	20.67	20.65	22.14	18.82	276.89	334.99	327.26
29	300	18.50	17.97	18.91	18.79	254.90	260.87	279.07
30	300	24.88	20.27	24.14	18.67	356.08	395.80	353.97
Mean		**21.96**	**19.49**	**21.67**	**18.41**	**308.85**	**339.65**	**315.13**

Note: * Image analysis;

** Manually;

*** Measured by image analysis, but calculated by the formula.

Table 4.2 Data of bruise surface area measured on stored apples impacted by the hockey ball from 200 mm drop height

Sample	IA *		MU **		Bruise surface area (mm^2)		
	D_1	D_2	D_1	D_2			
number	(mm)	(mm)	(mm)	(mm)	IA	IAC***	MU
1	17.38	17.25	18.15	15.41	220.65	235.55	219.67
2	19.31	16.61	17.51	17.30	225.84	251.99	237.92
3	19.18	16.85	18.87	18.46	245.94	253.83	273.59
4	16.66	16.54	17.91	16.68	211.52	216.39	234.63
5	17.07	16.93	18.06	16.94	212.72	226.99	240.28
6	18.13	18.11	16.85	16.62	243.77	257.95	219.95
7	17.48	16.11	18.10	16.14	216.23	221.06	229.44
8	20.05	16.69	16.94	16.11	228.53	262.82	214.34
9	20.25	15.04	18.11	16.50	186.53	239.20	234.69
10	18.18	18.22	17.88	17.26	229.74	260.15	242.38
Mean	**18.37**	**16.84**	**17.84**	**16.74**	**222.15**	**242.59**	**234.69**

Note: * Image analysis;

** Manually;

*** Measured by image analysis, but calculated by the formula.

Table 4.3 Data of bruise surface area measured on stored apples impacted with the pendulum from a 45 impact angles

Sample	IA *		MU **		Bruise surface area (mm^2)		
	D_1	D_2	D_1	D_2			
number	(mm)	(mm)	(mm)	(mm)	IA	IAC***	MU
1	18.86	18.63	22.56	21.20	226.92	275.82	375.63
2	17.86	15.22	21.69	16.90	189.55	213.39	287.90
3	21.03	17.58	22.52	17.42	251.61	290.22	308.11
4	20.08	17.74	21.18	16.67	241.95	279.63	277.30
5	21.63	18.61	19.66	15.61	210.26	315.99	241.03
6	17.93	16.76	20.89	16.74	212.84	235.90	274.65
7	18.91	18.86	19.89	17.82	249.20	279.96	278.38
8	20.03	16.92	20.10	17.76	237.88	266.04	280.37
9	21.31	20.93	22.21	18.46	307.23	350.12	322.01
10	24.67	18.68	23.45	19.32	315.35	361.76	355.83
Mean	**20.23**	**17.99**	**21.42**	**17.79**	**244.28**	**286.88**	**300.12**

Note: * Image analysis;

** Manually;

*** Measured by image analysis, but calculated by the formula.

Table 4.4 Data of bruise surface area measured on fresh apples impacted by the steel ball from 200 mm drop height

Sample	IA		MU		Bruise surface area		
	D_1	D_2	D_1	D_2	(mm^2)		
number	(mm)	(mm)	(mm)	(mm)	IA	IAC	MU
1	17.47	16.10	15.96	15.54	212.61	220.79	194.79
2	17.64	15.92	17.52	16.65	210.41	220.45	229.11
3	17.12	16.15	16.71	16.03	203.96	217.04	210.38
4	17.30	16.14	15.52	15.40	206.21	219.19	187.72
5	17.24	16.58	17.55	16.73	199.34	224.38	230.60
6	18.61	17.28	17.69	16.61	219.29	252.44	230.77
7	17.02	16.51	17.21	15.95	204.05	220.59	215.59
8	17.24	16.40	17.01	16.79	223.37	221.95	224.31
9	17.19	16.47	17.12	16.59	217.22	222.25	223.07
10	16.13	15.71	16.65	15.63	185.38	198.92	204.39
11	16.11	16.08	16.47	15.04	186.72	203.35	194.55
12	17.73	16.79	17.19	16.46	237.72	233.68	222.23
13	16.85	16.23	17.40	15.85	208.89	214.68	216.60
14	16.12	15.61	16.64	16.05	200.38	197.53	209.76
15	15.38	14.99	16.10	15.87	176.59	180.98	200.67
16	17.96	17.48	15.83	15.35	234.87	246.44	190.84
17	17.14	17.01	16.71	16.15	220.98	228.87	211.95
18	17.56	16.47	16.58	16.39	220.82	227.03	213.43
19	17.88	15.70	17.14	16.88	214.54	220.36	227.23
20	16.14	15.58	16.44	16.08	187.65	197.40	207.62
Mean	**17.09**	**16.26**	**16.77**	**16.10**	**208.55**	**218.42**	**212.28**

Table 4.5 Data of bruise surface area measured on fresh apples impacted by hockey ball from 200 mm drop height

Sample	IA		MU		Bruise surface area		
	D_1	D_2	D_1	D_2	(mm^2)		
number	(mm)	(mm)	(mm)	(mm)	IA	IAC	MU
1	19.07	16.46	18.18	16.59	233.58	246.41	236.88
2	17.70	17.21	18.89	16.67	223.53	239.12	247.32
3	17.43	16.47	17.24	17.21	216.14	225.35	233.03
4	17.37	17.19	17.77	16.69	223.76	234.39	232.93
5	17.64	16.44	17.58	16.62	223.57	227.65	229.48
6	17.09	16.92	17.73	17.48	213.58	226.99	243.41
7	16.36	15.83	17.13	16.78	200.25	203.30	225.76
8	17.45	17.21	17.26	16.36	226.78	235.75	221.78
9	17.09	16.71	18.23	16.73	219.32	224.18	239.54
10	16.77	15.68	16.94	16.50	199.51	206.42	219.53
11	18.96	17.15	17.84	17.29	243.99	255.25	242.26
12	17.23	16.42	17.90	16.33	214.54	222.09	229.58
13	17.60	16.59	17.87	17.09	227.89	229.21	239.86
14	17.38	16.86	17.49	16.55	222.74	230.03	227.34
15	16.57	16.19	16.91	15.81	204.48	210.59	209.97
16	17.60	15.97	17.62	16.83	216.79	220.64	232.91
17	17.25	16.63	17.53	17.09	220.78	225.19	235.30
18	16.38	16.00	17.27	16.76	201.54	205.73	227.33
19	17.42	16.72	17.17	15.83	224.31	228.64	213.47
20	16.52	16.46	17.26	16.39	208.86	213.46	222.18
Mean	**17.34**	**16.56**	**17.59**	**16.68**	**218.30**	**225.52**	**230.49**

Table 4.6 Data of bruise surface area measured on fresh apples impacted with the pendulum from a 60 impact angles

Sample	IA		MU		Bruise surface area (mm^2)		
	D_1	D_2	D_1	D_2			
number	(mm)	(mm)	(mm)	(mm)	IA	IAC	MU
1	25.82	25.50	25.36	24.68	501.12	516.85	491.55
2	27.96	24.67	26.66	24.45	540.41	541.47	511.95
3	25.58	22.38	25.64	22.85	440.71	449.40	460.15
4	25.43	21.45	25.38	22.06	412.47	428.20	439.72
5	25.27	23.85	25.17	24.09	464.64	473.11	476.25
6	25.47	24.42	25.63	24.29	475.66	488.25	488.87
7	24.85	21.37	26.38	20.45	402.52	416.87	423.68
8	23.33	22.96	23.92	21.74	414.75	420.49	408.41
9	27.83	23.56	27.46	23.92	507.38	514.70	515.88
10	27.51	23.80	27.00	23.10	517.34	513.97	489.74
11	23.04	22.76	23.77	22.13	396.82	411.65	412.98
12	23.70	21.94	23.98	21.87	399.23	408.18	411.97
13	27.04	23.64	26.53	22.81	484.95	501.79	475.35
14	25.62	25.22	25.88	23.51	489.27	507.22	477.96
15	24.28	23.98	24.95	23.05	435.82	457.05	451.64
16	25.23	21.35	24.94	21.79	407.00	422.85	426.76
17	26.82	22.31	27.05	22.90	446.96	469.71	486.51
18	26.43	23.53	26.25	23.82	476.71	488.19	491.23
19	25.02	22.32	25.50	22.13	427.57	438.38	443.12
20	24.70	23.65	24.88	22.80	452.53	458.56	445.47
Mean	**25.55**	**23.23**	**25.62**	**22.92**	**454.69**	**466.34**	**461.46**

APPENDIX 4

(Data from Chapter 5)

Table 5.1 Data of bruise volumes determined by image analysis (V_{IA}) and manually (V_{MU}) in which three formulae (Eq 2.2, 2.3, and 2.5) were used for the bruises produced by the steel ball from 100 mm drop height

Apple No.	Slice No.	Thick -ness (mm)	Bruise depth (mm)	Slice area (mm^2)	Slice volume (mm^3)	$V_{(IA)}$ (mm^3)	D_{max} (mm)	D_{min} (mm)	$V_{(MU)}$ (mm^3) Holt Eq2.3	Moh Eq2.2	Chen Eq2.5
1	1	2.05		89.20	182.86		12.67	10.99			
	2	1.05		98.69	103.62		11.94	11.60			
	3	0.67		97.04	65.02		11.91	11.84			
	4	1.47		56.55	83.13		9.93	8.59			
	5	0.45	5.69	27.54	12.40	447.02	8.33	6.04	486.39	455.15	478.27
2	1	1.41		125.56	177.04		14.43	11.63			
	2	0.39		117.18	45.70		13.38	12.46			
	3	1.74		101.11	175.93		12.86	10.96			
	4	1.77	5.31	28.82	51.02	449.69	6.73	6.34	565.27	512.59	578.93
3	1	0.59		77.20	45.55		11.26	9.82			
	2	1.26		78.34	98.71		10.70	10.54			
	3	1.15		42.67	49.07		8.44	7.65			
	4	1.39	4.39	5.39	7.49	200.83	3.95	2.42	282.75	262.87	291.43
4	1	2.48		141.38	350.62		15.86	13.16			
	2	0.98		60.56	59.35		9.53	8.63			
	3	1.37	4.83	22.14	30.33	440.31	5.84	5.50	678.1	608.09	688.18
5	1	1.28		79.60	101.89		11.78	11.28			
	2	0.98		96.02	94.10		11.51	11.01			
	3	1.50		91.00	136.50		10.38	10.32			
	4	0.58		62.59	36.30		10.18	9.37			
	5	0.51	4.85	48.31	24.64	393.43	9.24	9.17	348.31	324.03	352.39
6	1	1.13		128.24	144.91		14.21	12.91			
	2	1.17		128.10	149.88		13.48	12.89			
	3	1.30		98.40	127.92		12.42	11.35			
	4	1.40	5.00	62.93	88.10	510.80	9.75	9.39	513.52	461.93	528.63
7	1	2.12		128.55	272.52		15.32	12.47			
	2	0.95		101.72	96.64		12.16	11.85			
	3	1.39		85.27	118.52		12.81	9.74			
	4	1.14	5.60	11.33	12.91	500.59	5.52	4.27	678.1	608.09	688.18
8	1	1.38		143.68	198.28		15.02	13.77			
	2	1.37		117.86	161.47		13.13	12.65			
	3	1.24	3.99	102.45	127.03	486.78	12.98	10.97	451.4	386.75	471.31
9	1	0.77		122.43	94.27		14.09	12.11			
	2	1.36		122.53	166.64		13.68	12.47			
	3	1.06		102.51	108.67		12.33	11.57			
	4	0.99	4.18	86.26	85.39	454.97	11.59	10.83	416.37	364.12	434.5

Table 5.1 continues

10	1	1.43		146.18	209.03		16.51	12.83			
	2	1.22		123.31	150.44		13.57	13.45			
	3	0.87		97.30	84.65		12.35	10.92			
	4	0.72		72.94	52.52		11.23	10.94			
	5	1.41	5.65	43.37	61.16	557.80	8.91	8.30	705.1	628.18	711.65
11	1	0.99		114.21	113.07		14.15	11.65			
	2	1.90		129.29	245.66		14.07	13.05			
	3	1.17		111.71	130.70		12.29	12.07			
	4	0.57		81.08	46.22		11.52	10.14			
	5	0.82	5.45	49.30	40.43	576.07	9.25	7.99	565.23	513.28	571.35
12	1	1.78		127.25	226.51		13.43	12.54			
	2	1.28		143.19	183.28		15.69	12.75			
	3	0.84		100.81	84.68		11.79	11.69			
	4	1.37		85.62	117.30		11.26	10.66			
	5	0.67	5.94	16.09	10.78	622.55	6.00	4.71	572.57	530.46	560.96
13	1	0.98		141.90	139.06		14.99	14.09			
	2	1.19		112.34	133.69		13.09	12.25			
	3	1.71	3.88	47.49	81.21	353.96	9.38	7.75	439.18	372.95	456.49
14	1	0.94		147.34	138.50		16.42	12.52			
	2	1.49		71.93	107.17		10.77	9.62			
	3	1.10	3.53	48.55	53.40	299.08	8.61	8.44	492.39	396.78	498.32

Table 5.2 Data of bruise volumes determined by image analysis (V_{IA}) and manually (V_{MU}) for the bruises produced by steel ball from 200 mm drop height, in the manual method three formulae (Eq 2.2, 2.3, and 2.5) were used

Apple No.	Slice No.	Thick -ness (mm)	Bruise depth (mm)	Slice area (mm^2)	Slice volume (mm^3)	$V_{(IA)}$ (mm^3)	D_{max} (mm)	D_{min} (mm)	$V_{(MU)}$ (mm^3) Holt Eq 2.3	Moh Eq 2.2	Chen Eq2.5
1	1	1.29		171.55	221.30		15.72	14.99			
	2	1.45		173.02	250.88		15.20	15.13			
	3	2.11		154.60	326.20		14.73	14.71			
	4	0.73		120.48	87.95		14.85	11.35			
	4	1.06		65.89	69.84		10.65	9.55			
	4	0.99	7.63	21.38	21.17	977.35	7.35	4.51	1053.75	973.02	987.25
2	1	1.47		198.48	291.77		16.96	15.83			
	2	1.70		179.50	305.15		15.94	15.33			
	3	1.50		135.79	203.69		15.26	12.15			
	4	1.75	6.42	98.86	173.01	973.61	12.78	8.89	972.79	863.73	966.90
3	1	1.70		315.52	536.38		24.96	21.04			
	2	0.83		286.29	237.62		24.53	17.59			
	3	1.45		175.12	253.93		15.99	14.92			
	4	1.00		150.93	150.93		15.23	13.64			
	5	0.44		117.23	51.58		13.75	12.83			
	6	0.73		89.74	65.51		12.45	11.33			
	7	1.01	7.16	62.78	63.41	1359.35	10.80	9.49	2451.84	1943.90	2335.60
4	1	0.64		192.87	123.44		17.07	16.01			
	2	1.21		199.56	241.47		16.74	16.14			
	3	1.06		178.18	188.87		15.88	15.41			
	4	0.97		160.78	155.96		14.91	14.84			
	5	1.48		116.72	172.75		13.16	12.40			
	6	0.86		57.91	49.81		9.61	8.93			
	7	0.92	7.14	24.92	22.93	955.22	8.04	6.13	1113.80	1007.59	1089.33
5	1	1.29		200.32	258.41		17.36	15.60			
	2	1.07		204.63	218.95		17.37	15.55			
	3	0.93		171.95	159.92		15.86	14.68			
	4	1.07		134.80	144.24		14.14	13.52			
	5	1.08		93.27	100.73		11.94	10.98			
	6	1.34	6.78	41.02	54.97	937.22	8.87	8.70	1081.04	965.58	1069.85
6	1	1.07		176.93	189.31		15.97	15.10			
	2	1.29		161.07	207.78		14.95	14.89			
	3	1.31		155.97	204.33		14.77	13.86			
	4	1.21		122.24	147.91		13.54	12.43			
	5	0.75		74.90	56.17		11.10	9.98			
	6	0.86	6.49	34.30	29.50	835.00	8.08	7.37	876.86	793.13	866.66
7	1	1.32		186.20	245.78		16.38	15.45			
	2	1.05		186.79	196.13		15.72	15.70			
	3	0.56		193.12	108.15		16.94	15.46			
	4	1.48		173.84	257.28		15.22	15.12			
	5	3.36	7.77	117.53	394.89	1202.22	13.14	12.68	1159.09	1064.29	1091.55
8	1	0.82		181.69	148.99		15.91	15.14			
	2	1.54		179.11	275.83		15.87	15.14			
	3	1.36		171.88	233.76		15.72	15.16			
	4	0.99		114.75	113.61		12.72	12.47			
	5	0.70		83.19	58.23		11.42	10.61			
	6	1.39	6.80	51.68	71.83	902.25	9.74	8.14	923.46	840.58	901.25

Table 5.4 Data of bruise volumes determined by image analysis (V_{IA}) and manually (V_{MU}) for the bruises produced by steel ball from 300 mm drop height, in the manual method three formulae (Eq 2.2, 2.3, and 2.5) were used

Apple No.	Slice No.	Thick -ness (mm)	Bruise depth (mm)	Slice area (mm^2)	Slice volume (mm^3)	$V_{(IA)}$ (mm^3)	D_{max} (mm)	D_{min} (mm)	$V_{(MU)}$ (mm^3) Eq 2.3 Holt	Eq 2.2 Moh	Eq 2.5 Chen
1	1	1.13		371.58	419.88		23.44	22.40			
	2	1.65		334.94	552.65		23.77	19.65			
	3	0.89		328.25	292.14		21.54	21.15			
	4	0.88		295.10	259.69		20.22	19.87			
	5	0.60		249.56	149.74		18.94	17.80			
	6	0.65		203.23	121.94		18.18	16.49			
	7	0.73		163.62	106.36		15.60	15.09			
	8	1.11		138.36	153.58		15.37	12.66			
	9	1.19		84.02	99.99		12.78	10.53			
	10	1.06	9.89	46.20	48.97	2204.94	11.95	6.92	3054.49	2640.40	2845.18
2	1	1.20		386.30	463.56		25.62	22.44			
	2	1.23		297.93	366.46		21.71	20.38			
	3	1.38		222.61	307.20		18.14	16.69			
	4	0.65		192.43	125.08		17.19	16.58			
	5	2.38		133.26	317.17		14.49	14.45			
	6	1.32	8.16	72.30	95.44	1674.91	14.26	10.05	2983.05	2387.83	2804.45
3	1	0.82		409.13	335.49		30.61	19.94			
	2	1.75		327.24	572.67		22.42	20.36			
	3	0.46		280.22	128.90		19.60	18.75			
	4	1.56		268.40	418.71		19.34	18.33			
	5	1.60		226.49	362.38		18.05	17.55			
	6	0.78		165.06	128.75		15.50	15.42			
	7	1.20		97.89	117.47		12.92	11.05			
	8	1.19	6.79	55.12	65.60	2129.96	11.60	9.18	3900.56	2662.28	3331.16
4	1	1.14		333.46	380.15		26.65	17.75			
	2	1.56		312.07	486.84		22.88	18.82			
	3	0.97		302.81	293.72		22.86	18.38			
	4	1.30		235.92	306.69		19.12	17.13			
	5	0.63		180.76	113.88		16.78	14.97			
	6	1.35		146.29	197.49		16.45	13.04			
	7	1.11		114.33	126.91		16.71	11.21			
	8	2.26	10.32	60.70	137.18	2042.85	15.40	8.65	3723.66	3023.27	3465.84
5	1	2.54		302.39	768.08		23.80	18.87			
	2	1.13		395.79	447.25		23.15	22.69			
	3	1.04		328.12	341.24		22.12	19.70			
	4	1.18		216.27	255.20		18.80	17.28			
	5	1.09		137.83	150.24		14.52	14.37			
	6	1.34	8.32	86.41	115.79	2077.80	12.23	11.58	2578.80	2152.26	2467.61
6	1	1.52		352.46	535.73		27.27	17.46			
	2	1.13		340.92	385.23		25.44	19.03			
	3	1.11		308.66	342.61		22.90	18.82			
	4	1.01		257.74	260.32		20.83	17.11			
	5	1.10		205.93	226.52		17.92	16.82			
	6	0.97		98.47	95.51		14.96	11.01			
	7	1.22	8.06	54.26	66.20	1912.12	11.55	7.84	3371.33	2627.94	3138.37
7	1	1.01		430.17	434.48		29.04	21.04			
	2	0.92		361.31	332.41		26.32	18.58			
	3	0.97		249.06	241.59		19.72	17.64			
	4	1.45		239.75	347.64		18.24	18.18			

Table 5.4 continues

	5	1.20		143.57	172.29		14.37	13.95			
	6	2.65		111.37	295.13		13.50	12.12			
	7	1.07	9.27	32.62	34.91	1858.43	10.24	6.06	4446.00	3487.06	4093.28
8	1	1.19		324.36	385.99		22.87	21.10			
	2	2.41		324.56	782.19		21.78	20.58			
	3	1.37		223.03	305.55		17.85	17.57			
	4	1.72		123.69	169.46		14.56	13.79			
	5	0.75	7.44	63.33	108.92	1752.11	10.66	10.45	2105.32	1743.78	2037.53
9	1	1.84		338.40	622.66		25.14	19.49			
	2	2.08		311.93	648.81		23.15	18.86			
	3	2.72		219.81	597.87		17.71	16.91			
	4	0.86		159.46	137.13		16.10	14.06			
	5	1.68		100.90	169.52		12.45	12.31			
	6	0.44	9.62	28.24	12.43	2188.41	7.06	6.78	3370.41	2853.77	3183.50
10	1	1.62		309.92	502.08		21.64	20.16			
	2	1.55		277.43	430.01		19.83	18.55			
	3	1.38		211.22	291.49		17.30	17.16			
	4	1.07		175.20	187.46		15.70	15.51			
	5	0.94		89.54	84.16		11.52	10.48			
	6	1.47		89.39	131.40		11.65	11.29			
	7	0.97	9.00	27.02	26.21	1652.81	8.06	6.03	2323.86	2036.78	2206.76
11	1	1.49		209.51	312.18		18.63	15.94			
	2	1.39		242.91	337.65		18.03	18.62			
	3	1.63		234.87	382.83		17.20	17.39			
	4	1.14		160.82	183.33		16.47	13.92			
	5	1.46		128.18	146.12		13.66	13.51			
	6	0.94	8.05	55.52	81.05	1443.16	11.06	7.85	1317.74	1208.36	1246.96
12	1	1.08		268.05	289.49		19.78	18.73			
	2	0.51		286.08	145.90		19.65	19.22			
	3	1.25		271.16	338.95		19.28	18.37			
	4	1.95		209.54	408.60		17.81	16.02			
	5	0.86		165.10	141.98		16.38	15.03			
	6	1.49	7.14	94.44	140.72	1465.64	13.08	11.65	1489.66	1287.60	1462.68
13	1	1.48		302.87	448.25		21.59	19.87			
	2	1.45		267.47	387.83		20.24	18.21			
	3	1.57		266.62	418.59		19.80	18.82			
	4	1.17		213.50	249.79		17.31	17.02			
	5	0.70		157.52	110.27		16.14	13.72			
	6	2.83	9.20	88.23	249.68	1864.41	14.79	9.32	2374.04	2091.76	2245.39
14	1	1.12		312.39	349.88		21.64	19.44			
	2	2.71		299.58	811.85		21.00	19.96			
	3	1.26		238.30	300.26		18.52	17.70			
	4	1.44		181.77	261.74		16.48	16.01			
	5	1.16	7.69	134.46	155.98	1879.70	14.97	14.12	1926.47	1652.28	1885.56
15	1	1.72		459.54	790.40		29.06	22.44			
	2	1.14		288.51	328.90		20.69	19.45			
	3	1.27		221.54	281.35		18.15	16.48			
	4	0.88		193.76	170.51		16.50	15.93			
	5	0.88		136.43	120.06		14.77	12.26			
	6	1.35		72.90	98.41		12.15	9.94			
	7	0.96	8.20	56.68	54.41	1844.05	14.00	8.91	3988.30	3008.04	3625.80
16	1	1.13		276.89	312.88		20.67	20.65			
	2	0.57		240.71	137.20		18.33	18.11			
	3	1.53		247.77	379.09		19.48	18.83			
	4	1.18		213.14	326.11		17.18	16.98			

Table 5.4 continues

	5	1.33		160.97	189.95		15.99	14.32			
	6	1.87	7.61	123.42	230.79	1576.02	14.35	13.05	1744.05	1507.56	1702.41
17	1	1.25		254.90	318.62		18.50	17.97			
	2	1.62		283.41	459.13		19.85	19.61			
	3	2.03		247.04	501.24		18.43	17.87			
	4	0.81		196.44	159.31		16.61	16.48			
	5	2.17	7.88	114.88	249.30	1687.61	13.99	12.86	1684.52	1475.49	1625.72
18	1	1.68		356.08	598.21		24.88	20.27			
	2	0.93		358.72	333.61		23.55	20.67			
	3	2.56		298.76	764.83		21.71	18.90			
	4	0.37		197.06	72.91		16.70	15.73			
	5	1.04		153.90	160.06		14.97	14.63			
	6	1.65	8.23	88.63	146.24	2075.86	12.91	11.64	2792.81	2292.48	2667.47

Table 5.5 Data of bruise volumes determined by image analysis (V_{IA}) and manually (V_{MU}) for the bruises produced by pendulum with a 45° impact angle, in the manual method three formulae (Eq 2.2, 2.3, and 2.5) were used

Apple No.	Slice No.	Thick -ness (mm)	Bruise depth (mm)	Slice area (mm^2)	Slice volume (mm^3)	$V_{(IA)}$ (mm^3)	D_{max} (mm)	D_{min} (mm)	$V_{(MU)}(mm^3)$ Eq 2.3 Holt	Eq 2.2 Moh	Eq 2.5 Chen
1	1	1.33		226.92	301.80		18.86	18.63			
	2	2.13		194.84	415.01		18.32	16.67			
	3	1.78	5.24	80.19	142.74	859.55	11.32	10.95	978.78	807.27	975.92
2	1	2.40		189.55	454.92		17.86	15.22			
	2	0.78		109.70	85.57		12.91	12.39			
	3	1.62	4.80	59.63	96.60	637.09	10.59	9.11	792.22	659.17	801.68
3	1	0.26		251.61	65.42		21.03	17.58			
	2	0.93		191.83	178.40		18.64	14.59			
	3	2.28	3.47	107.39	244.85	488.67	13.56	11.44	885.37	624.53	803.54
4	1	1.43		241.95	345.99		20.08	17.74			
	2	0.99		98.28	97.30		16.62	16.14			
	3	1.98	4.40	95.73	189.55	632.83	12.61	11.70	950.38	741.29	928.92
5	1	1.90		210.26	399.49		21.63	18.61			
	2	1.65		179.70	296.51		17.88	16.15			
	3	1.08	4.63	179.70	194.08	890.08	8.04	6.13	1195.26	902.62	1134.21
6	1	1.68		212.84	357.57		17.93	16.76			
	2	1.60		223.71	357.94		19.70	16.32			
	3	0.82		201.95	165.60		17.65	16.44			
	4	0.94	5.04	79.93	75.13	956.24	12.10	11.89	843.17	703.32	848.38
7	1	1.55		249.20	386.26		18.91	18.86			
	2	2.14		216.20	462.67		18.42	18.02			
	3	1.42		142.85	202.85		14.32	13.14			
	4	1.11	6.22	15.98	17.74	1069.51	9.45	3.76	1166.90	999.44	1164.59
8	1	1.01		237.88	240.26		20.03	16.92			
	2	1.33		199.85	265.80		19.31	15.21			
	3	0.59		118.04	69.64		14.74	11.14			
	4	1.04	3.97	44.67	46.46	622.16	8.69	8.14	876.55	658.24	833.97
9	1	1.03		307.23	316.45		21.31	20.93			
	2	1.44		225.65	324.94		20.28	17.69			
	3	1.15	3.62	117.24	134.83	776.21	14.27	12.81	948.66	670.40	860.74
10	1	0.10		315.35	31.54		24.67	18.68			
	2	2.39		244.67	584.76		20.75	17.31			
	3	2.88	5.37	132.38	381.25	997.55	16.73	12.72	1799.70	1327.33	1661.66